Report No. BMI-APDA-660

Special Distribution to APDA Only

IRRADIATION STUDIES OF URANIUM-10 w/o MOLYBDENUM FUEL ALLOY

by

John E. Gates
William E. Murr
Arthur A. Bauer
Frank A. Rough

to

ATOMIC POWER DEVELOPMENT ASSOCIATES

January 26, 1961

BATTELLE MEMORIAL INSTITUTE
505 King Avenue
Columbus 1, Ohio

DISCLAIMER

TABLE OF CONTENTS

	Page
ABSTRACT	1
INTRODUCTION	1
EXPERIMENTAL PROCEDURES AND RESULTS	5
Specimen Fabrication	5
Hot-Rolling Fabrication Techniques	6
Coextrusion Fabrication Techniques	6
Fabrication of Specimens for Reference-Diameter Phase	6
Heat Treatments	7
Preirradiation Measurements	13
Encapsulation and Irradiation	13
Temperature-Effects Series	19
Reference-Diameter Series	21
Postirradiation Examination of Specimens	28
Fission-Gas Analysis	28
Capsule Opening	28
Dosimetry	28
Measurement of Physical Dimensions and Relative Density	29
Visual Examination of Specimens	29
Measurement of Linear Thermal Expansion	29
POSTIRRADIATION HEAT TREATMENTS	58
METALLOGRAPHIC EXAMINATION	58
DISCUSSION AND EVALUATION OF RESULTS	68
Heat-Treatment Phase	72
Burnup Phase	73
Composition-Effects Phase	73
Cladding-Thickness Phase	74
Burnup-and-Heat-Treatment Phase	75
Temperature-Effects Phase	77
Reference-Diameter Phase	78
Release of Krypton-85 From Specimens During Irradiation	78
Specimen Swelling	79
Thermal Expansion and Postirradiation Heat Treatments	80
General Discussion	89
CONCLUSIONS	90

IRRADIATION STUDIES OF URANIUM-10 w/o MOLYBDENUM FUEL ALLOY

by

John E. Gates, William E. Murr, Arthur A. Bauer,
and Frank A. Rough

Bare and zirconium-clad uranium-10 w/o molybdenum specimens were irradiated in NaK-filled capsules in the MTR. Irradiation conditions vaired to include central-core temperatures ranging from 300 to over 1200 F, fuel burnups ranging from 0.36 to over 3.0 total a/o, and fission rates in the range of 0.35 to 1.9 x 10^{14} fissions/(sec)(cm^3) of alloy. Other parameters studied included the effects of heat treatment, changes in composition, different fabrication techniques, and changes in cladding thickness on the behavior of the fuel alloy. The objective of the irradiations was to determine the behavior of the fuel alloy under conditions approaching as closely as possible those to be encountered in the Enrico Fermi Atomic Power Plant as they were known at the time.

The results indicate that the volume of the fuel alloy would increase conservatively at a rate of about 3.0 per cent per a/o burnup as long as the critical temperature of 1000 to 1100 F was not exceeded and the gamma phase of the alloy did not transform during irradiation. If the critical temperature was exceeded, the alloy swelled until rupture or complete disintegration occurred. The occurrence of transformation during irradiation was noted at burnups in the range of 2.5 total a/o at fission rates of 1.5 x 10^{14} to 1.9 x 10^{14} fissions/(sec)(cm^3) and temperatures of 800 to 1000 F. The alloy was normally maintained in the gamma phase during irradiation, even at temperatures below 1100 F and at fission rates in the range of 0.7 x 10^{14} fissions per sec. Transformation during irradiation was accompanied by excessive swelling of the alloy.

INTRODUCTION

Atomic Power Development Associates, Inc. (APDA) has been designing a fast-breeder power reactor. This reactor is to be installed in the Enrico Fermi Atomic Power Plant being constructed by the Power Reactor Development Company (PRDC) and The Detroit Edison Company under the Atomic Energy Commission Power Reactor Demonstration Program. APDA, with the assistance of Battelle Memorial Institute, has devoted considerable effort over the past 7 years to selecting a suitable fuel alloy for use in the Fermi reactor and in investigating the radiation stability of the selected alloy. This report summarizes the results of these studies.

Preliminary studies of a series of zirconium-uranium and molybdenum-uranium alloys irradiated to low burnups indicated that the uranium-10 w/o molybdenum alloy possessed the best radiation stability, and also that this stability was apparently improved by heat treating the alloy to retain the gamma phase prior to irradiation. The results of these irradiations were reported in the October 1955, December 1955, and April 1956, quarterly reports to APDA. As a result of this information, in addition to that available in the literature at the time, the uranium-10 w/o molybdenum alloy was selected as a reference alloy. With the selection of a reference alloy, an intensive

irradiation program was initiated to obtain detailed information on the ability of this alloy to withstand the conditions of burnup and temperature expected to be achieved in the first core of the fast-breeder power reactor. The MTR was selected for use in the irradiations since this reactor provides the highest neutron flux available.

The intensive irradiation program was initiated in January, 1956. This program was divided into several phases, each designed to provide a particular type of information concerning the radiation stability of the reference fuel alloy. Although some of the various phases have been described in previous reports, all phases will be described again for orientation purposes.

Heat-Treatment Phase

The preliminary irradiations in NaK at low burnups, about 0.1 total a/o, had indicated that the gamma structure of the reference fuel alloy was apparently more stable to irradiation than the partially transformed structures. However, the differences in the radiation stability of the various structures were small at low burnups and 12 additional unclad specimens were irradiated to higher burnups while immersed in NaK. The irradiations were conducted in Capsules BMI-302-19 and -20 and BMI-9-7 and -8 in the MTR. The specimens irradiated in the first two capsules were fabricated by hot rolling, while the specimens in the other two capsules were fabricated by coextrusion with the cladding being removed prior to irradiation. The data obtained from the irradiation of Capsules BMI-302-19 and -20 were included in Report No. BMI-APDA-625, May, 1957. The details of the irradiation of Capsules BMI-9-7 and -8 are included in this report.

Burnup Phase

A series of unclad reference fuel specimens with retained-gamma structures were irradiated in contact with NaK for the purpose of determining whether the alloy could withstand burnups as high as 3 total a/o at temperatures of 1065 F. The specimens were fabricated by hot-rolling techniques. The irradiations were conducted in capsules designed to maintain two specimens, positioned end to end, in NaK at 1065 F in a specified neutron flux. Seven such capsules, designated BMI-9-1, -2, -3, -4, -5, -12, and -13, were irradiated. Although the data obtained from Capsules BMI-9-1, -2, -3, and -4 were included in BMI-APDA-625, they are also discussed in this report along with the results of the remaining irradiations.

Composition-Effects Phase

It was considered that the composition of the reference fuel alloy might vary slightly during fabrication of a core loading. Since variations in composition could have serious effects on the radiation stability of the alloy, a total of four specimens of uranium-9 w/o molybdenum and four of uranium-11 w/o molybdenum, heat treated to retain the gamma phase, were irradiated immersed in NaK in two capsules. All specimens were coextruded and clad with nominally 4 mils of zirconium except for the bare ends. The capsules were designated BMI-9-10 and -11 and were designed to maintain the specimens at 1065 F in a specified neutron flux. The results of these irradiations are discussed in this report.

Cladding-Thickness Phase

A zirconium cladding thickness of 4 mils had been chosen as the reference fuel-pin cladding thickness. In order to investigate the effects of increasing the thickness of the cladding, a group of coextruded specimens clad with selected thicknesses of zirconium was irradiated. Six specimens were irradiated in Capsule BMI-9-9 and seven in Capsule BMI-9-14. Capsule BMI-9-14 was equipped with thermocouples for temperature measurement. The design irradiation temperature was 1065 F and all specimens were immersed in NaK. Two specimens with nominal zirconium cladding thicknesses of 4, 8, and 11 mils, except for the bare ends, were irradiated in each capsule. An extra specimen with a 4-mil cladding was included in one capsule for use in neutron-dosimetry studies. The results of these irradiations are discussed in this report.

Burnup-and-Heat-Treatment Phase

A reference heat treatment of 24 hr at 1652 F followed by quenching in water was selected for use early in the program to produce the gamma phase in the reference alloys. As the technology of the reference alloy advanced, it became important to know whether the radiation stability of the alloy could be enhanced by other, possibly more economical, heat treatments. Twelve coextruded specimens of the reference alloy, clad with a nominal 4 mils of zirconium except for the bare ends, were irradiated immersed in NaK in six capsules. The specimens were given one of three different heat treatments prior to irradiation. These capsules were designated BMI-9-22, -23, -24, -25, -30 and -31, and were designed to maintain the specimens at 1065 F in a specified neutron flux. Capsule BMI-9-6, which contained two reference-alloy specimens clad by pressure-bonding techniques, is also included in this phase for convenience. The results of these irradiations are discussed in this report.

End-Cap Phase

One phase of the program at Battelle involved the development of a method for end capping the reference fuel pins. Methods involving the use of swaging, butt-welding, and pressure-bonding techniques to attach end caps to the fuel pins were studied. Since the selected method for preparation of the first reactor core loading would require the production of end caps which could survive the rigorous conditions in the reactor core, a series of irradiations of end-capped specimens was initiated. Two specimens fabricated by hot-rolling techniques and clad and end capped with zirconium by pressure-bonding techniques were irradiated in Capsule BMI-9-15. Six coextruded zirconium-clad specimens with zirconium end caps attached by butt-welding techniques were irradiated in Capsules BMI-9-16, -17, and -18. Four coextruded zirconium-clad specimens with their ends swaged to a point were irradiated in Capsules BMI-9-26 and -27. Four coextruded zirconium-clad specimens with a swaged zirconium end cap on one end and a swaged stainless steel end cap on the other, were irradiated in Capsules BMI-9-28 and -29. All specimens were immersed in NaK for the irradiations. The design irradiation temperature was 1065 F at the center of the specimens. The results of these irradiations were discussed in detail in BMI-APDA-652 dated January 1960. However, the data are also used in this report to facilitate a general discussion of the radiation stability of the reference fuel.

Temperature-Effects Phase

With but two exceptions in the early parts of the program, Capsules BMI-302-1 and BMI-9-14, irradiations were conducted in capsules which were not equipped with thermocouples or an external heat supply. The irradiation temperature of the specimens was calculated from neutron-dosimeter data, the known thermal conductivity of the fuel and capsule components, and the known temperatures of the MTR coolant water. These calculations were fully described in BMI-APDA-648.

Using the calculation method, the average temperature of the specimens was not known until after the irradiations were completed, the capsules opened, and the dosimeters analyzed. Since it was difficult to predict the neutron flux present in a given position in the MTR due to the effect of other experiments and the reactor control rods, and since the calculated temperatures gave only the average value for the complete irradiation, three irradiations were planned involving the use of capsules equipped with thermocouples and electrical heaters. A continuous record of the irradiation temperature could thus be maintained and, if the neutron flux fluctuated during the irradiation, the desired temperature could be maintained by use of the electrical heaters. Three such capsules, BMI-9-19, -20, and -21, were designed to maintain central specimen temperatures of 750, 1290, and 1065 F, respectively.

Each of the three capsules contained three coextruded zirconium-clad specimens of the reference alloy. The specimens were given one of three different heat treatments and were sealed in small individual containers filled with NaK. Three such containers were included in each capsule. The results of these irradiations are discussed in this report.

Reference-Diameter Phase

Six specimens, each about 5.5 in. long and 0.159 in. in diameter, were fabricated by techniques being considered for use in fabricating the first core loading. These pins were fabricated by coextrusion techniques and end capped by cold-swaging techniques. Four of these specimens were individually encapsulated in NaK for irradiation in the MTR at design temperatures of 1200 F to burnups of 1.5 total a/o. The capsules were designated as BMI-9-32, -33, -34, and -35. One of the capsules, BMI-9-32, was equipped with thermocouples.

The irradiation of Capsules BMI-9-34 and -35 was discontinued after it was discovered that specimens fabricated from natural rather than enriched uranium had been loaded into the capsules. These capsules were never opened for recovery of the specimens. The irradiation of Capsules BMI-9-32 and -33 was completed and the results are discussed in this report.

Measurements of Selected Physical Properties

The routine postirradiation examination of the irradiated specimens provided data concerning the condition of the specimen surface, changes in the physical dimensions and density, microstructures, and burnup. Measurements of fission-gas release were made in selected instances. In addition to these routine measurements, experiments were conducted to measure the effects of radiation on the thermal conductivity,

mechanical properties, electrical resistivity, and linear thermal expansion of the reference fuel alloy.

The thermal conductivity of several specimens irradiated to burnups ranging from 0.36 to 1.2 total a/o was measured. The results of these measurements were included in BMI-APDA-625. The mechanical properties of specimens with burnups ranging from 0.36 to 2.1 total a/o were measured. Data were obtained on the ultimate strength, 0.2 per cent offset yield strength, modulus of elasticity, and fracture strain. The results of the measurements were included in BMI-APDA-638. The measured electrical resistivity of several specimens irradiated to various burnups was included in BMI-APDA-625.

The coefficient of linear thermal expansion of several specimens with burnups ranging from 0.36 to 2.0 total a/o was measured at temperatures up to 1472 F. Although the measured thermal expansion was a combination of metal expansion and swelling due to fission-gas agglomeration, the data obtained from the measurements can be used to good advantage in studying the swelling of the fuel alloy at various temperatures. The results of these measurements are discussed in this report.

Postirradiation Heating Studies

Heat treatment of irradiated specimens was performed at various stages of the program in attempts to obtain additional information about the swelling of the irradiated reference fuel at selected temperatures. The major phase of these studies was reported in BMI-APDA-646, March, 1959. The results of other miscellaneous studies are included in this report.

Metallographic Examinations

Selected specimens were sectioned after irradiation and prepared for metallographic examination. The results of the microstructural studies are included in this report.

EXPERIMENTAL PROCEDURES AND RESULTS

Specimen Fabrication

Specimens used in the irradiations were fabricated by either hot rolling followed by cold swaging or by coextrusion with zirconium cladding. After fabrication, the specimens were given selected heat treatments. A list of all specimens used in the program is given in Table 1*. Each of the two fabrication techniques is described below.

*All tables are at the end of the report.

Hot-Rolling Fabrication Techniques

The core material used in the preparation of specimens by hot-rolling techniques was tungsten-electrode arc melted seven times to insure homogenity. The metal was shaped into a finger bar about 3/8 in. in diameter by 1.0 in. in length during the melting. After the melting procedure was completed, the bar was heated to 1796 F under helium, hot rolled in air to a diameter of 0.265 in., and quenched in water. The hot-rolled rod was vapor blasted to clean the surface and cold swaged to a diameter of 0.148 in. The swaged rod was heat treated at 1094 F for 0.5 hr under helium, and then quenched in water. Following this, the rod was vapor blasted to clean the surface, sealed in Vycor, heated for 24 hr at 1652 F, and quenched in water. This heat treatment produced the gamma phase in the fuel alloy. The fuel rod was then machined to a diameter of 0.100 in. and sectioned into fuel pins of the desired length. Additional heat treatments as listed in Table 1 were given after the fuel rods were machined to size.

Coextrusion Fabrication Techniques

The core material for the coextruded specimens was arc melted several times, induction melted in zirconia, and cast at 2696 F into cold copper molds. The casting, which was about 0.875 in. in diameter, was machined to a diameter of 0.673 in. and a length of 1.765 in. for coextrusion. After machining, the billet was shipped to Nuclear Metals, Inc., for coextrusion. The details of the coextrusion process were reported to APDA by NMI. The end product of the extrusion was a fuel rod clad with about 0.004 in. of zirconium with an over-all diameter of 0.100 in. The rod was cut into appropriate lengths for irradiation.

Fabrication of Specimens for Reference-Diameter Phase

Billets of uranium-10 w/o molybdenum fuel alloy were cast at Battelle. Two types of fuel alloy were prepared. Billets of one type of alloy contained uranium enriched to 9.49 per cent of uranium-235; the second type of alloy contained uranium enriched to 19.35 per cent of uranium-235. It was desired that these specimens be fabricated by the same technique as the prototype fuel pins to be used in the reactor. Therefore, the billets were sent to the Babcock & Wilcox facility at Alliance, Ohio, for fabrication into fuel pins using standard production methods.

Three pins of each fuel alloy were prepared by Babcock & Wilcox using coextrusion techniques. The fuel pins were nominally 5.5 in. long and 0.159 in. in diameter including a 4-mil-thick zirconium cladding. All six pins were solution heat treated for 1 hr at 1472 F and slow cooled. The 9.49 per cent enriched pins were identified as Pins 10-1, -2, and -3, and the 19.35 per cent enriched pins were identified as Pins 20-1, -2, and -3. The end caps were then swaged on the pins by the Nuclear Metals, Inc., plant in Concord, Massachusetts.

Two different end caps were swaged on the six pins. A zirconium end cap was swaged on one end of each pin and a Type 304 stainless steel end cap was swaged on the other end. The end caps overlapped the fuel pins about 0.5 in. The zirconium end caps, which extended about 0.45 in. beyond the end of the fuel pins, were tapered to a point. Each Type 304 stainless steel end cap, which extended about 0.85 in. beyond the end of the fuel pin, contained an oval hole about 0.06 in. wide and 0.45 in. long near the end.

A zirconium spacer about 0.1 in. long was inserted between the stainless steel end cap and the end of the fuel pin before swaging. The assembled specimens, which were about 6.8 in. long, had the appearance of large sewing needles. Figures 1 and 2 show the six specimens after fabrication. The joints between the Type 304 stainless steel end caps and the fuel pins are shown in Figures 3 and 4, and the joints between the zirconium end caps and the fuel pins are shown in Figures 5 and 6. The tapered ends of the zirconium end caps of Specimens 10-1, -2, and -3 are shown in Figure 7. Figure 8 presents an X-ray photograph of the six specimens. Note the zirconium spacer between the fuel pins and the stainless steel end caps. After the six specimens had been prepared by Nuclear Metals, Inc., they were sent to Battelle. Four of the specimens were encapsulated for irradiation while the other two were retained as controls.

Heat Treatments

Specimens were given various heat treatments prior to irradiation. The conditions for each heat treatment were selected to produce various phases in the alloy or to relieve possible stresses. In some cases the heat treatments were almost identical except that varying lengths of time at temperature were used.

(1) 24 hr at 1652 F followed by water quenching. This treatment produced the gamma phase in the reference fuel alloy.

(2) 1 hr at 1472 F followed by water quenching, and then 1/4 hr at 662 F, followed by air cooling. The first part of the treatment was considered a realistic production gamma heat treatment which would not cause excessive diffusion of uranium from the core into the cladding. The second part was designed to relieve any stresses in the specimens without causing transformation.

(3) 1/4 hr at 662 F followed by air cooling. This treatment was essentially for the relief of stresses in the specimens. The alloy was in the gamma-phase condition because of the conditions of fabrication.

(4) 24 hr at 1652 F followed by water quenching and then 1/4 hr at 662 F followed by air cooling. This treatment was used to determine if a low-temperature stress relief was beneficial with the gamma-phase heat treatment.

(5) 1 hr at 1472 F followed by slow (4-1/2 hr) cooling to 212 F. This treatment was selected to study the effects of slow cooling as opposed to quenching on the radiation stability of the alloy.

(6) The specimens were fabricated at 1544 F and furnace cooled.

(7) 1 hr at 1472 F followed by water quenching, 2 weeks at 932 F, and air cooling. This treatment results in essentially complete transformation of the gamma phase.

(8) 24 hr at 1652 F followed by water quenching, 100 hr at 932 F, and furnace cooling. This treatment produced about 80 per cent transformation of the gamma phase.

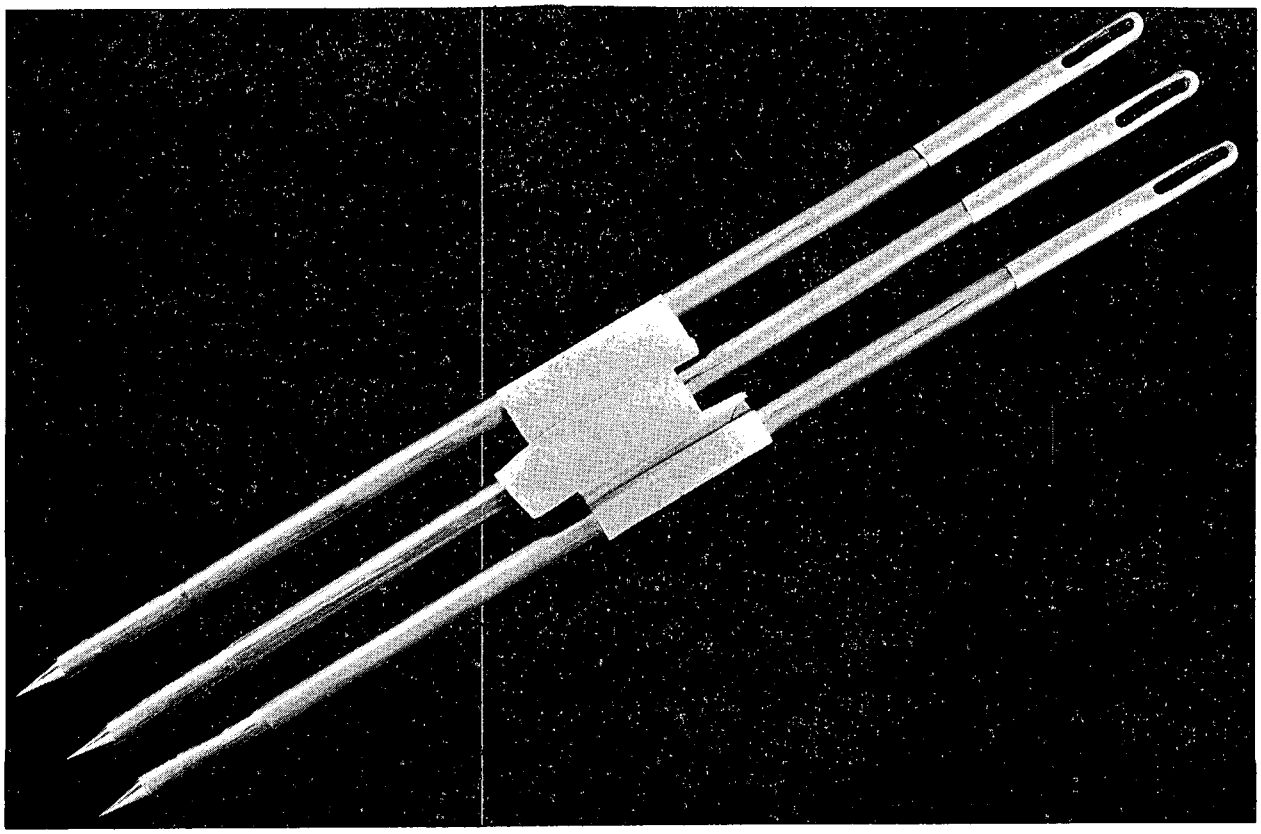

1X RM8700

FIGURE 1. SPECIMENS 10-1, -2, AND -3 AFTER FABRICATION

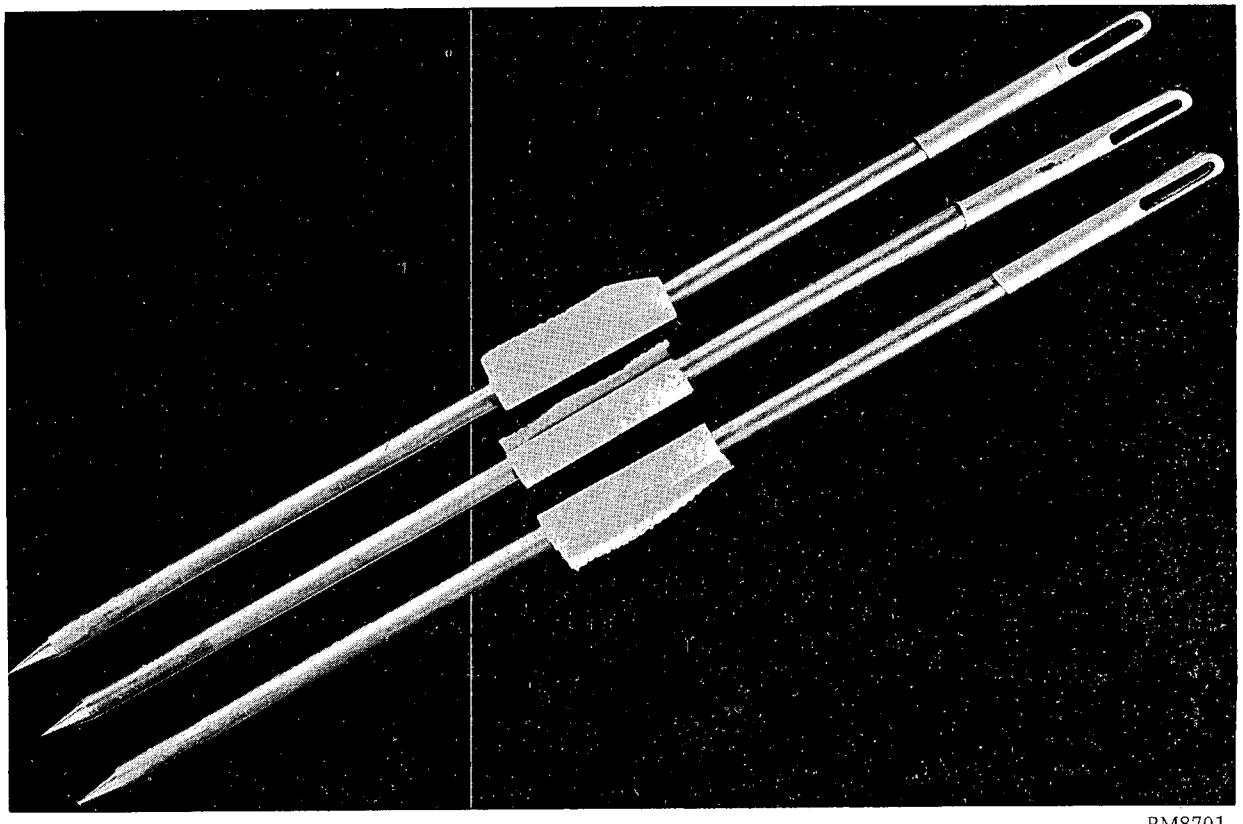

1X RM8701

FIGURE 2. SPECIMENS 20-1, -2, AND -3 AFTER FABRICATION

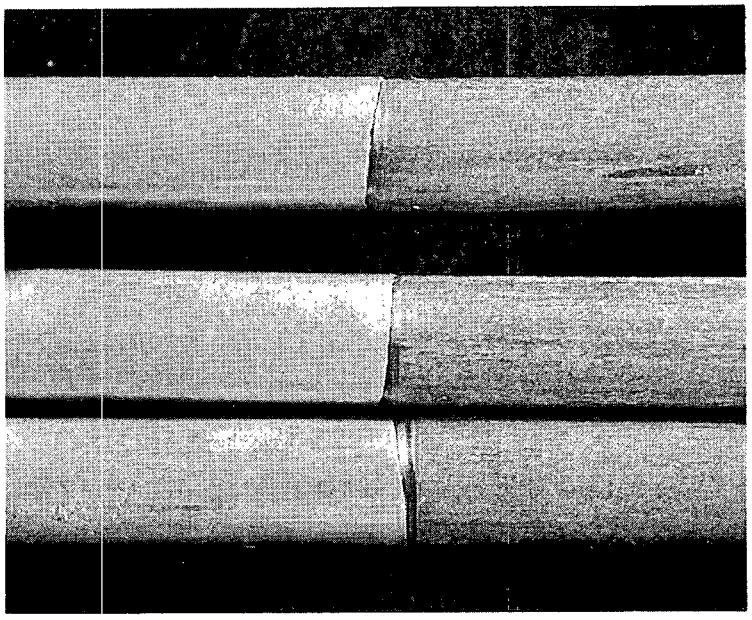

4X RM8705

FIGURE 3. JOINT BETWEEN TYPE 304 STAINLESS STEEL END CAP AND FUEL-PIN SECTION OF SPECIMENS 10-1, -2, AND -3

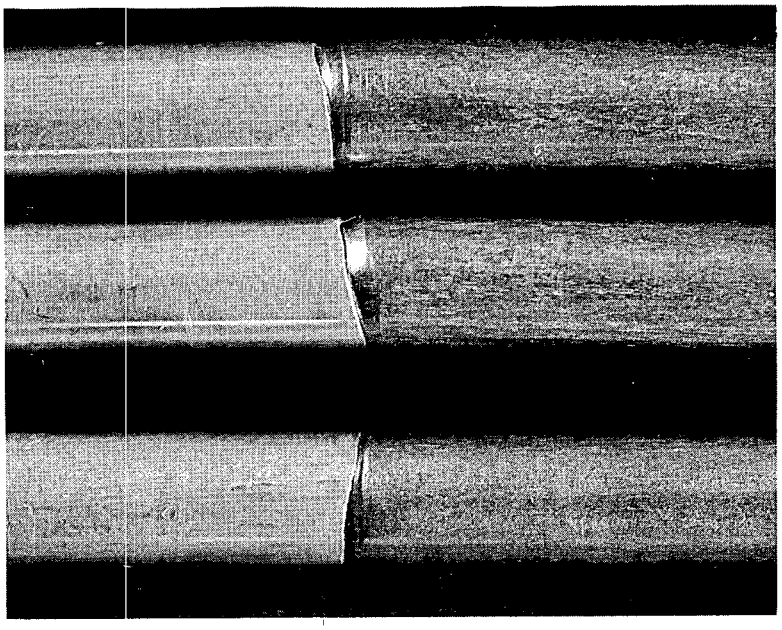

4X RM8706

FIGURE 4. JOINT BETWEEN TYPE 304 STAINLESS STEEL END CAP AND FUEL-PIN SECTION OF SPECIMENS 20-1, -2, AND -3

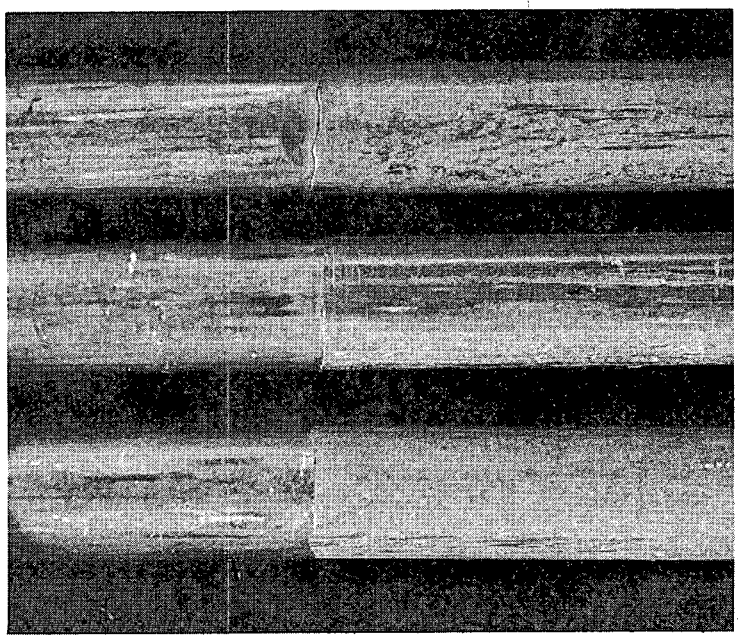

4X RM8703

FIGURE 5. JOINT BETWEEN ZIRCONIUM END CAPS AND FUEL-PIN SECTION OF SPECIMENS 10-1, -2, AND -3

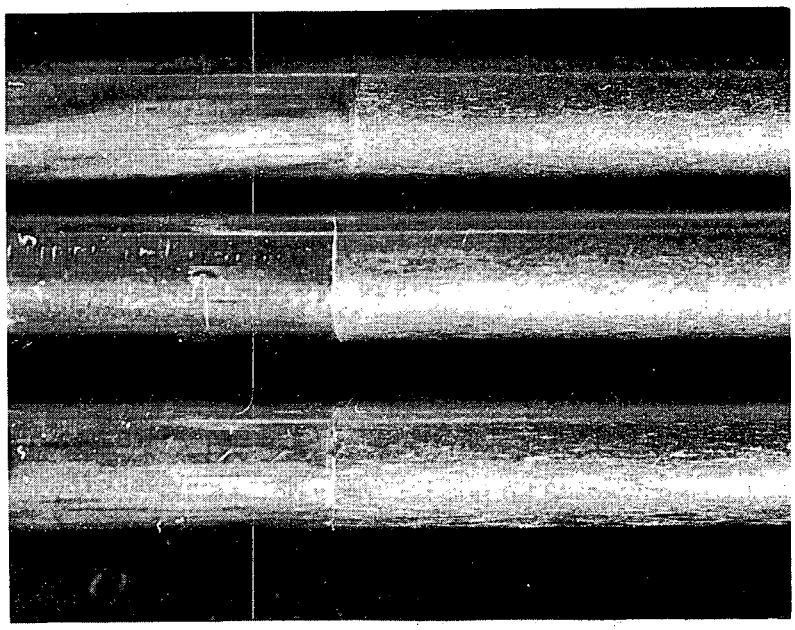

4X RM8709

FIGURE 6. JOINT BETWEEN ZIRCONIUM END CAPS AND FUEL-PIN SECTION OF SPECIMENS 20-1, -2, AND -3

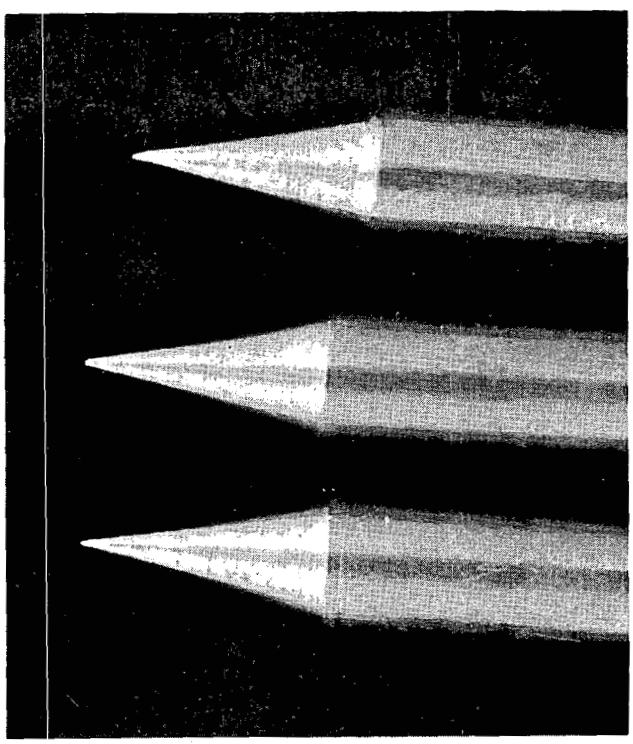

4X RM8711

FIGURE 7. TAPERED ENDS OF ZIRCONIUM END CAPS OF SPECIMENS 10-1, -2, AND -3

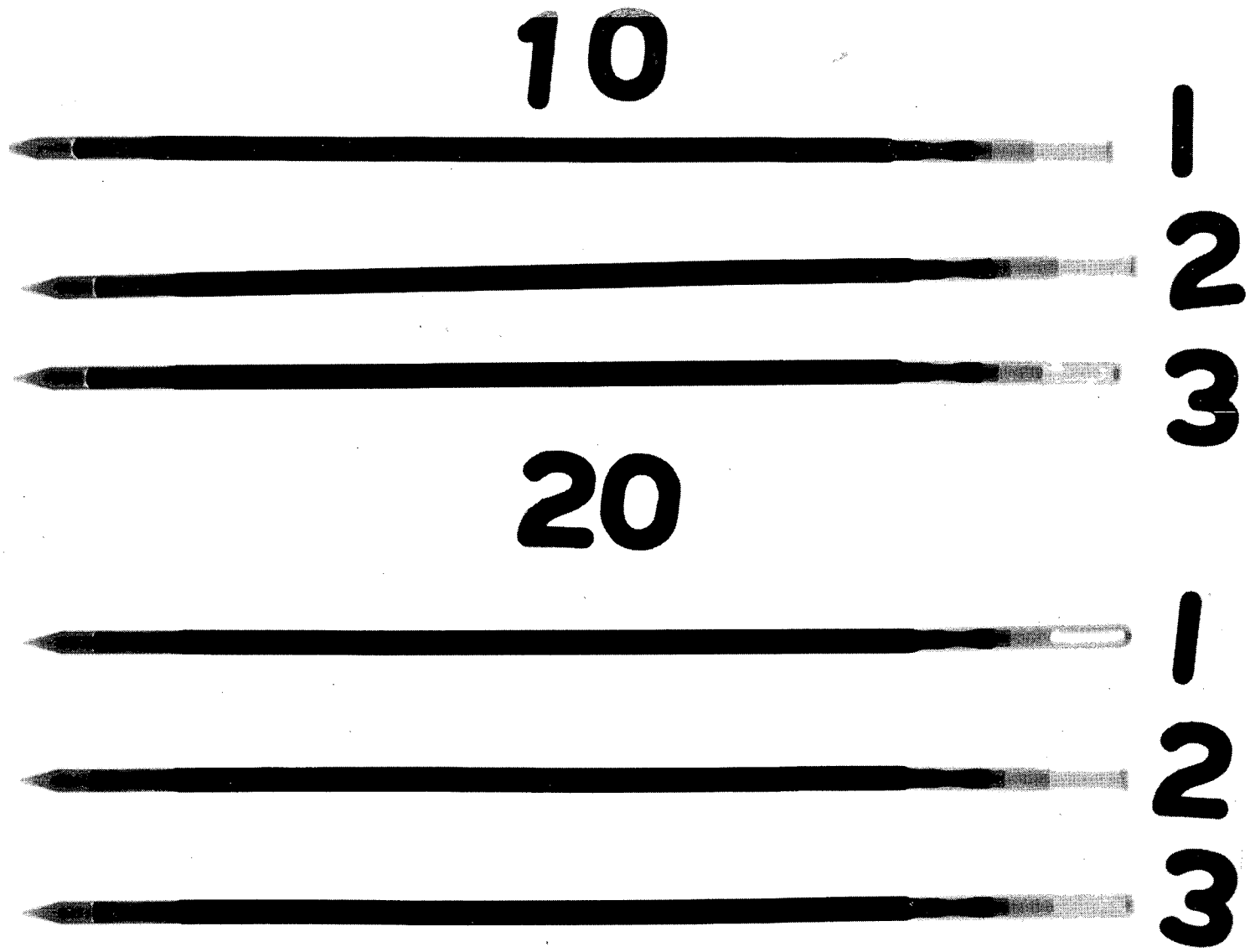

FIGURE 8. X-RAY OF THE SIX REFERENCE-DIAMETER SPECIMENS AFTER FABRICATION

(9) 24 hr at 1652 F followed by water quenching, 2 weeks at 932 F, and furnace cooling. This treatment produced essentially complete transformation of the gamma phase.

Preirradiation Measurements

After fabrication and heat treatment, the specimens were measured and photographed in preparation for encapsulation and irradiation. The preirradiation dimensions and density of each specimen are listed in Table 2. Photomacrographs showing the condition of the specimen prior to irradiation are presented later in the report along with photomacrographs showing the condition of the specimens after irradiation.

Encapsulation and Irradiation

All irradiations were conducted in NaK-filled capsules in the MTR. The design of the irradiation capsules and techniques of temperature and burnup calculation were discussed in an earlier report, BMI-APDA-648. General details of the capsule and specimen configuration used in the heat-treatment, burnup, composition-effects, cladding-thickness, burnup-and-heat-treatment, temperature-effects, and the reference-diameter Phases, are shown in Figures 9 through 15.

Dosimeter wires fabricated from either aluminum or nickel with additions of 0.6 w/o cobalt were included in each capsule. The wires were fastened in various positions in the capsule in order to permit a determination of the neutron-flux distribution over the length of the specimens. The amount of cobalt-60 formed in the wires was used as a basis for determining the neutron flux. Small temperature-indicator wires were also included in several of the capsules. These wires were designed to melt at different temperatures thus giving an indication of the temperatures occurring during irradiation. However, as discussed in an earlier report, BMI-APDA-652, it was not possible to determine whether the wires had melted after irradiation and detailed examination of the wires was terminated early in the program.

The irradiations were planned to produce selected burnups and temperatures (see Table 3). These conditions were generally difficult to achieve with any accuracy, principally because of the uncertainty in the knowledge of the neutron flux in the MTR. During some of the long-term irradiations, the capsules were shifted to different positions in the MTR which further complicated the problem. The irradiation history of each capsule, as supplied by the MTR, is given in Table 4. Although the MTR neutron-flux data do not in most instances agree with the capsule dosimeter flux data, the MTR data were used to provide a relative indication of the irradiation conditions and to estimate the burnup during the irradiation. Accumulated data and experience with other programs were also brought into play in estimating the burnup from MTR data. This improved the chances of obtaining the desired temperature and burnup conditions for a particular irradiation.

Each irradiation was followed carefully and running estimates were maintained of the burnup and temperature of the specimens in each capsule. At selected times, the capsules were discharged from the MTR and were returned to the Battelle hot cells for the postirradiation examination.

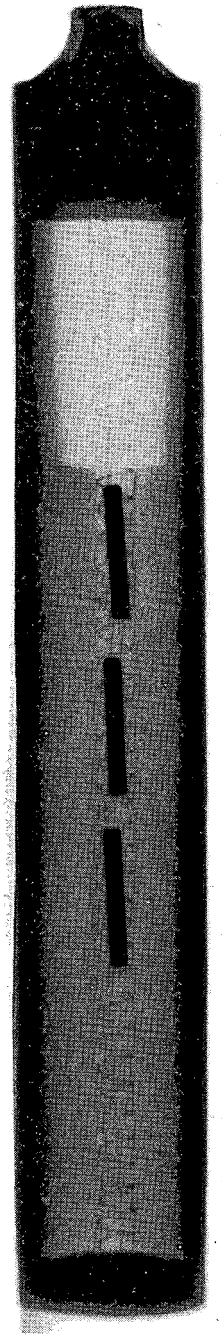

FIGURE 9. X-RAY PHOTOGRAPH OF TYPE OF CAPSULE USED IN HEAT-TREATMENT PHASE

Capsule BMI-9-7 is shown.

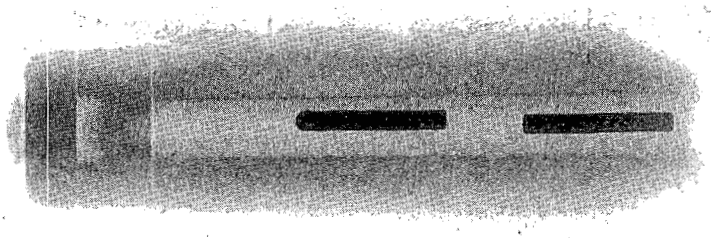

FIGURE 10. X-RAY PHOTOGRAPH OF TYPICAL CAPSULE CONFIGURATION USED IN BURNUP PHASE

Capsule BMI-9-12 is shown.

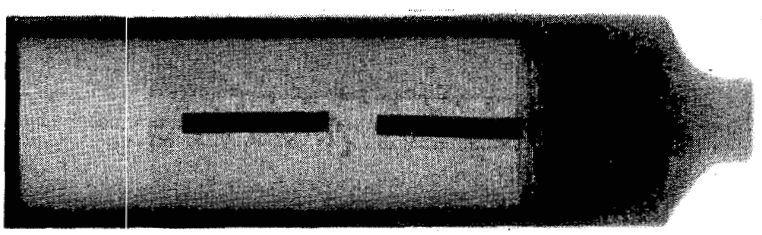

FIGURE 11. X-RAY PHOTOGRAPH OF TYPICAL CAPSULE CONFIGURATION USED IN COMPOSITION-EFFECTS PHASE

This capsule, BMI-9-10, is of the double-compartment type. The other compartment is identical to the one shown.

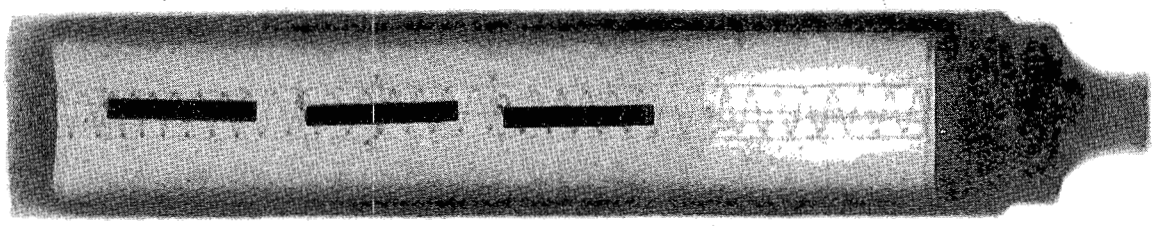

FIGURE 12. X-RAY PHOTOGRAPH OF TYPICAL CAPSULE CONFIGURATION USED IN CLADDING-THICKNESS PHASE

This capsule, BMI-9-9, is of the double-compartment type. Only one compartment is shown.

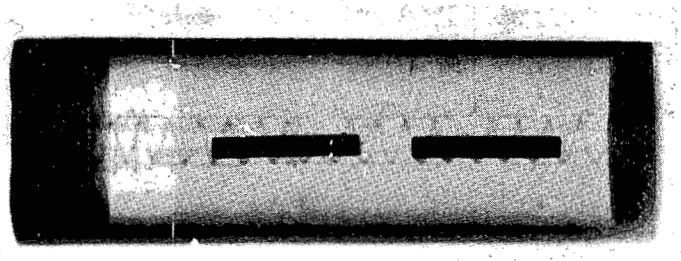

FIGURE 13. X-RAY PHOTOGRAPH OF TYPICAL CAPSULE CONFIGURATION USED IN BURNUP-AND-HEAT-TREATMENT PHASE

Capsule BMI-9-23 is shown.

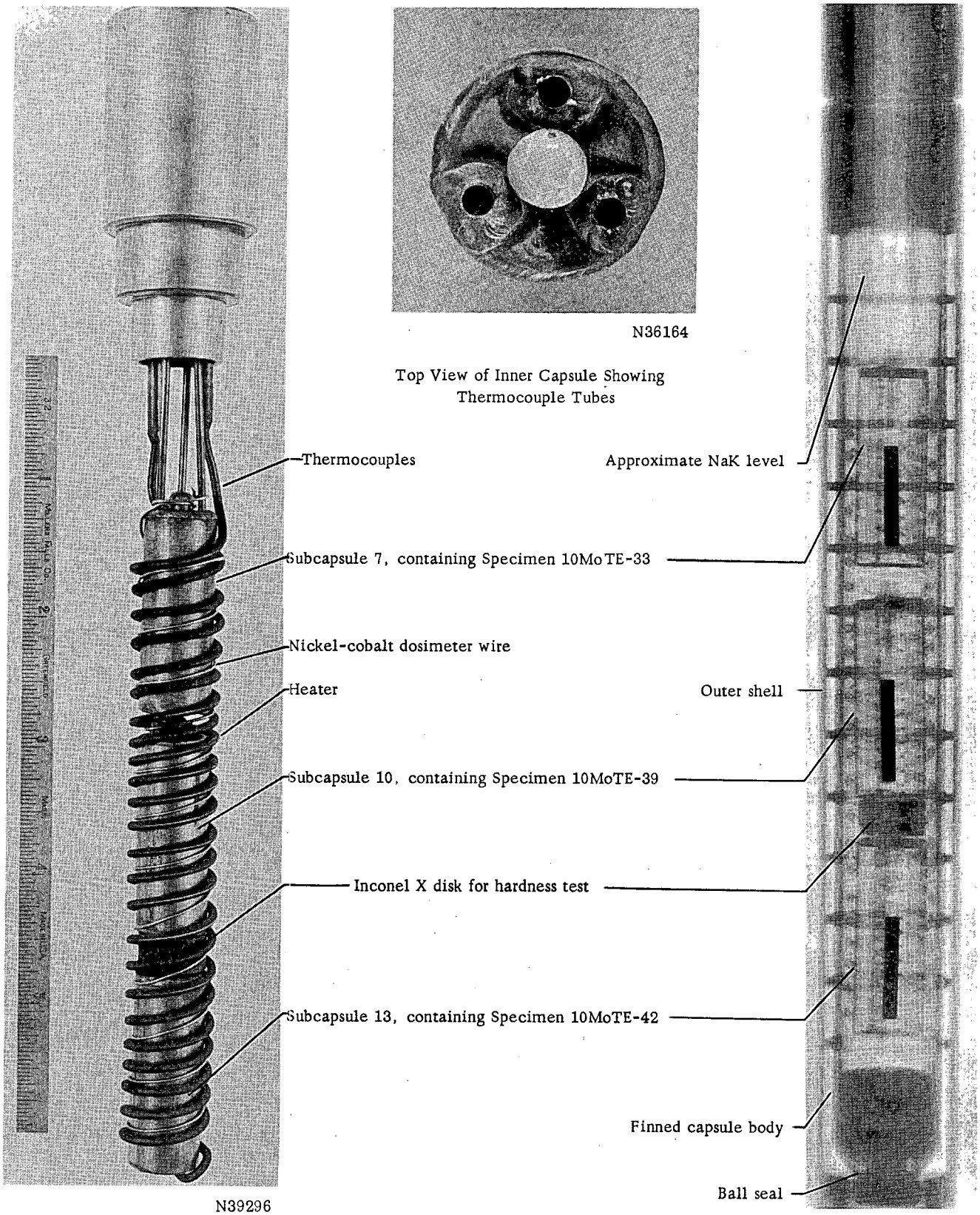

FIGURE 14. PHOTOGRAPH OF SPECIMEN ASSEMBLY AND RADIOGRAPH OF LOADED FINNED-WALL CAPSULE USED IN THE TEMPERATURE-EFFECTS PHASE

Capsule BMI-9-21 is shown.

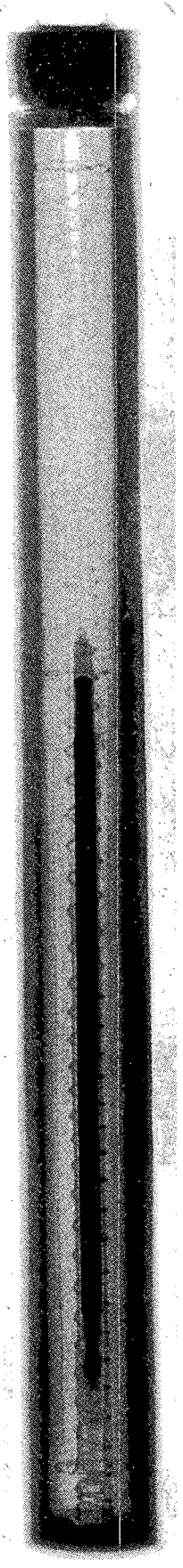

FIGURE 15. X-RAY PHOTOGRAPH OF CAPSULE CONFIGURATION USED IN REFERENCE-DIAMETER PHASE

Capsule BMI-9-32 is shown.

Temperature-Effects Series

Capsules BMI-19, -20, and -21 were of basically similar design. Each contained specimens located within spirally wound zirconium wire baskets in small sealed subcapsules. NaK filled the inner subcapsule cavity, covering the specimen but allowing approximately 20 per cent expansion space within the subcapsule. Each large capsule contained three subcapsules stacked on top of each other and within a spirally wound, externally controlled, 1-kw Kanthal resistance heater. The subcapsules were immersed in NaK to provide an efficient heat-transfer medium. A photograph of the assembled capsule, showing heater and thermocouple placement, and a radiograph of the loaded capsule was shown in Figure 14. Additional information concerning the capsule design employed for this series of experiments has been reported in BMI-APDA-648.

Capsule BMI-9-19 was irradiated in the MTR in Position A-13-SE during MTR Cycles 85 through 91. Reported unperturbed fluxes for this position are 7 and 11 x 10^{13} nv. The irradiation period was 106.1 days, the specimens' surface temperature calculated from thermocouple data during irradiation ranged from 610 to 860 F. Capsule BMI-9-20 was irradiated during MTR Cycles 88 through 94 in Position A-7-SE. The reported unperturbed fluxes for this position were 7 to 7.6 x 10^{13}, with a peak near the center of the hole to about 9.8 x 10^{13} nv. The capsule was in pile during 101.2 days of operation, achieving average surface temperatures calculated from thermocouple data ranging between 1000 and 1140 F. Capsule BMI-9-21 was irradiated during MTR Cycle 88 in MTR Position A-9-SE and during MTR Cycles 89 through 97 in the MTR Position A-9-SW. The reported unperturbed fluxes in this position were between 4.2 and 7.2 x 10^{13} nv. The irradiation period was 145.3 days; the average specimen surface temperature calculated from thermocouple data was about 540 F.

Each large capsule contained a resistance wire-wound heater and three or more thermocouples. The thermocouples were located inside wells adjacent to the specimens, so that each thermocouple monitored the temperature of an individual specimen. The electrical heater of Capsule BMI-9-19 operated during the seven cycles that the capsule was inserted in the MTR, failing near the end of the seventh, or last, cycle. The heater in BMI-9-20 operated for approximately seven cycles; however, the heaters failed during the seventh cycle, and the temperatures obtained thereafter were approximately 450 F lower. The heater in Capsule BMI-9-21 was inoperative during the entire irradiation; although specimen temperatures were recorded by the thermocouples.

On the basis of detailed temperature charts obtained from MTR records, the temperatures shown in Table 5 have been determined for specimens from the three capsules on a cycle-by-cycle basis. Temperatures reported are the calculated maximum surface and center-line temperatures obtained from thermocouple readings. In addition, a continuous temperature record of the three capsules versus operating time above 400 F is shown in Figure 16. The figure shows that the most uniform specimen surface temperature was obtained on Capsule BMI-9-20. Temperature charts were never received from the MTR for Capsule BMI-9-21 for MTR Cycles 88, 89, 90, and 91; consequently, both the irradiation temperature table and the temperature graph of this capsule are incomplete.

The subcapsules did not contain temperature-indicator wires as a means of checking on the temperatures attained during irradiation. However, an indirect indication of the temperature reached in subcapsules from Capsule BMI-9-20 was afforded by the condition of aluminum-0.6 w/o cobalt dosimeter wires placed inside the subcapsule for the

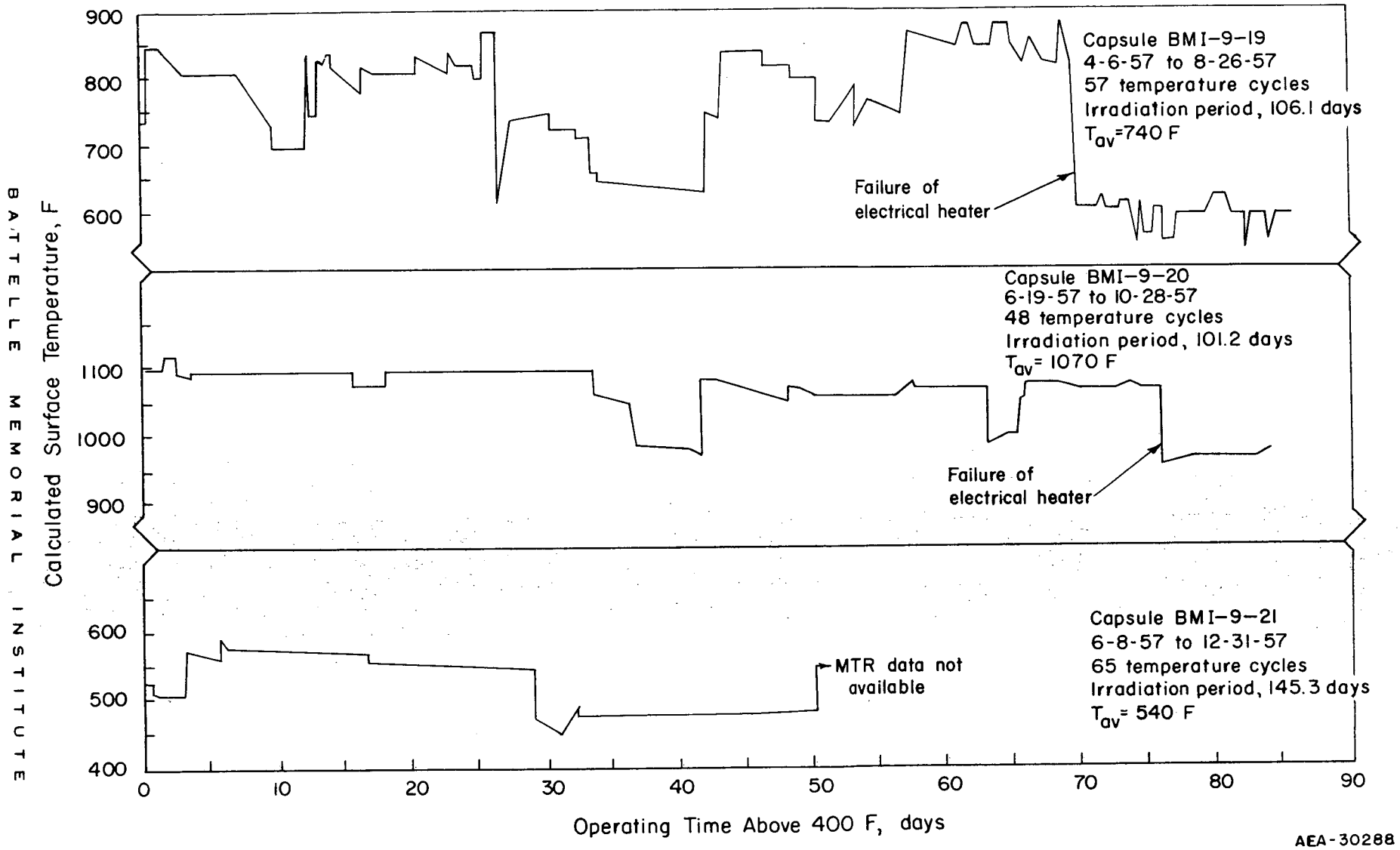

FIGURE 16. SURFACE TEMPERATURES IN INSTRUMENTED CAPSULES VERSUS OPERATING TIME ABOVE 400 F

purpose of neutron-flux monitoring. Upon opening the subcapsules from this capsule, the dosimeter wires were found missing from all of the capsules with the exception of a portion of the wire that was still intact from Specimen 10-MoTE-41. It is believed that the wire from Specimen 10-MoTE-41, and the wires from the other two subcapsules were attacked by the NaK during irradiation at temperatures approaching the melting point of aluminum. Data obtained from dosimeter wires outside the subcapsules were used to calculate the neutron flux incident on the specimens in the Capsule BMI-9-20, as noted later in Table 10.

Reference-Diameter Series

Capsules BMI-9-34 and -35 were irradiated simultaneously in two irradiation positions in the reflector of the MTR. Capsules BMI-9-32 and -33 were irradiated consecutively in the same position as Capsule BMI-9-34 after it was discharged from the reactor.

Capsule BMI-9-32 was positioned in a zone of almost uniform thermal-neutron flux, while the other three capsules experienced extreme flux gradients over their lengths. The flux at the bottom of Capsule BMI-9-32 was about 10 per cent greater than at the top, while fluxes at the bottom of the other three capsules were from three to ten times greater than the flux at the top. The greater fission rate at the bottom of the capsules due to the higher thermal-neutron flux would be expected to cause a greater burnup and higher temperatures near the bottom of the specimens than at the top. However, the only capsule which was equipped with thermocouples for temperature measurement (Capsule BMI-9-32) experienced a very small flux gradient and the effect of the slightly higher fission rate at the bottom was not observed in the data obtained from the thermocouples.

The thermocouples in Capsule BMI-9-32 were positioned at approximately equal intervals along the length of the specimen and were held against the outside of the zirconium basket by one wire ring near the top of the specimen. The hot junctions of the thermocouples were nominally 0.173 in. from the center line of the specimen. However, because the thermocouples were restrained only at one point, it is possible that vibration caused by the flow of the cooling water past the capsule may have caused a variation in the position of the hot junction by as much as ±0.030 in. The uncertainties in the recorded temperature caused by the possible movement of the thermocouples together with the normal uncertainties associated with these thermocouples when operating at near 930 to 1110 F require the application of a 150 F tolerance to the recorded temperature.

The thermocouple data recorded during the three irradiation cycles are presented in Figures 17, 18, and 19. Figure 20 graphically presents the average temperature recorded by each thermocouple for each of the three irradiation cycles.

The recorded temperatures at the thermocouple along with the calculated specimen surface and center temperatures are summarized in Table 6. Calculated heat generation rates and fuel burnups are also included. Burnup, heat-generation, and temperature data for Capsule BMI-9-33 are included in Table 7. Several methods for determining specimen burnup and irradiation temperatures were available. Two methods involved calculations based upon available flux data. One of these methods employed reactor-quoted flux information and the other used flux data obtained from the analyses

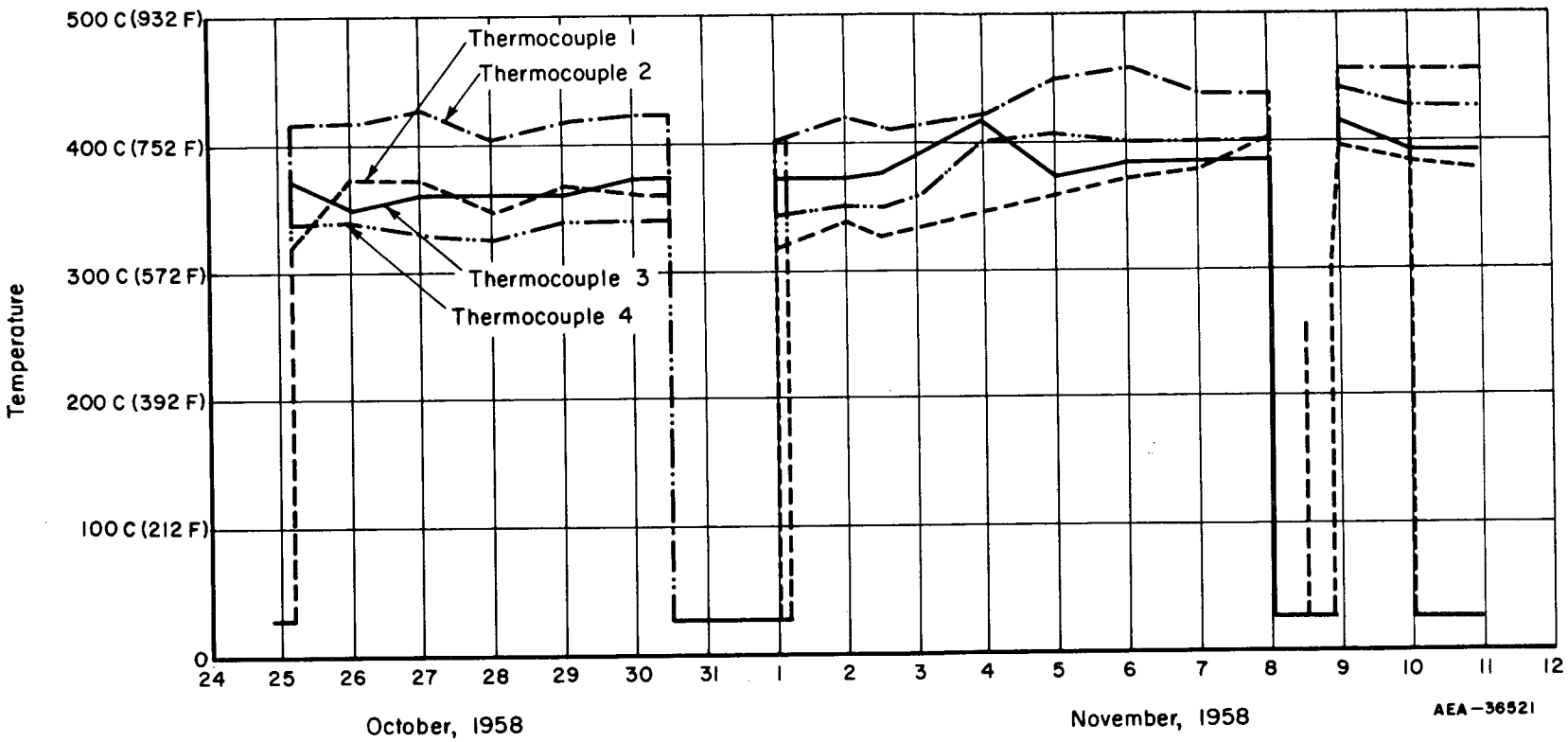

FIGURE 17. MEAN IRRADIATION TEMPERATURES RECORDED BY THERMOCOUPLES IN CAPSULE BMI-9-32 DURING MTR CYCLE 112

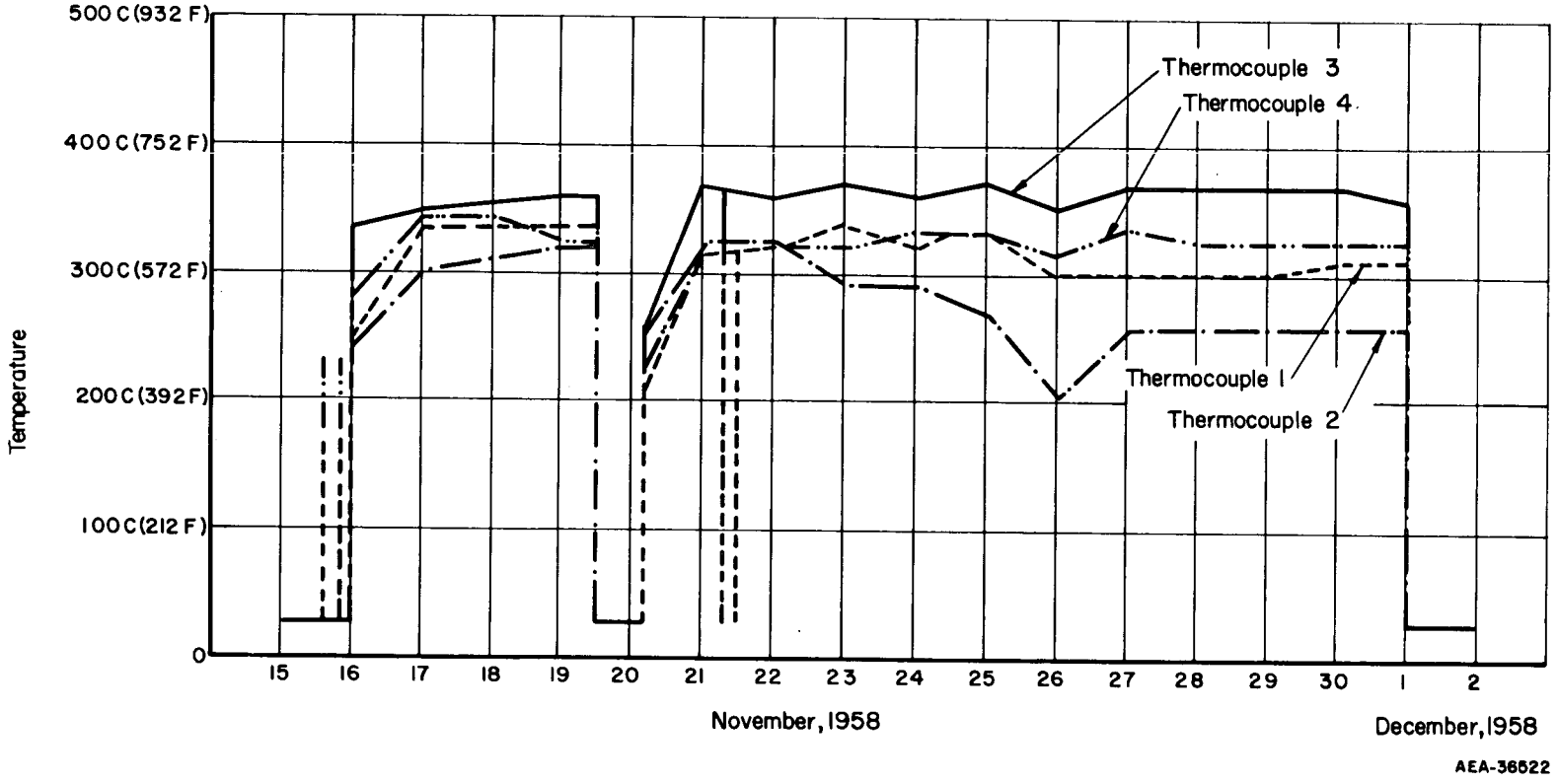

FIGURE 18. MEAN IRRADIATION TEMPERATURES RECORDED BY THERMOCOUPLES IN CAPSULE BMI-9-32 DURING MTR CYCLE 113

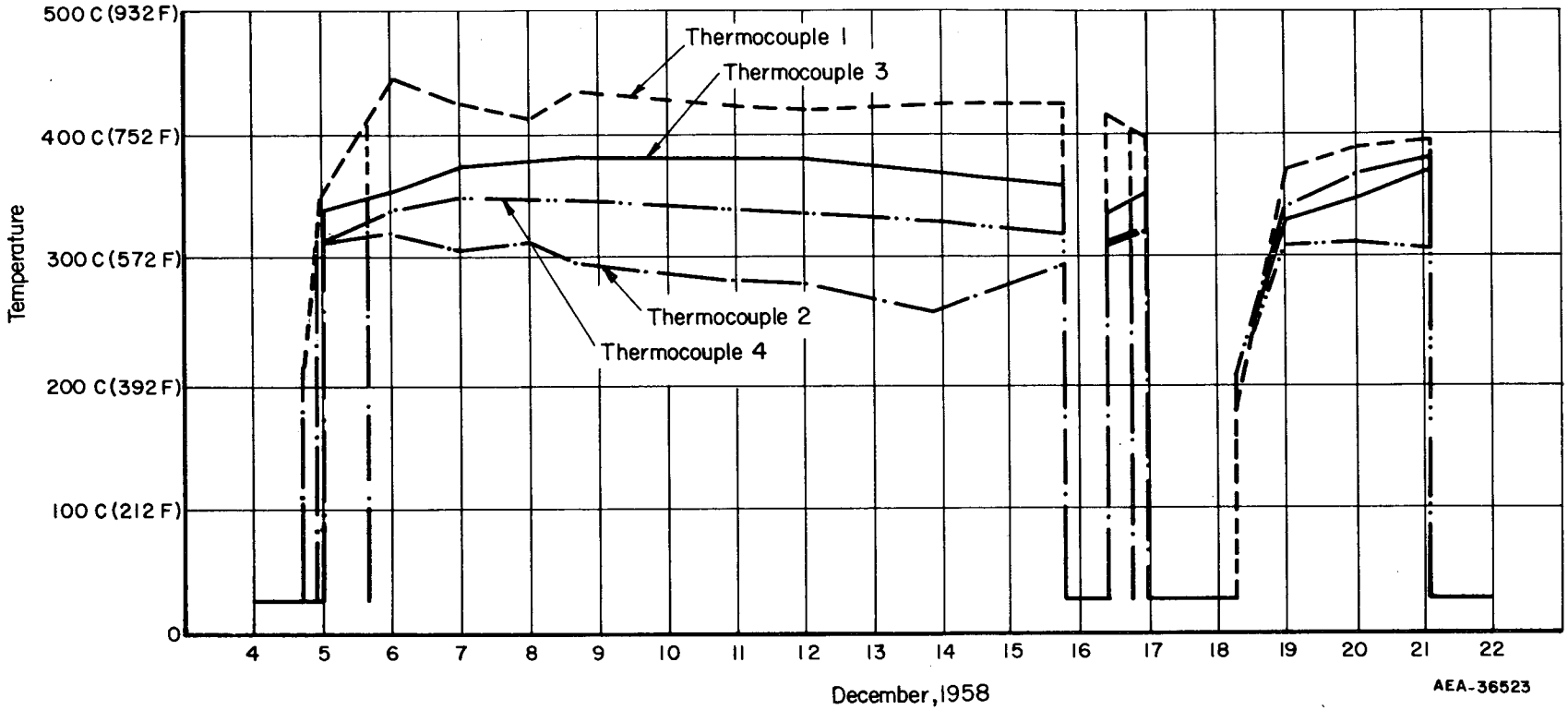

FIGURE 19. MEAN IRRADIATION TEMPERATURES RECORDED BY THE THERMOCOUPLES IN CAPSULE BMI-9-32 DURING MTR CYCLE 114

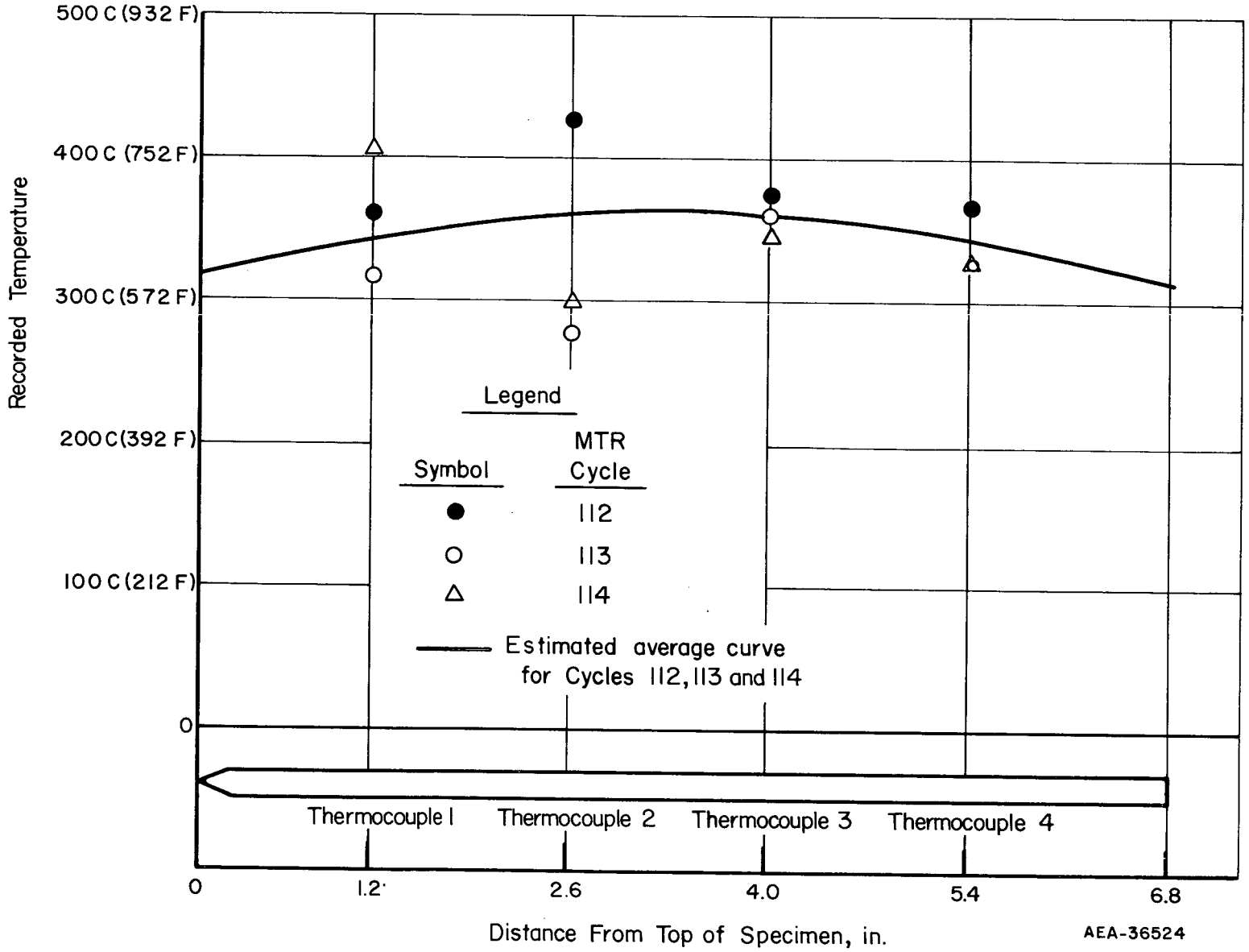

FIGURE 20. AVERAGE TEMPERATURES RECORDED BY THERMOCOUPLES DURING IRRADIATION OF CAPSULE BMI-9-32

of dosimeters irradiated adjacent to the specimens. A third method was based upon the results of burnup analyses performed on a section of the irradiation specimen. The last two methods, often referred to as heat-meter techniques, employ temperature data obtained during irradiation from thermocouples. One of these last two methods requires the additional knowledge of the reactor coolant temperature while the other employs flux data obtained from dosimetry. All five methods have certain accuracy limits due to the necessity of assuming various nuclear and thermal properties of the fuel material and the irradiation capsule.

Calculations based upon reactor-quoted flux are considered the most inaccurate and were not considered in the analyses of the results of this experiment. The radiochemical analyses of sections of the irradiated specimens are considered to be the most accurate means of determining the radiation conditions, provided a representative sample can be obtained. However, this method was not employed in this case because the poor condition of the specimens indicated the probable loss of fission products from the fuel material and thus the inability to obtain a representative sample. The remaining three methods were employed to calculate the most probable irradiation conditions.

The conditions experienced during irradiation by Specimn 10-1 as determined by the three methods are presented in Table 6. The average temperatures presented are the weighted average temperatures for the three irradiation cycles. The maximum temperatures indicated in the table are the maximum temperatures experienced during any of these irradiation cycles. The data indicate that although the average temperatures recorded by all four thermocouples were about the same, the maximum temperatures recorded by Thermocouples 1 and 2 were somewhat greater than those recorded by Thermocouples 3 and 4. Examination of the thermocouple recorder charts indicated that the temperatures recorded by Thermocouples 1 and 2 were much more erratic than those recorded by Thermocouples 3 and 4.

An arbitrary criterion was defined to study the behavior of the thermocouples during irradiation. A term called the "temperature variation" was defined as being "the maximum excursion in the recorded temperature during any 5-min period". Table 8 presents the temperature variations of each thermocouple for each irradiation cycle. The daily maximum average temperature variation presented in the table is the average of the maximum temperature variations recorded during each day of irradiation. In general, the maximum temperature variation recorded during each day was repeated several times during the day. The cycle maximum temperature variation is the maximum temperature variation recorded during each cycle. The maximum temperature variation recorded during each cycle usually occurred several times during only one day of the irradiation cycle. The temperature-variation data presented in Table 8 indicate that Thermocouples 1 and 2 behaved more erratically than Thermocouples 3 and 4. This agrees with the data presented in Table 6. The erratic behavior exhibited by Thermocouples 1 and 2 could have been caused by bad thermocouple junctions, or by movement of the thermocouples with respect to the specimen.

Estimated surface and center-core temperature curves are presented in Figures 21 and 22, respectively. The curves were prepared employing the data recorded by Thermocouples 3 and 4, and extrapolating to the ends of the specimen. The burnups calculated by the heat-meter technique and from data obtained from dosimeter analyses agree within the tolerance limits of the required thermal- and nuclear-property assumptions, Table 6. The burnup calculated from data recorded by Thermocouple 4 is lower than the burnup calculated from data recorded by Thermocouple 3 or dosimeter data.

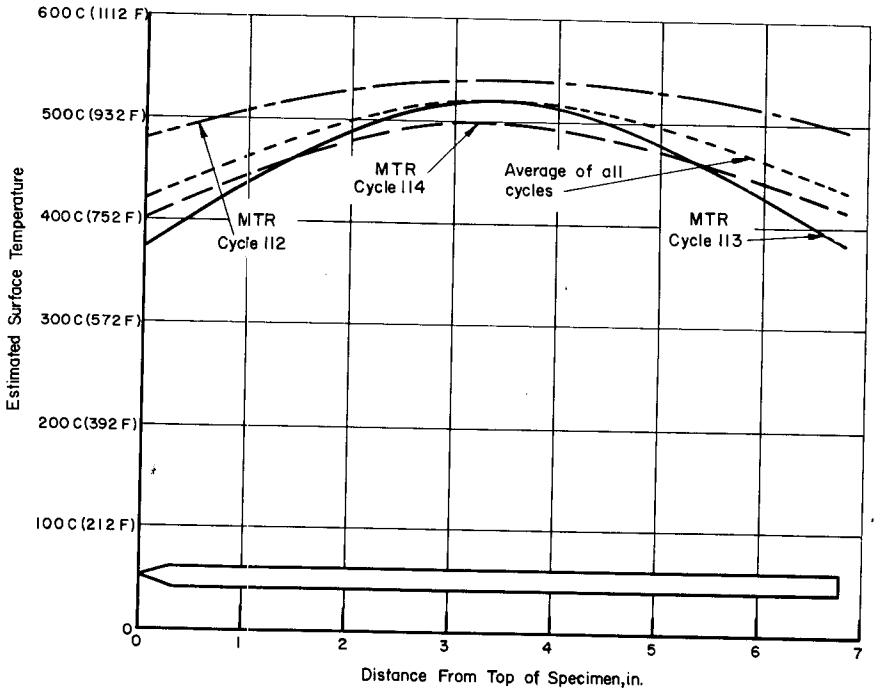

FIGURE 21. ESTIMATED AVERAGE SURFACE TEMPERATURE OF SPECIMEN 10-1, CAPSULE BMI-9-32, DURING EACH MTR IRRADIATION CYCLE

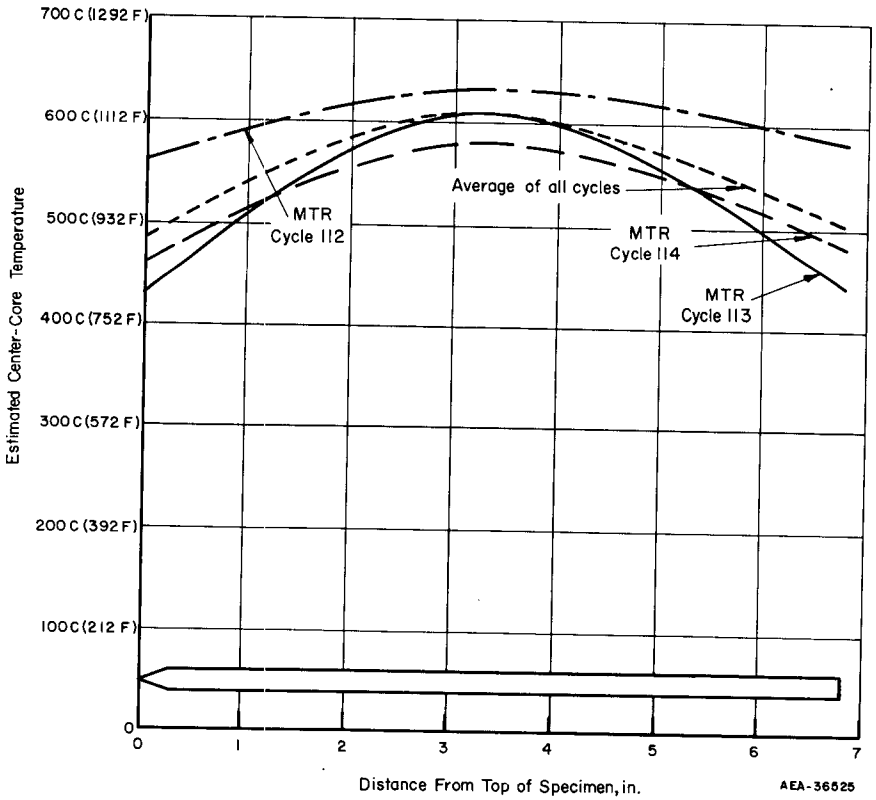

FIGURE 22. ESTIMATED AVERAGE CENTER-CORE TEMPERATURE OF SPECIMEN 10-1, CAPSULE BMI-9-32, DURING EACH MTR IRRADIATION CYCLE

However, the temperatures recorded by Thermocouple 4 appear to be influenced by thermal end effects and thus the indicated burnup would be lower at the end than at the center even though the burnup would normally be expected to be greater at the end due to nuclear end effects. The average specimen burnup is estimated to be 0.78 total per cent ±10 per cent and the average midlength center-core temperatures during irradiation are estimated to have been 1170, 1130, and 1080 F for MTR Cycles 112, 113, and 114, respectively. However, during short periods of time, temperatures as high as 1400 F may have been attained.

Postirradiation Examination of Specimens

The postirradiation examination of the fuel specimens involved several different operations: sampling the capsule for fission gas; opening the capsule for recovery of the specimens; visual inspection of the specimens; preparation of stereomacrographs; measurements of dimensions and density; analysis of neutron-dosimeter wires; radiochemical analyses to determine specimen burnup; metallographic examinations. The experimental details of these operations are discussed separately below.

Fission-Gas Analysis

Fission gases released from the specimens during irradiation were accumulated in the gas-expansion space provided in the capsules. A hole was punched in selected capsules after irradiation and the gases were collected in an evacuated manifold. Small aliquots of the gas were then analyzed with a gamma-ray spectrometer. The intensity of the characteristic 0.52-Mev gamma ray emitted during the radioactive decay of krypton-85 was measured in each aliquot and the data used to calculate the total quantity of krypton-85 released from the specimen during irradiation. A complete description of the analytical techniques and the necessary calculations was included in the report BMI-APDA-625.

The fission gas released from specimens irradiated in Capsules BMI-9-1, -2, -3, -4, -12, -13, -19, -20, and -21, was collected and analyzed. The results are included in Table 9.

Capsule Opening

The ends of the capsules were cut off with a pipe cutter exposing the NaK capsule coolant and the specimens. The NaK was reacted with butyl alcohol and the specimens and dosimeters were recovered.

Dosimetry

Each capsule contained at least one aluminum or nickel neutron-dosimeter wire. The wires were prepared with 0.6 w/o cobalt and were generally wrapped around the specimen basket in a spiral fashion in as close proximity to the specimens as possible. After irradiation, the wire was recovered and cut into sections, each section corresponding to the length of one specimen.

The amount of cobalt-60 formed in the wires during irradiation was determined by radiochemical analyses and the data were used to calculate the average neutron flux to which the wire was exposed. The calculated neutron-flux data obtained by dosimetry are presented in Table 10. A complete description of the analytical techniques for examining the dosimeter wires was included in an earlier report, BMI-APDA-625.

Measurement of Physical Dimensions and Relative Density

The physical dimensions of each intact specimen were measured with vernier micrometers after irradiation. Continual measurement of control specimens by different remote manipulator operators has indicated that the dimensions of small specimens can be measured remotely to ±0.0005 in. or better.

The relative density of the irradiated specimens was determined by the difference in weight in air and in carbon tetrachloride at ambient room temperature (68 to 77 F). Experience with this type of measurement indicates that the relative density of small (about 0.2 cm^3 volume) specimens can be measured to within ±0.03 density unit.

All measurements were designed to duplicate the preirradiation measurements as closely as possible. The results of the postirradiation measurements were included in Table 2. The changes occurring in the density and dimensions of the specimens as a result of the irradiation are included in Table 11 along with the burnup and irradiation temperature data.

Visual Examination of Specimens

All of the specimens were examined stereoscopically at magnifications up to 32X as they were removed from the capsules. Photographs were made of each specimen showing its general condition and any unusual defects, Figures 23 through 45.

Measurement Of Linear Thermal Expansion

The linear thermal expansion of both irradiated and unirradiated specimens was measured at temperatures up to 1472 F. The measurements were performed with a quartz vacuum dilatometer. The specimens were positioned between two quartz rods in the furnace vacuum chamber. As the temperature was gradually increased (about 37.4 F per min), the expansion of the specimen was measured with a dial gage attached to one end of the quartz rods.

The unirradiated control specimens of the reference alloy were given two thermal cycles to 1472 F. The use of two cycles is normal procedure in such measurements, since it has been observed that metal specimens seem to "settle down" after the first run and produce smoother heating and cooling curves. It was observed that the control specimens were reduced slightly in length with a negligible change in density after the thermal cycles. The electrical-resistivity measurements indicated that some transformation had occurred. The density and electrical resistivity of the control specimens prior to the dilation measurements were estimated from data obtained from numerous

specimens of this type. Data concerning the changes in physical properties of the specimens as a result of the thermal-expansion measurements are included in Table 12.

The dilation curves for the unirradiated control specimens are shown in Figures 46 and 47. The heating and cooling curves for both specimens are smooth without any major changes in slope. The point at which transformation from the gamma to the alpha-plus-delta phase occurs is not sharply defined due to the rate of temperature rise (6 F per min) which is sufficiently fast to prevent any measurable degree of transformation of the gamma phase. The mean linear thermal-expansion coefficients were calculated from:

$$\text{Mean linear thermal-expansion coefficient, in. per in.} = \frac{\ell_t - \ell_b}{\ell_b\,(t - b)} \text{ per deg C or F,}$$

where

ℓ_b = specimen length at the base temperature, b

ℓ_t = specimen length at temperature, t.

The calculated coefficients are included in Table 13. The coefficients calculated for a selected range of temperature from both the heating and cooling curves will not be identical unless the heating and cooling curves coincide. The coefficients are actually the slopes of the curves over a particular temperature range.

The mean linear thermal-expansion coefficients of irradiated specimens of the reference alloy are also included in Table 13. The data indicate that the specimens swelled during the one thermal cycle to 932 F which three of the four irradiated specimens received. The swelling appeared to increase with increasing burnup, as evidenced by the density changes. This behavior was the reverse of that of the control specimens. The electrical-resistivity measurements appeared to indicate that more transformation had occurred in the specimen with the highest burnup at 932 F.

The dilation curves for the three irradiated specimens cycled to 932 F are shown in Figures 48, 49, and 50. One of the specimens, 10MoU-24, had been used previously for thermal-conductivity measurements and still had some nickel and tin remaining on one end. These materials had been applied to this specimen as a part of the experimental techniques involved in the thermal-conductivity measurements. The small amount of nickel and tin remaining on the specimen might have affected the dilation data and only the average of one heating and cooling cycle is shown in Figure 47. In general, the curves for all the specimens were rather smooth during cycling to 932 F. In contrast to the unirradiated specimens, the irradiated specimens were longer after the thermal cycling rather than shorter.

One irradiated specimen, HT-7, with a burnup of 1.3 total a/o was cycled to 1472 F. This specimen exhibited a greater elongation and a larger density change than the other specimens. The dilation curve, Figure 51, for this specimen shows an abrupt change in slope at about 1022 to 1112 F. The increase in the rate of dilation at this temperature was probably the result of rapid swelling due to the presence of fission gases in the specimens. It is unlikely that the peculiar configuration of the curve was the result of transformation, since transformation in this material normally produces only a

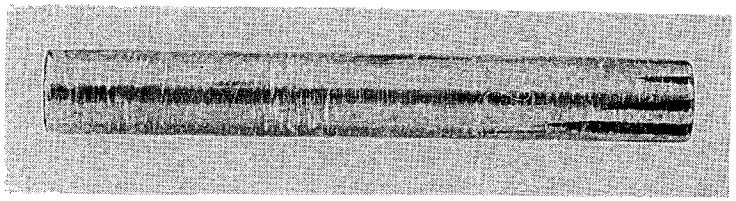

4X Unirradiated RM5918

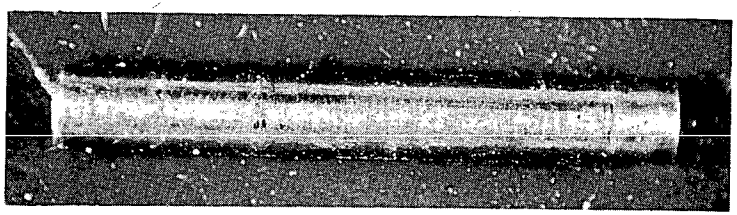

4X Irradiated HC770

a. Specimen HT-4

Burnup: 1.1 total a/o; center-line irradiation temperature: 730 to 810 F.

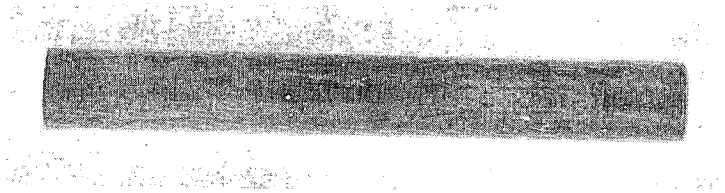

4X Unirradiated RM5906

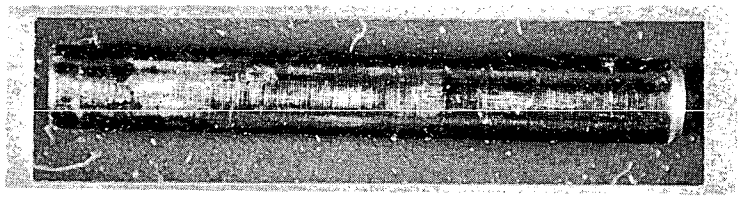

4X Irradiated HC769

b. Specimen HT-1

Burnup: 1.2 total a/o; center-line irradiation temperature: 770 to 860 F.

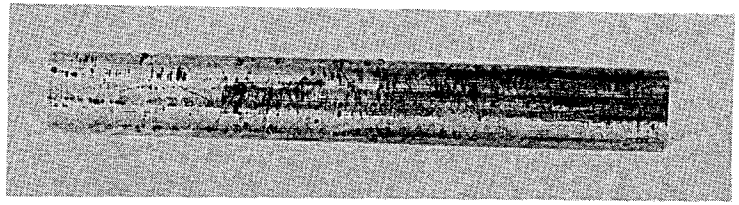

4X Unirradiated RM5930

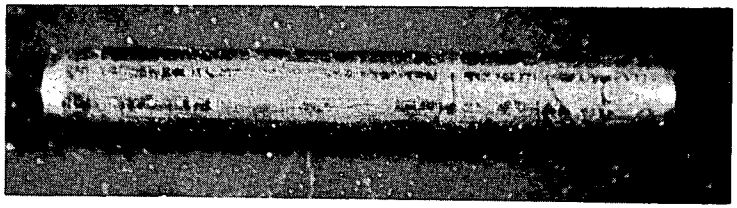

4X Irradiated HC777

c. Specimen HT-7

Burnup: 1.3 total a/o; center-line irradiation temperature: 820 to 920 F.

FIGURE 23. SPECIMENS FROM CAPSULE BMI-9-7 BEFORE AND AFTER IRRADIATION

There was little change in the appearance of the specimen surface.

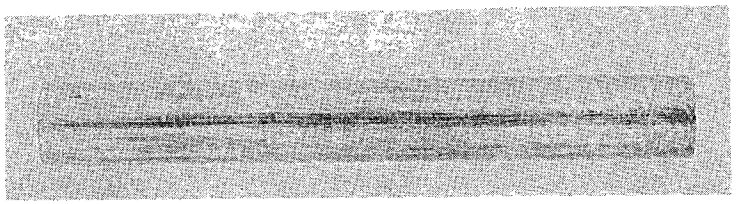

4X Unirradiated RM5922

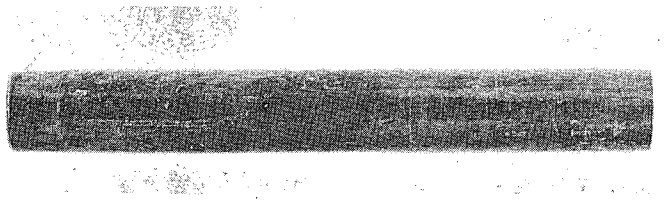

4X Unirradiated RM5910

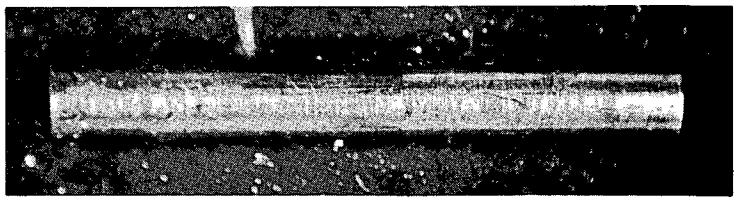

4X Irradiated HC785

a. Specimen HT-5

Burnup: 1.6 total a/o; center-line irradiation temperature: 880 to 1000 F.

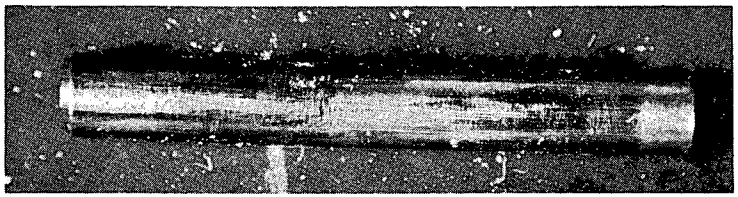

4X Irradiated HC778

b. Specimen HT-2

Burnup: 1.6 total a/o; center-line irradiation temperature: 880 to 1000 F.

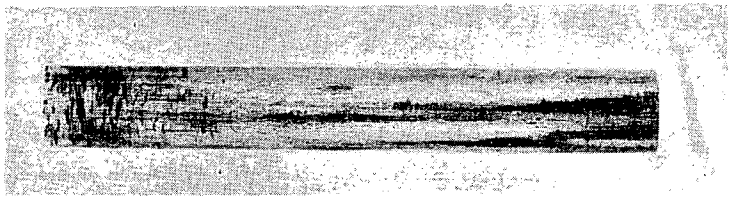

4X Unirradiated RM5934

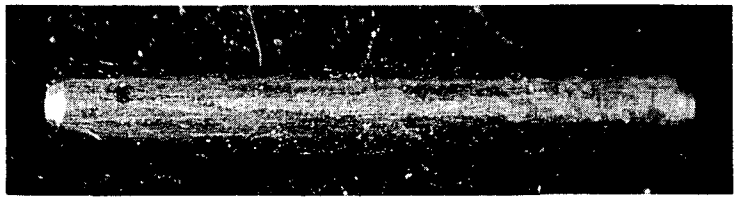

4X Irradiated HC786

c. Specimen HT-8

Burnup: 1.6 total a/o; center-line irradiation temperature: 880 to 1000 F.

FIGURE 24. SPECIMENS FROM CAPSULE BMI-9-8 BEFORE AND AFTER IRRADIATION

There was little change in the appearance of the specimen surface.

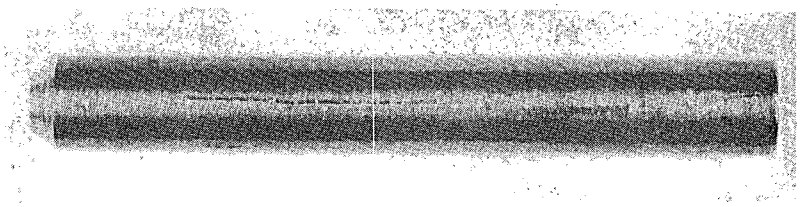

5X Unirradiated RM4418

a. Specimen 10MoU-20

Burnup: 2.6 total a/o; center-line irradiation temperature: 2200 F (estimated).

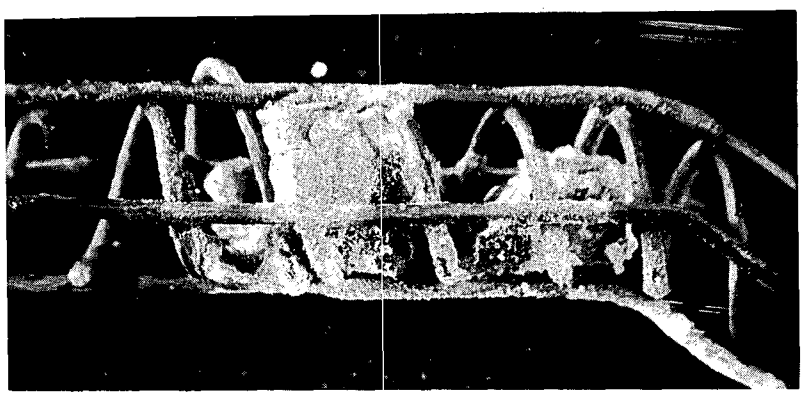

4X Irradiated HC1049

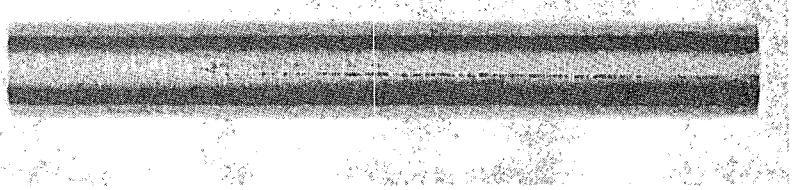

5X Unirradiated RM4423

b. Specimen 10MoU-25

Burnup: 2.6 total a/o; center-line irradiation temperature: 1200 to 1600 F (estimated).

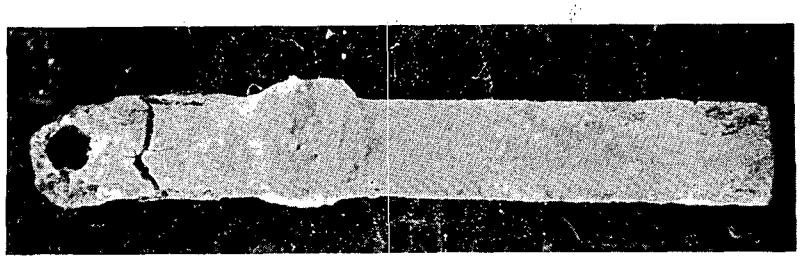

4X Irradiated HC1048

FIGURE 25. SPECIMENS FROM CAPSULE BMI-9-5 BEFORE AND AFTER IRRADIATION

This capsule was irradiated in several locations in the MTR in neutron fluxes as high as 17×10^{13} nv, thus producing center-line temperatures on the order of 1600 F. It is also probable that this capsule was irradiated in an inverted position for at least one MTR cycle, thus allowing Specimen 10MoU-20 to protrude from the NaK and reach melting temperatures (2250 F).

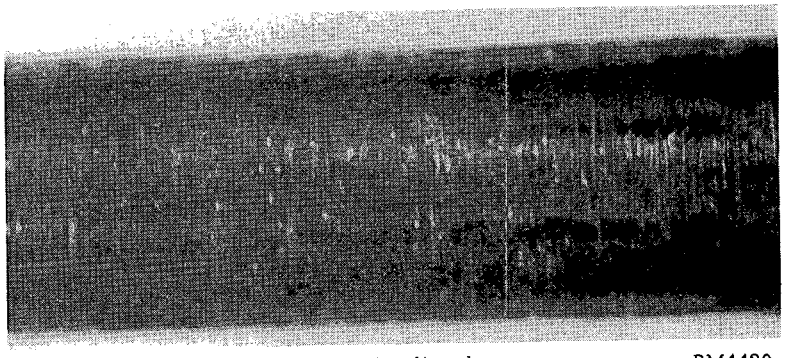

15X Unirradiated RM4430

a. Specimen 10MoU-18

Burnup: 1.9 total a/o; center-line irradiation temperature: 430 to 550 F.

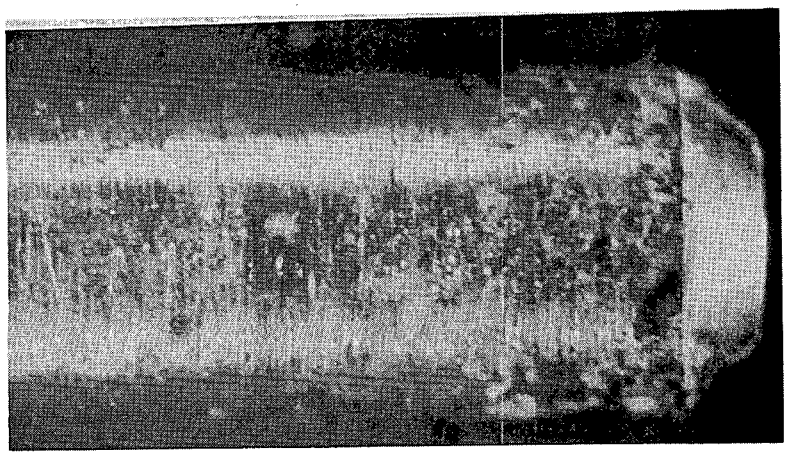

16X Irradiated HC1101

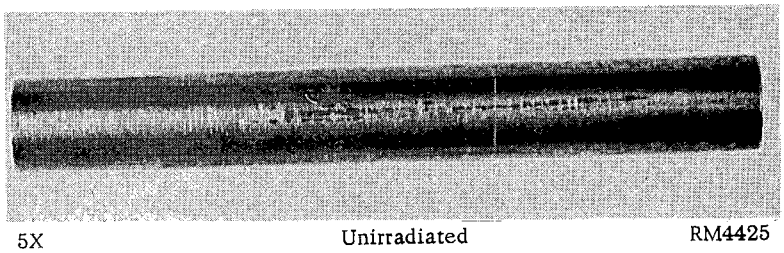

5X Unirradiated RM4425

b. Specimen 10MoU-27

Burnup: 1.7 total a/o; center-line irradiation temperature: 420 to 530 F.

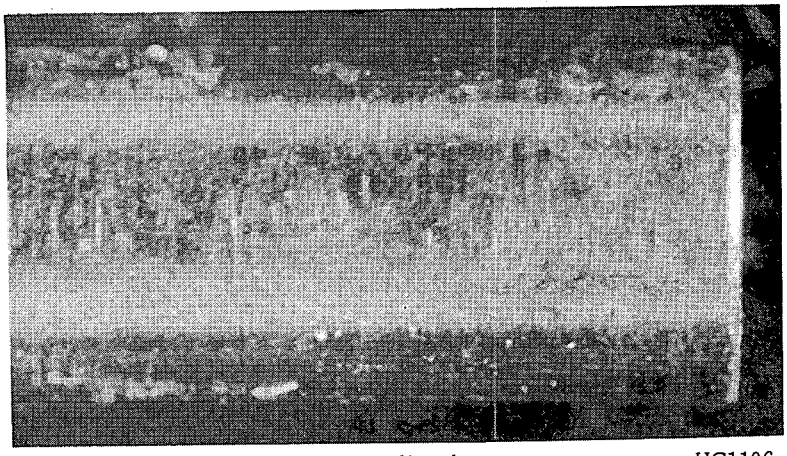

16X Irradiated HC1106

FIGURE 26. SPECIMENS FROM CAPSULE BMI-9-12 BEFORE AND AFTER IRRADIATION

There was little noticeable change in the specimens.

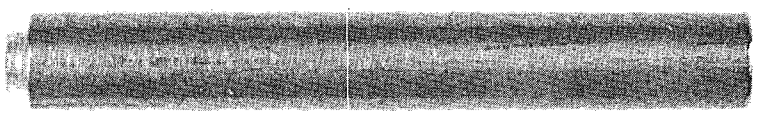

5X Unirradiated RM4419

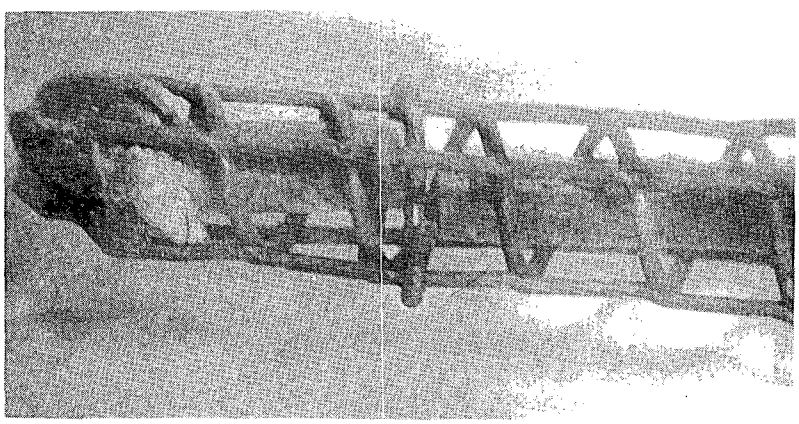

4X Irradiated HC1928

a. Specimen 10MoU-21

Burnup: 5 total a/o (estimated); center-line irradiation temperature: 1000 to 1500 F (estimated).

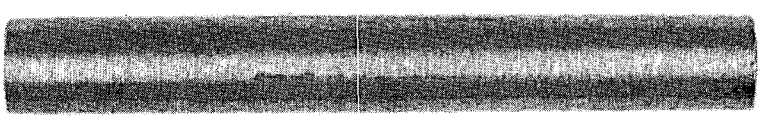

5X Unirradiated RM4426

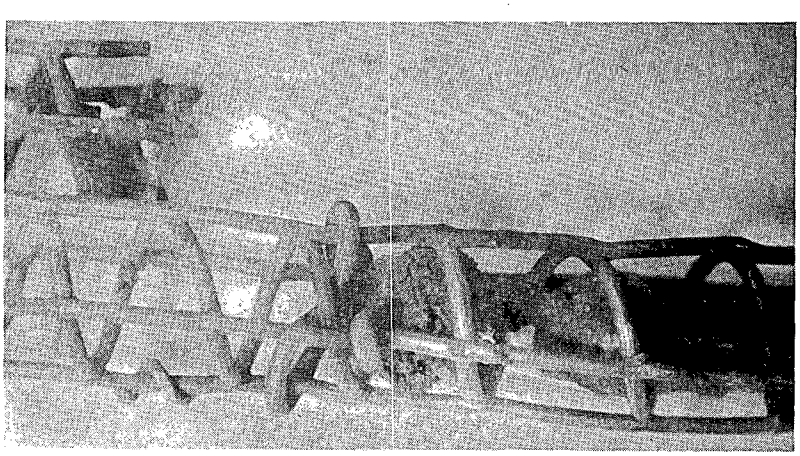

4X Irradiated HC1930

b. Specimen 10MoU-29

Burnup: 5 total a/o (estimated); center-line irradiation temperature: 1000 to 1500 F (estimated).

FIGURE 27. SPECIMENS FROM CAPSULE BMI-9-13 BEFORE AND AFTER IRRADIATION

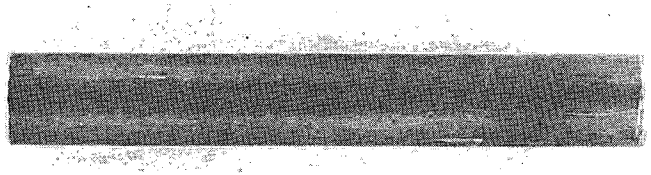

4X Unirradiated RM6223

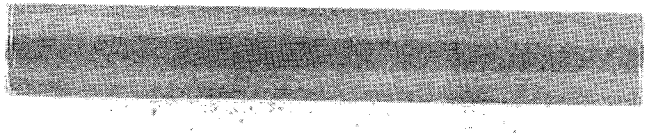

4X Unirradiated RM6215

a. Specimen 11MoCE-6

Burnup: 2.2 total a/o (estimated); center-line irradiation temperature: 1100 to 2100 F (estimated).

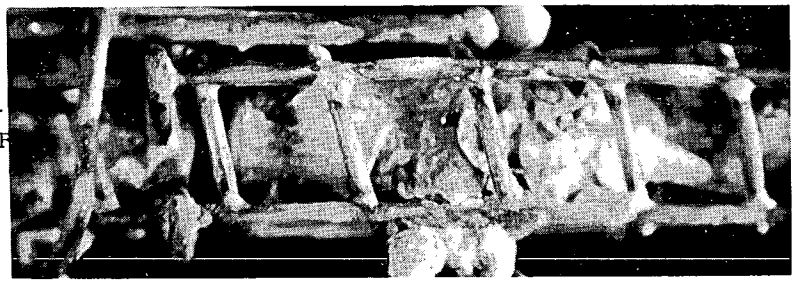

4X Irradiated HC1019

b. Specimen 11MoCE-2

Burnup: 2.2 total a/o (estimated); center-line irradiation temperature: 1100 to 2100 F (estimated).

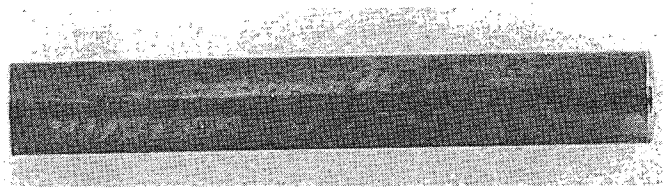

4X Unirradiated RM6199

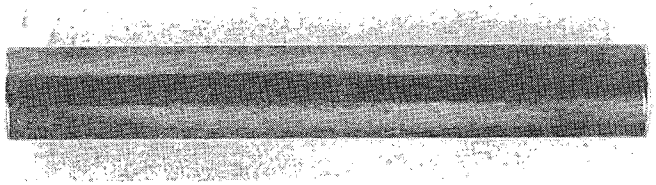

4X Unirradiated RM6207

c. Specimen 9MoCE-4

Burnup: 2.2 total a/o (estimated); center-line irradiation temperature: 1100 to 2100 F (estimated).

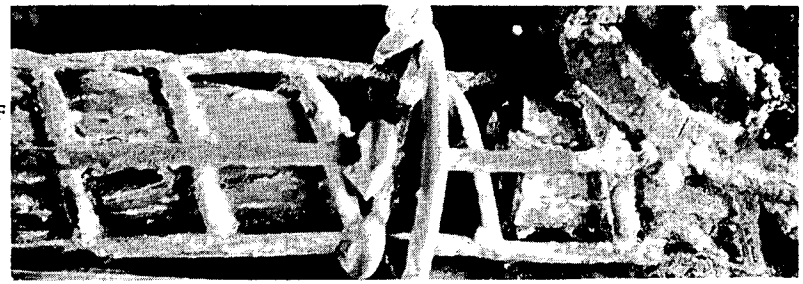

4X Irradiated HC1018

d. Specimen 9MoCE-8

Burnup: 2.2 total a/o (estimated); center-line irradiation temperature: 1100 to 2100 F (estimated).

FIGURE 28. SPECIMENS FROM CAPSULE BMI-9-10 BEFORE AND AFTER IRRADIATION

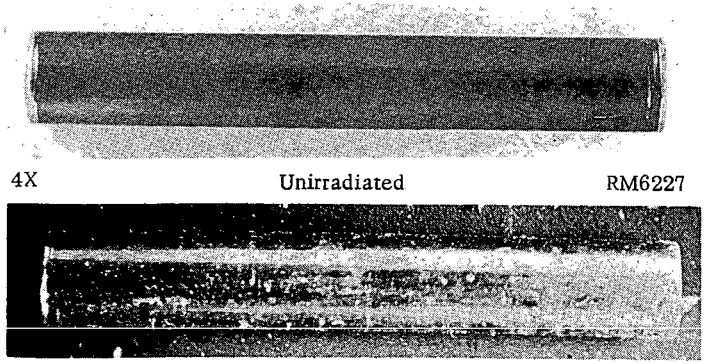

a. Specimen 11MoCE-9

Burnup: 1.1 total a/o; center-line irradiation temperature: 750 to 840 F.

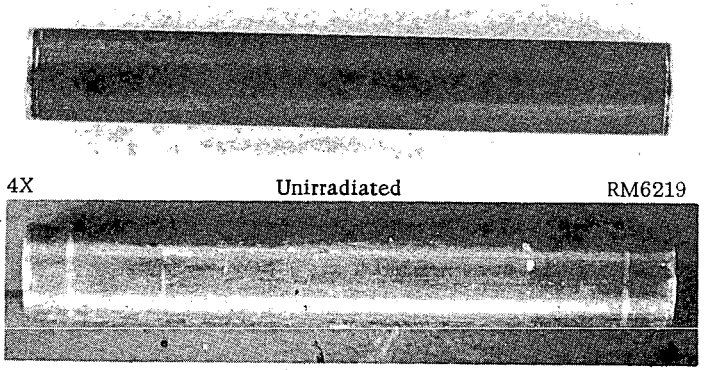

b. Specimen 11MoCE-4

Burnup: 1.2 total a/o; center-line irradiation temperature: 800 to 900 F.

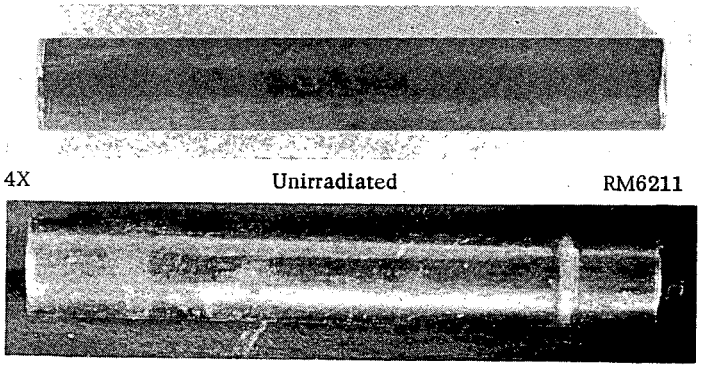

c. Specimen 9MoCE-9

Burnup: 1.3 total a/o; center-line irradiation temperature: 850 to 970 F.

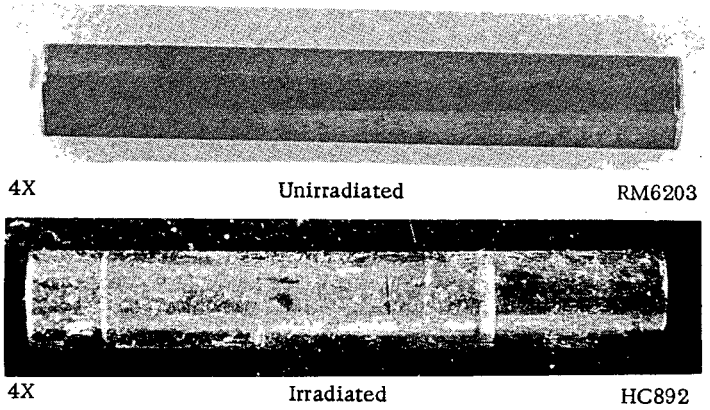

d. Specimen 9MoCE-6

Burnup: 1.4 total a/o; center-line irradiation temperature: 910 to 1040 F.

FIGURE 29. SPECIMENS FROM CAPSULE BMI-9-11 BEFORE AND AFTER IRRADIATION

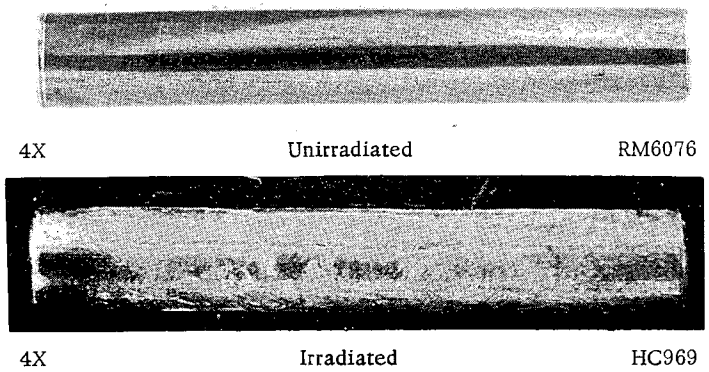

4X Unirradiated RM6076

4X Irradiated HC969

a. Specimen 10CT4-26

Burnup: 3.4 total a/o; center-line irradiation temperature: 1020 to 1440 F.

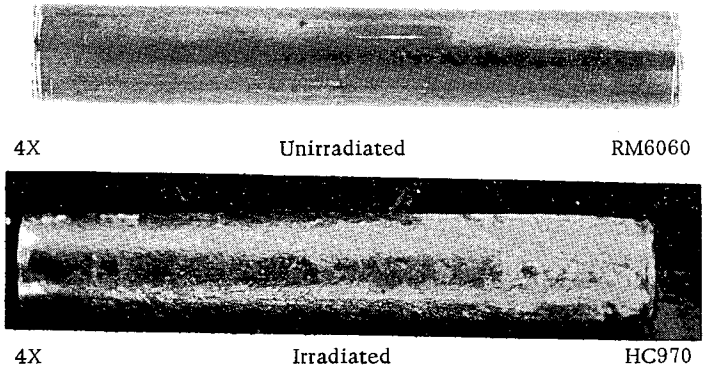

4X Unirradiated RM6060

4X Irradiated HC970

b. Specimen 10CT8-3

Burnup: 2.7 total a/o; center-line irradiation temperature: 860 to 1120 F.

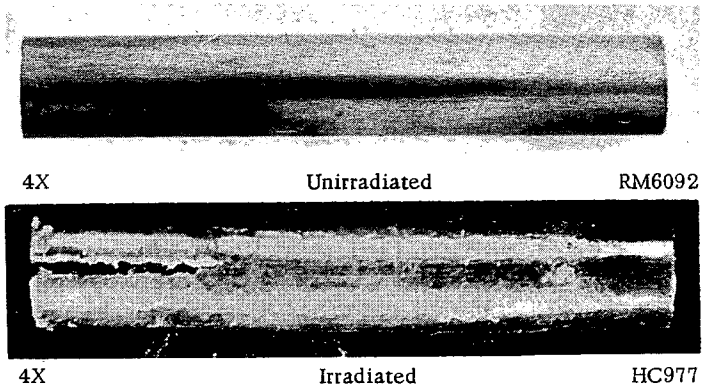

4X Unirradiated RM6092

4X Irradiated HC977

c. Specimen 10CT11-3

Burnup: 3.0 total a/o; center-line irradiation temperature: 930 to 1260 F.

FIGURE 30. SPECIMENS FROM CAPSULE BMI-9-9 BEFORE AND AFTER IRRADIATION

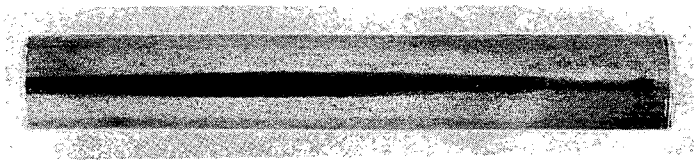

4X Unirradiated RM6072

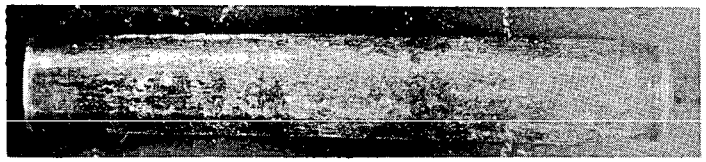

4X Irradiated HC986

d. Specimen 10CT4-25

Burnup: 2.7 total a/o; center-line irradiation temperature: 860 to 1120 F.

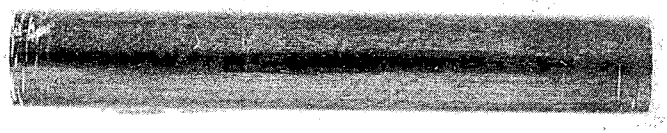

4X Unirradiated RM6056

4X Irradiated HC978

e. Specimen 10CT8-2

Burnup: 2.7 total a/o; center-line irradiation temperature: 860 to 1120 F.

4X Unirradiated RM6088

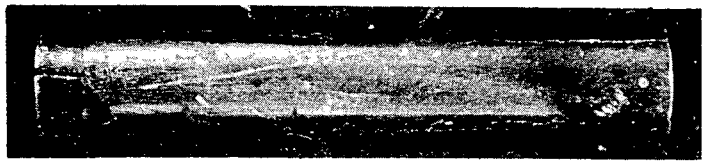

4X Irradiated HC985

f. Specimen 10CT11-2

Burnup: 2.5 total a/o; center-line irradiation temperature: 820 to 1040 F.

FIGURE 30. (CONTINUED)

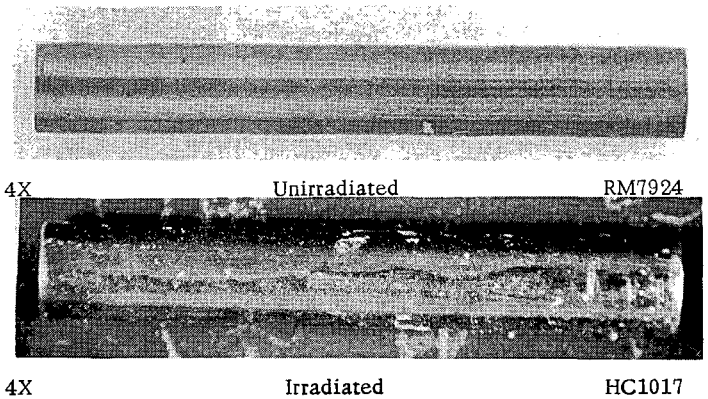

4X Unirradiated RM7924

4X Irradiated HC1017

a. Specimen 10CT4-34

Burnup: 0.70 total a/o (dosimeter test specimen.)

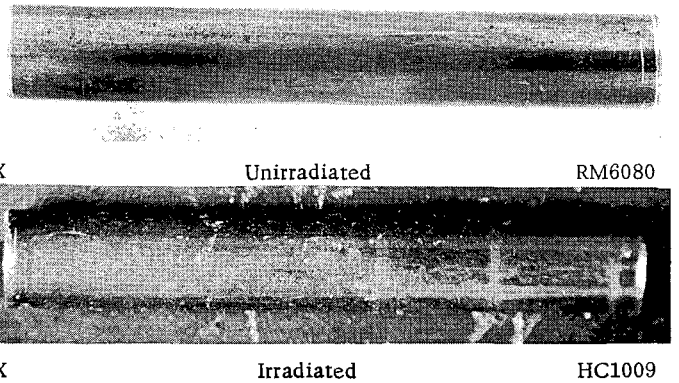

4X Unirradiated RM6080

4X Irradiated HC1009

b. Specimen 10CT4-27

Burnup: 0.45 total a/o; center-line irradiation temperature: 310 to 320 F.

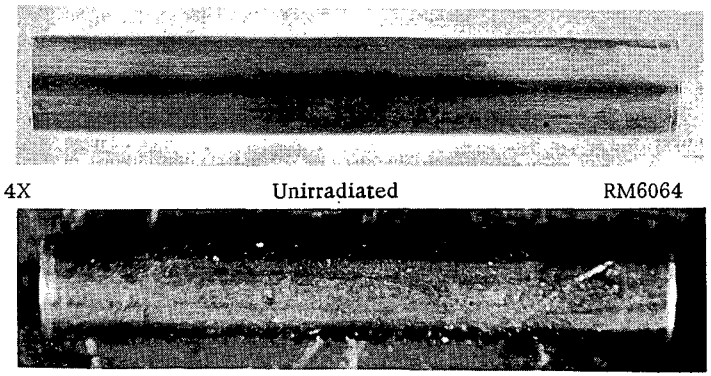

4X Unirradiated RM6064

4X Irradiated HC1002

c. Specimen 10CT8-4

Burnup: 0.54 total a/o; center-line irradiation temperature: 340 to 360 F.

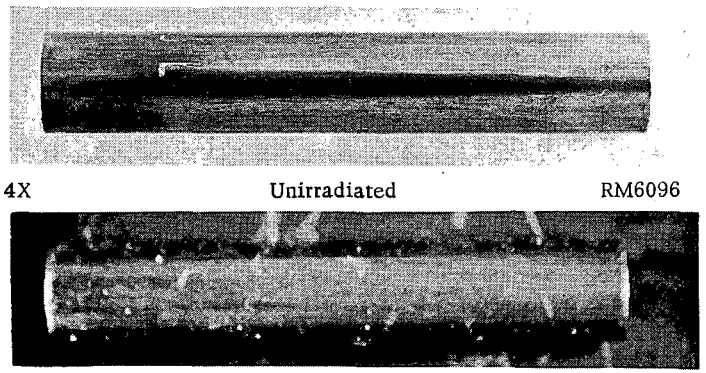

4X Unirradiated RM6096

4X Irradiated HC1010

d. Specimen 10CT11-4

Burnup: 0.92 total a/o; center-line irradiation temperature: 500 to 540 F.

FIGURE 31. SPECIMENS FROM CAPSULE BMI-9-14 BEFORE AND AFTER IRRADIATION

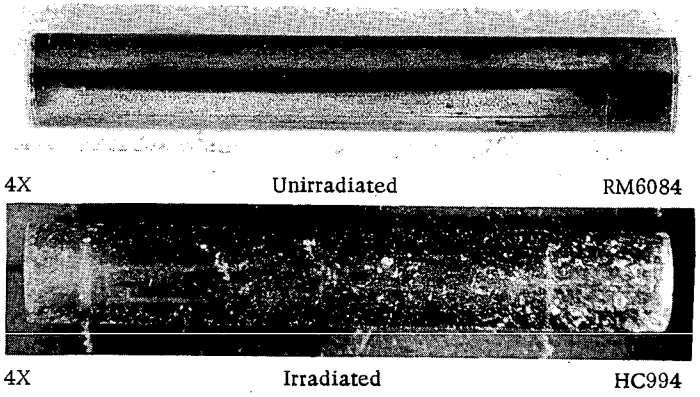

e. Specimen 10CT4-28

Burnup: 1.2 total a/o; center-line irradiation temperature: 590 to 660 F.

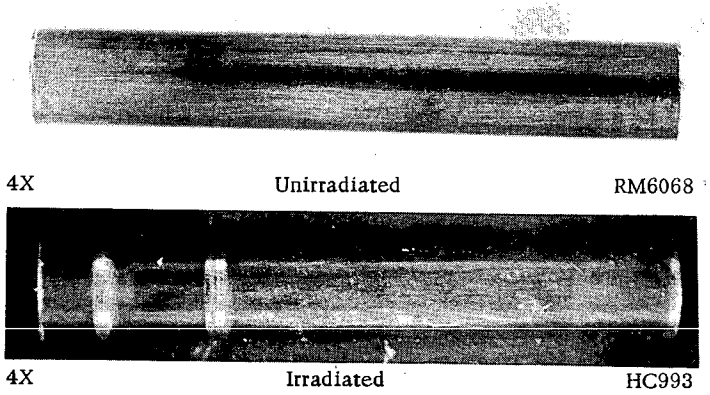

f. Specimen 10CT8-6

Burnup: 1.0 total a/o; center-line irradiation temperature: 540 to 590 F.

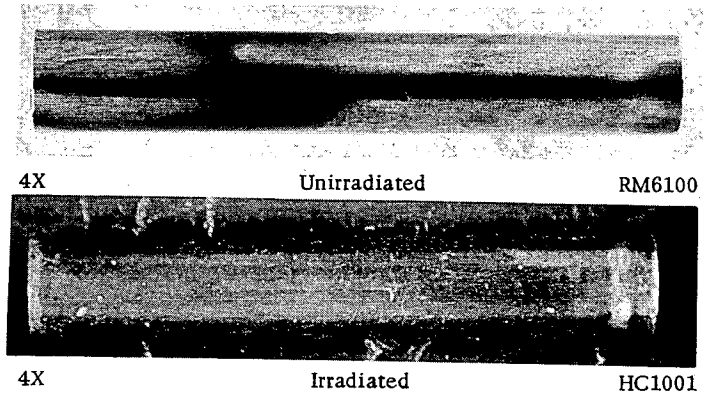

g. Specimen 10CT11-5

Burnup: 1.2 total a/o; center-line irradiation temperature: 610 to 680 F.

FIGURE 31. (CONTINUED)

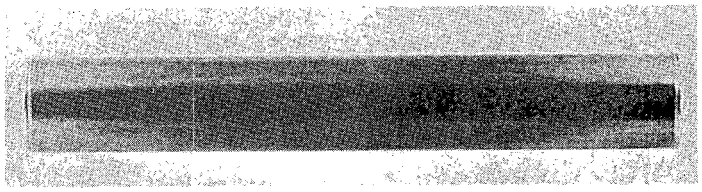

4X Unirradiated RM6243

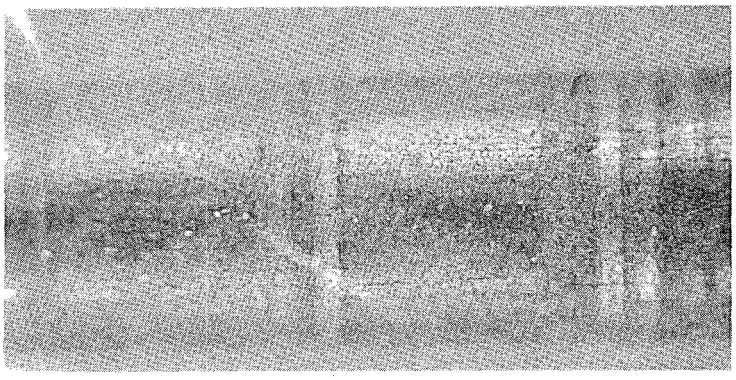

12X Irradiated HC2607

a. Specimen 10MoBH-35

Burnup: 1.9 total a/o; center-line irradiation temperature: 620 to 840 F. Note the circumferential marks apparently due to the specimen contacting the basket.

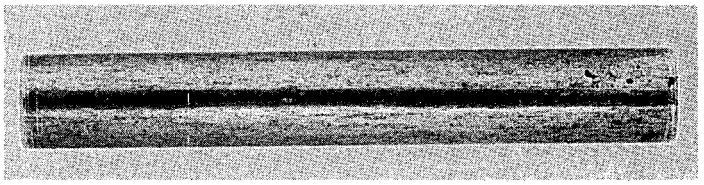

4X Unirradiated RM6738

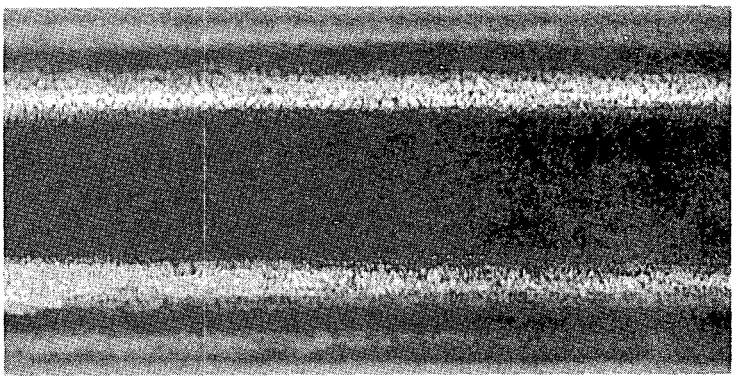

12X Irradiated RM6749

b. Specimen 10MoBH-43

Burnup: 1.9 total a/o; center-line irradiation temperature: 620 to 840 F.

FIGURE 32. SPECIMENS FROM CAPSULE BMI-9-22 BEFORE AND AFTER IRRADIATION

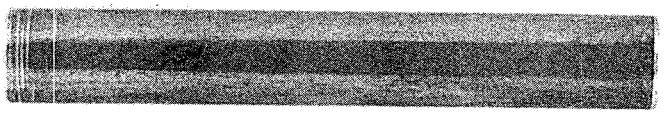

4X Unirradiated RM6247

4X Irradiated HC1931

a. Specimen 10MoBH-37

Burnup: 3.7 total a/o; center-line irradiation temperature: 620 to 920 F (near end of irradiation).

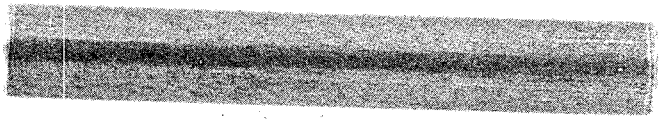

4X Unirradiated RM6739

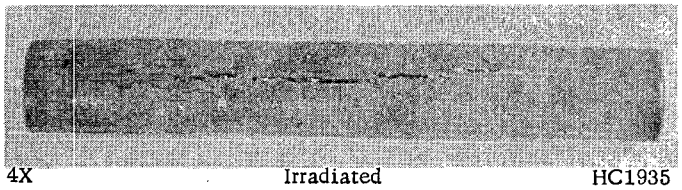

4X Irradiated HC1935

b. Specimen 10MoBH-44

Burnup: 3.9 total a/o; center-line irradiation temperature: 650 to 970 F (near end of irradiation).

FIGURE 33. SPECIMENS FROM CAPSULE BMI-9-23 BEFORE AND AFTER IRRADIATION

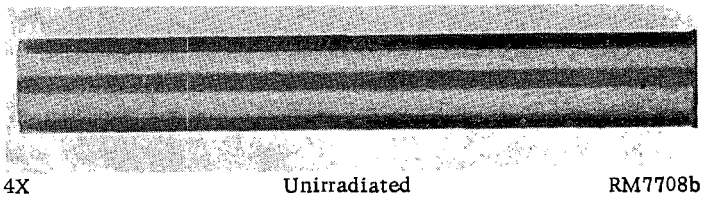

4X Unirradiated RM7708b

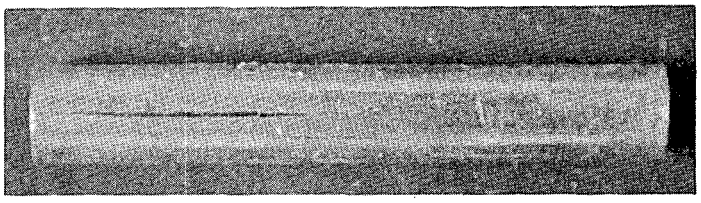

4X Irradiated HC1432

a. Specimen 10MoBH-1B

Burnup: 1.6 total a/o; center-line irradiation temperature: 710 to 730 F.

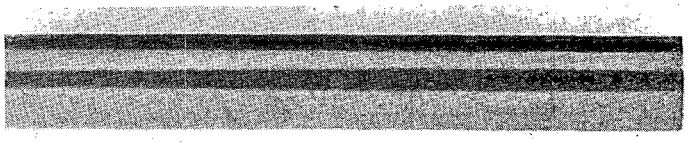

4X Unirradiated RM7708a

b. Specimen 10MoBH-1A

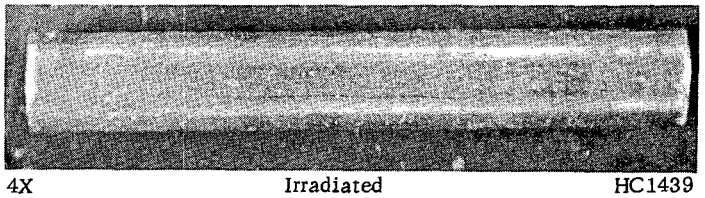

4X Irradiated HC1439

b. Specimen 10MoBH-1A

Burnup: 1.8 total a/o; center-line irradiation temperature: 800 to 820 F.

FIGURE 34. SPECIMENS FROM CAPSULE BMI-9-24 BEFORE AND AFTER IRRADIATION

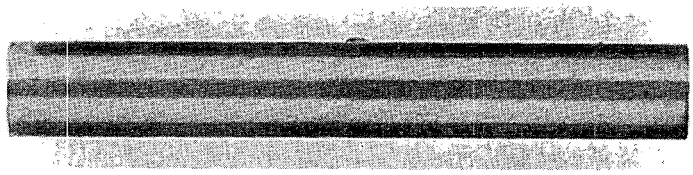

4X Unirradiated RM7708c

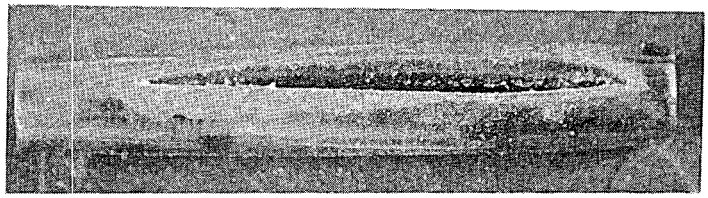

4X Irradiated HC1427

a. Specimen 10MoBH-1C

Burnup: 2.2 total a/o; center-line irradiation temperature: 620 to 790 F.

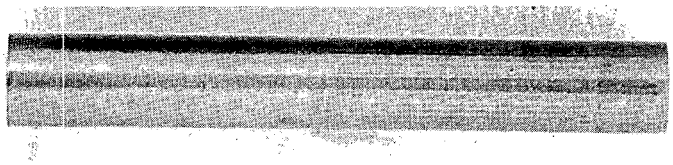

4X Unirradiated RM7708d

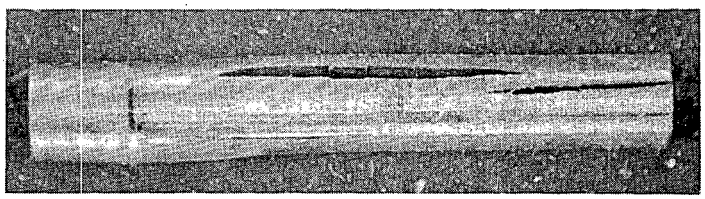

4X Irradiated HC1431

b. Specimen 10MoBH-5

Burnup: 2.3 total a/o; center-line irradiation temperature: 650 to 840 F.

FIGURE 35. SPECIMENS FROM CAPSULE BMI-9-25 BEFORE AND AFTER IRRADIATION

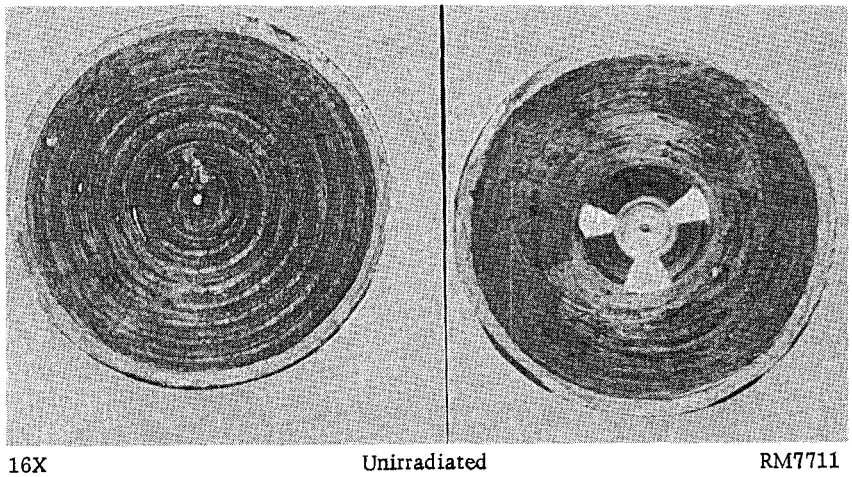

16X Unirradiated RM7711

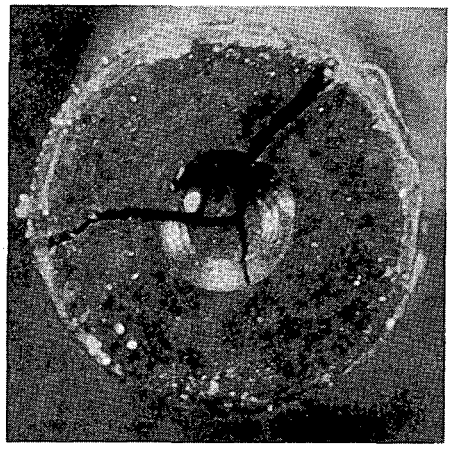

16X Irradiated HC1421

a. Specimen 10MoBH-6

Burnup: 1.4 total a/o; center-line
irradiation temperature: 540 to 610 F.

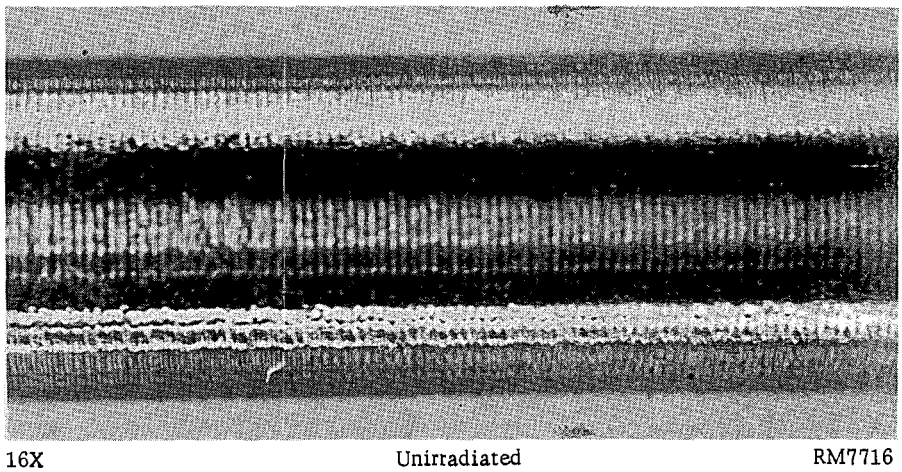

16X Unirradiated RM7716

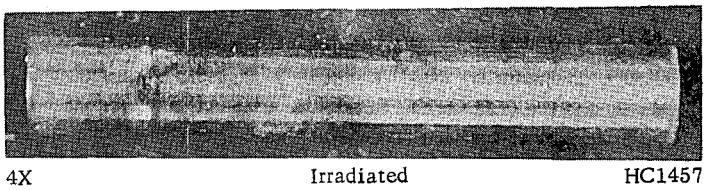

4X Irradiated HC1457

b. Specimen 10MoBH-8

Burnup: 1.6 total a/o; center-line
irradiation temperature: 590 to 680 F.

FIGURE 36. SPECIMENS FROM CAPSULE BMI-9-30 BEFORE AND AFTER IRRADIATION

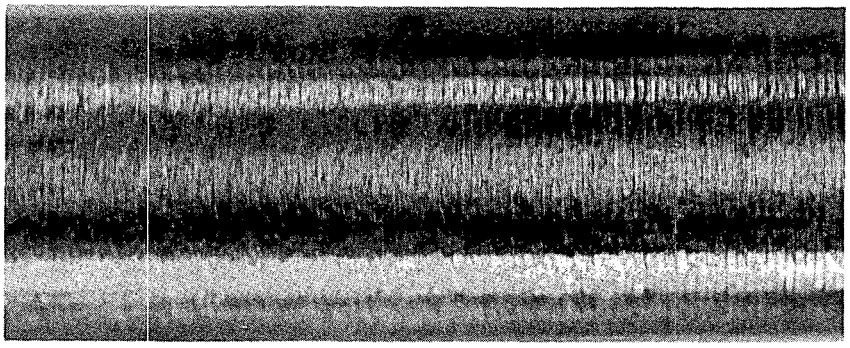

16X Unirradiated RM7925

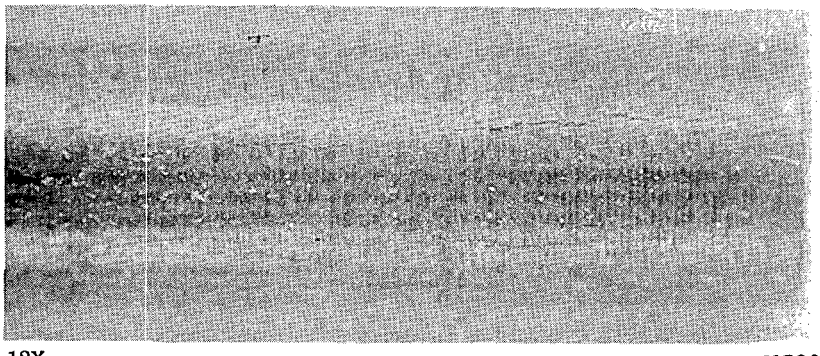

12X Irradiated HC2605

FIGURE 37. SPECIMEN 10MoBH-9 FROM CAPSULE BMI-9-31 BEFORE AND AFTER IRRADIATION

Burnup for this specimen was 2.7 total a/o, center-line irradiation temperature was 720 to 840 F.

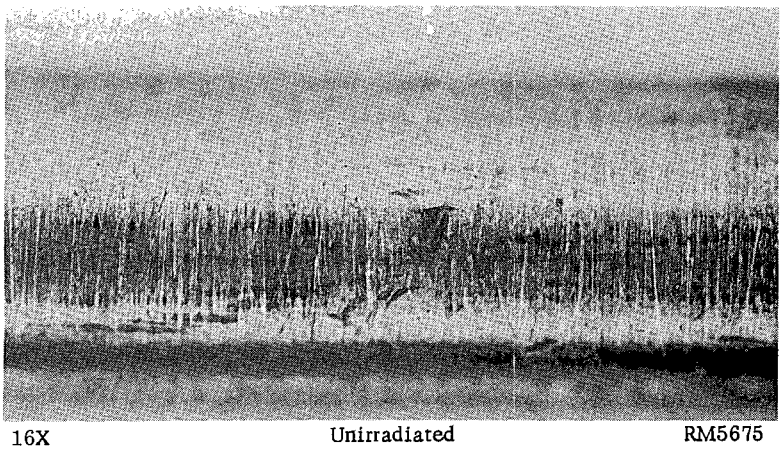

16X Unirradiated RM5675

a. Specimen 10PB-2

Burnup: 3.5 total a/o (estimated); center-line irradiation temperature: 1500 to 2000 F (estimated).

4X Irradiated HC913

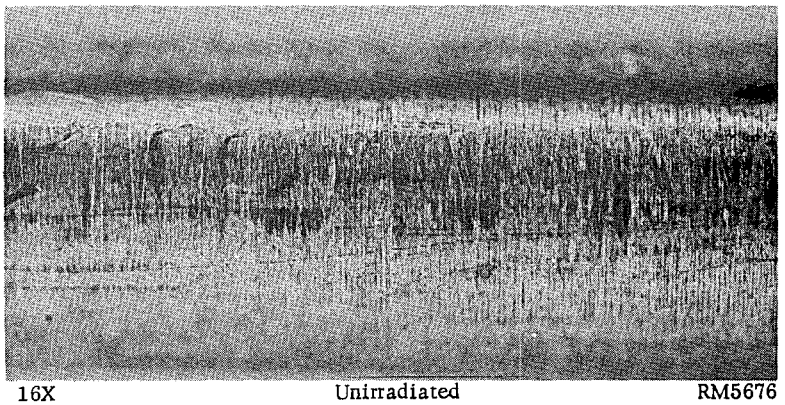

16X Unirradiated RM5676

b. Specimen 10PB-3

Burning: 3.5 total a/o (estimated); center-line irradiation temperature: 1500 to 2000 F (estimated).

6X Irradiated HC915

FIGURE 38. SPECIMENS FROM CAPSULE BMI-9-6 BEFORE AND AFTER IRRADIATION

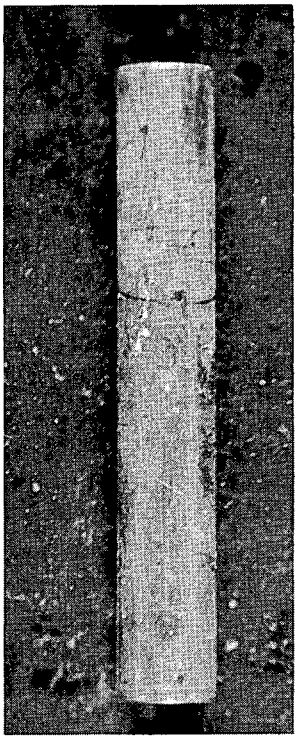

4X HC1132

Specimen 10MoTE-30

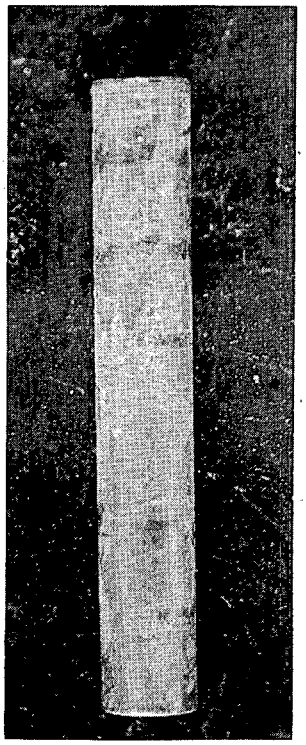

4X HC1139

Specimen 10MoTE-40

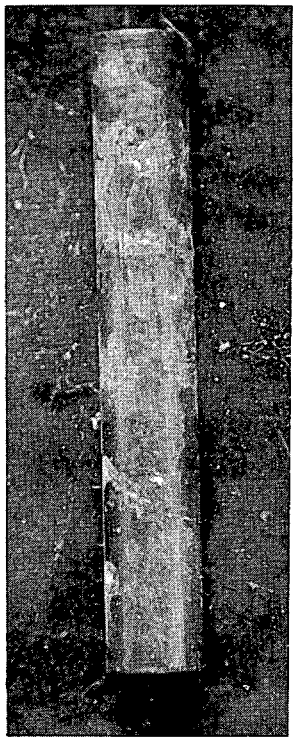

4X HC1135

Specimen 10MoTE-31

a. Over-All View of Specimen

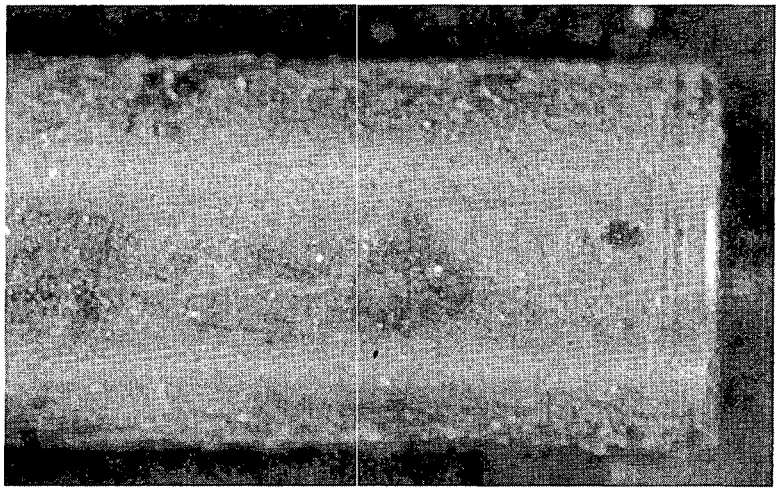

16X HC1133

Specimen 10MoTE-30

b. Side View

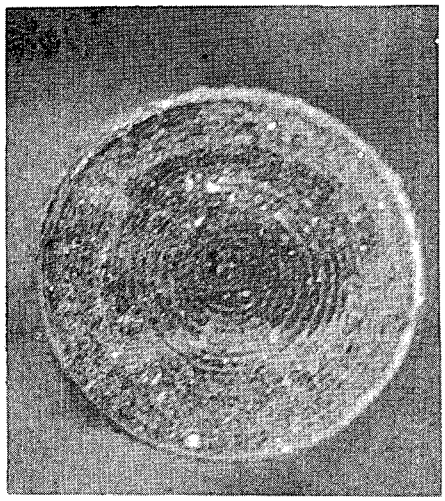

16X HC1130

Specimen 10MoTE-30

c. End View

FIGURE 39. APPEARANCE OF SPECIMENS IRRADIATED IN CAPSULE BMI-9-19

Detail views are shown only of one specimen because of similarity.

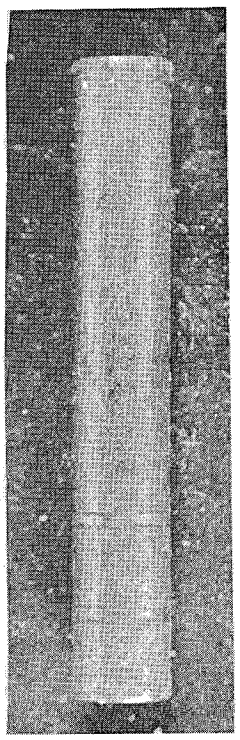

4X HC1417

Specimen 10MoTE-33

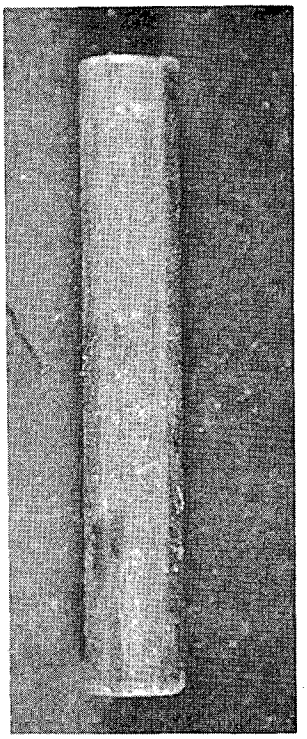

4X HC1449

Specimen 10MoTE-39

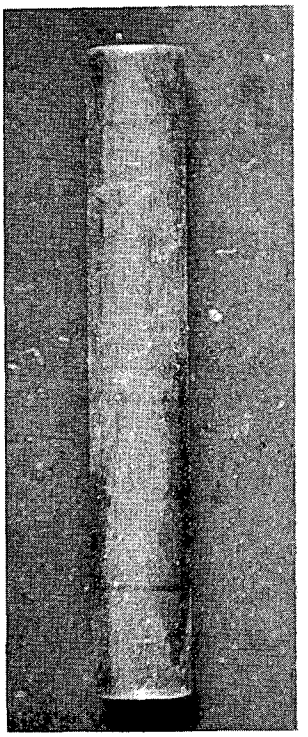

4X HC1450

Specimen 10MoTE-42

a. Over-All View

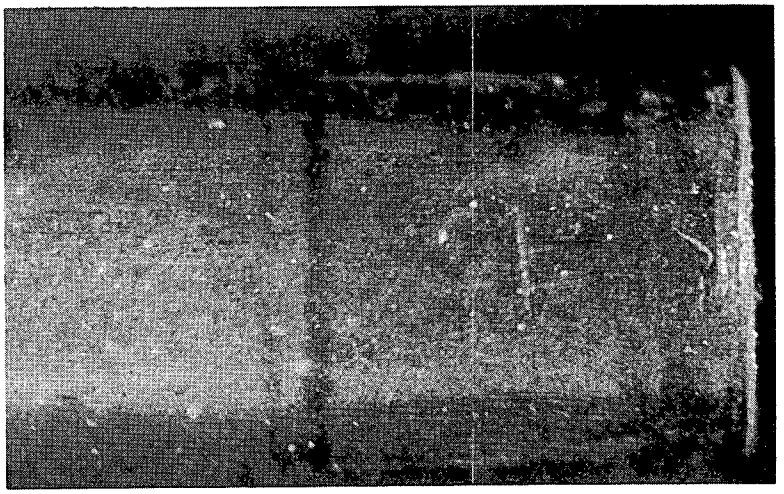

16X HC1451

Specimen 10MoTE-42

b. Side View

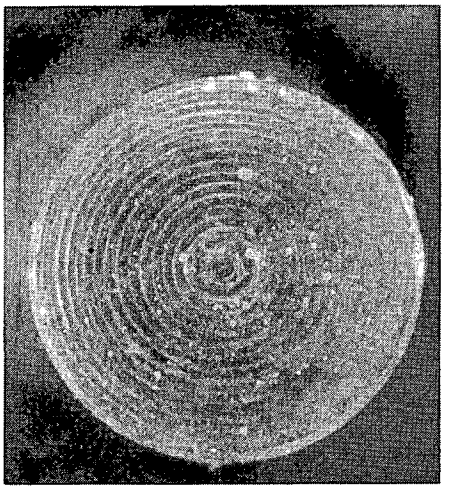

16X HC1452

Specimen 10MoTE-42

c. End View

FIGURE 40. APPEARANCE OF SPECIMENS IRRADIATED IN CAPSULE BMI-9-21

Detail views are shown only of one specimen because of similarity.

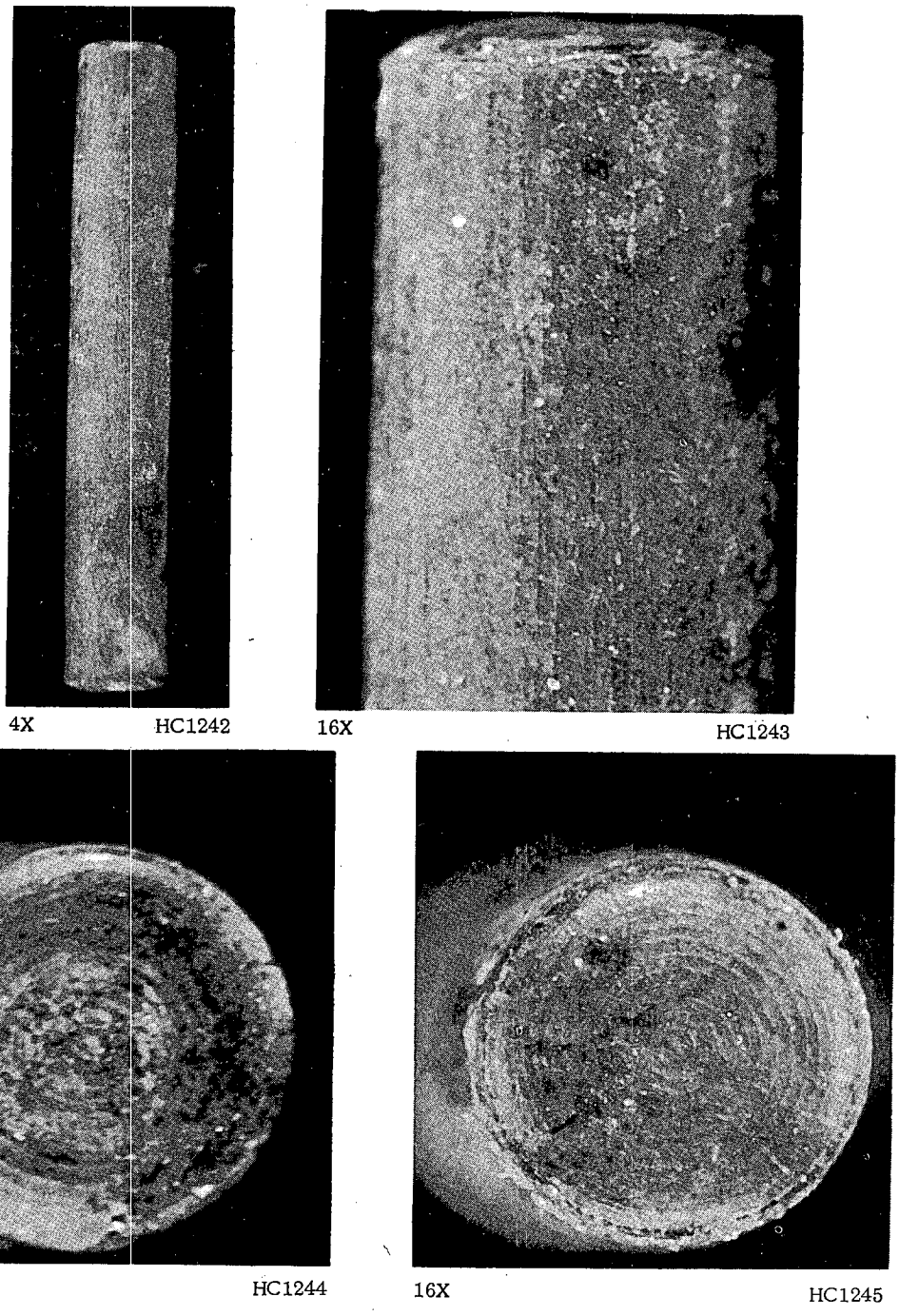

FIGURE 41. SPECIMEN 10MoTE-32 IRRADIATED IN CAPSULE BMI-9-20

Preirradiation heat treatment was 1 hr at 1472 F, water quenched, plus 15 min at 662 F, air cooled. Specimen underwent a 23 per cent density decrease, 8.3 per cent length increase and 11.9 per cent diameter increase. Note fuel extruded from ends of specimen and numerous fine cracks.

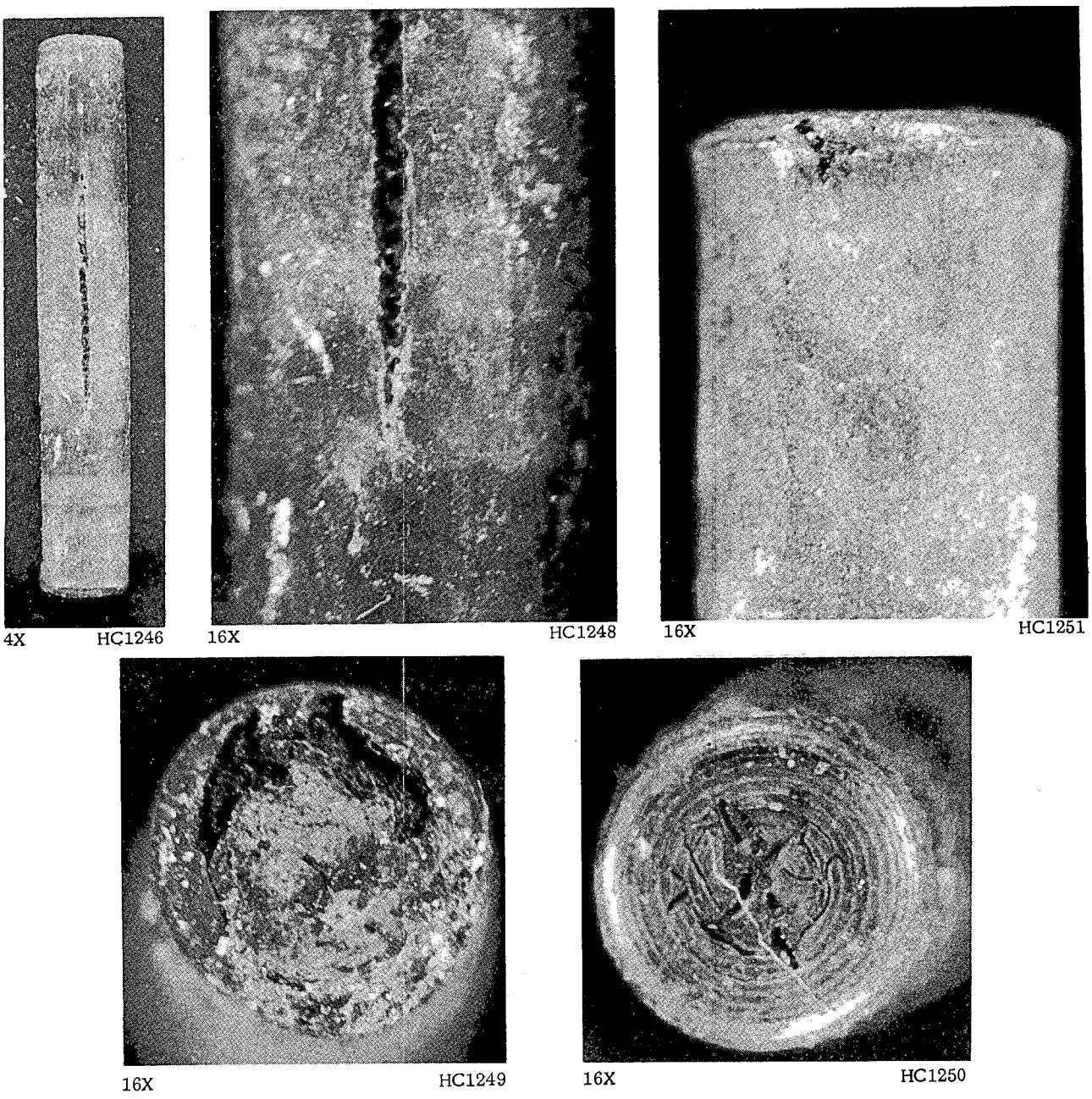

FIGURE 42. SPECIMEN 10MoTE-36 IRRADIATED IN CAPSULE BMI-9-20

Preirradiation heat treatment was 1 hr at 1472 F, slow cooled (4-1/2 hr) to 212 F. The specimen underwent a 19.8 per cent density decrease, 6.3 per cent length increase, and 11.2 per cent diameter increase.

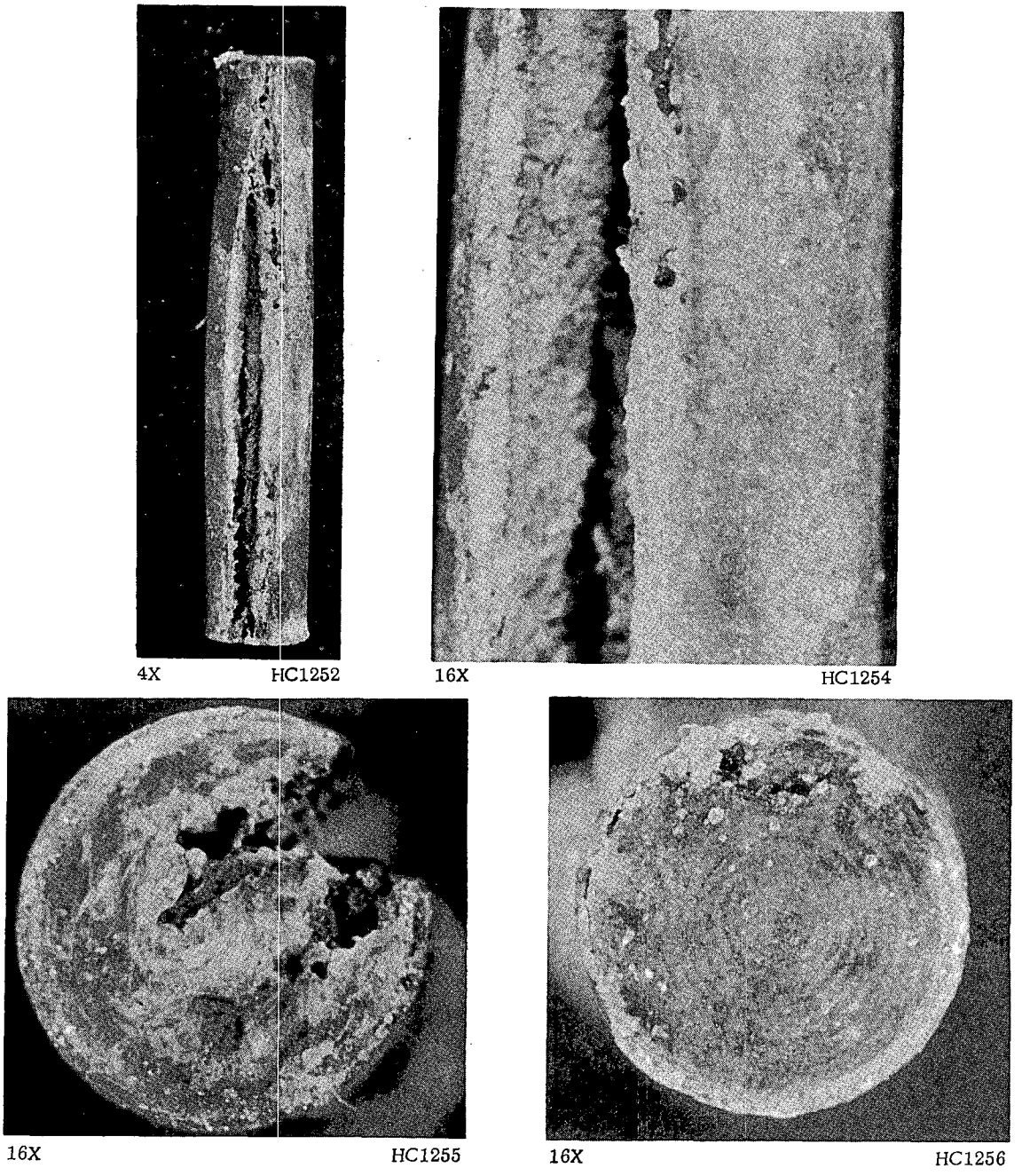

FIGURE 43. SPECIMEN 10MoTE-41 IRRADIATED IN CAPSULE BMI-9-20

Preirradiation heat treatment was 1 hr at 1472 F, water quenched, plus 2 weeks at 932 F, air cooled. The specimen underwent a 46.8 per cent decrease in density, 5.8 per cent length increase and 19.5 per cent diameter increase.

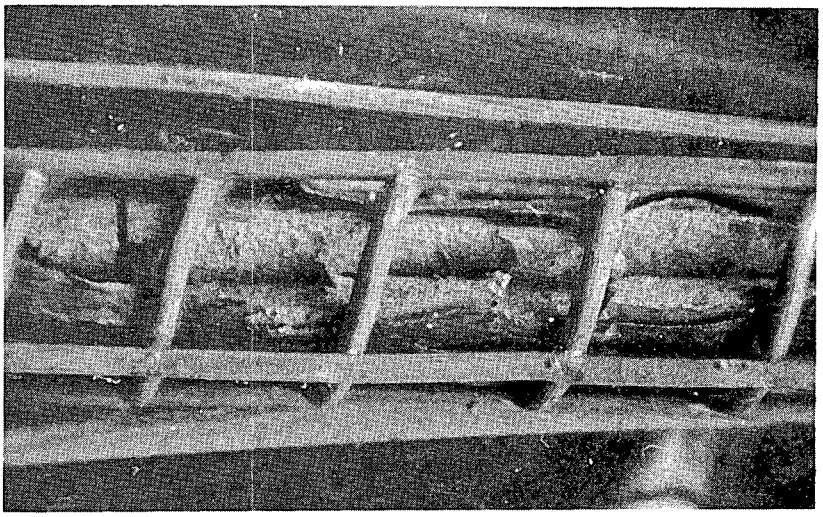

4X HC2373

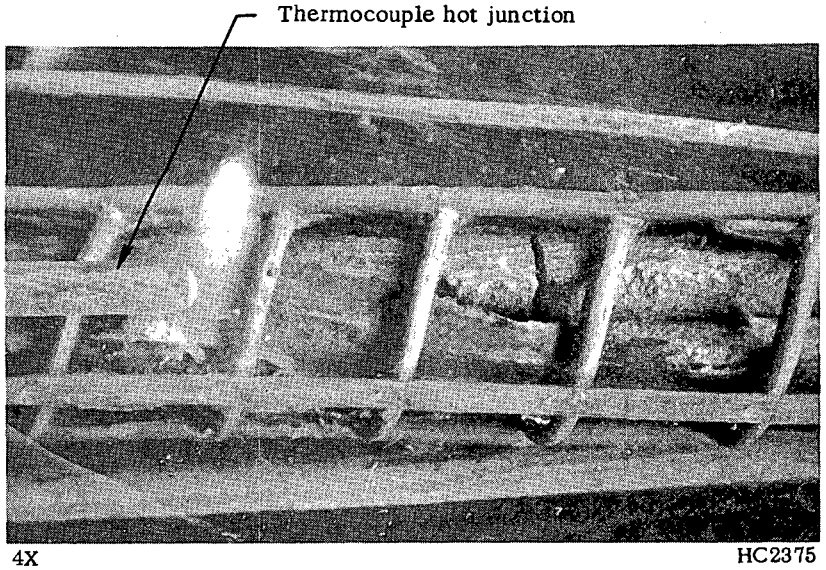

4X HC2375

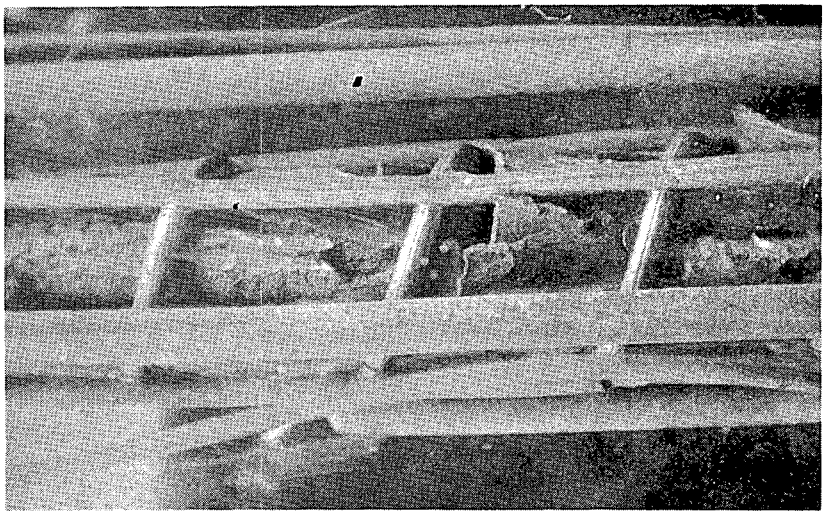

4X HC2377

FIGURE 44. SPECIMEN 10-1 IRRADIATED IN CAPSULE BMI-9-32

Photograph taken through wall of plastic vial.

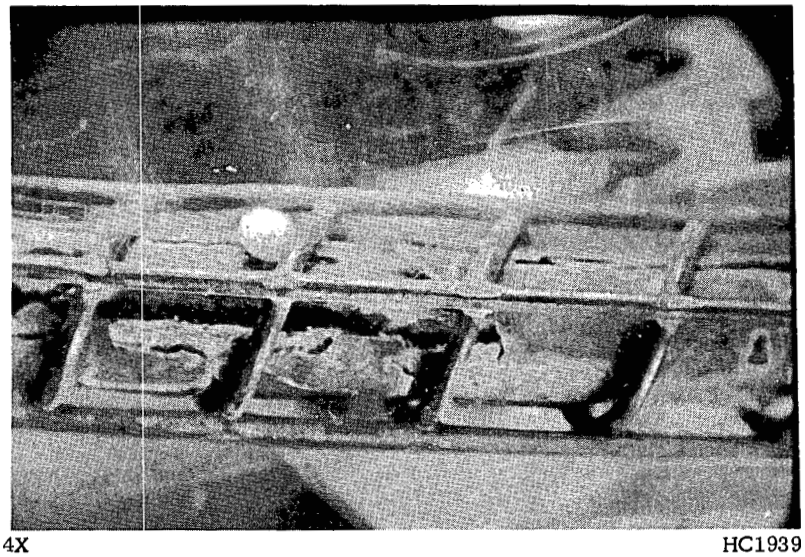

4X HC1939

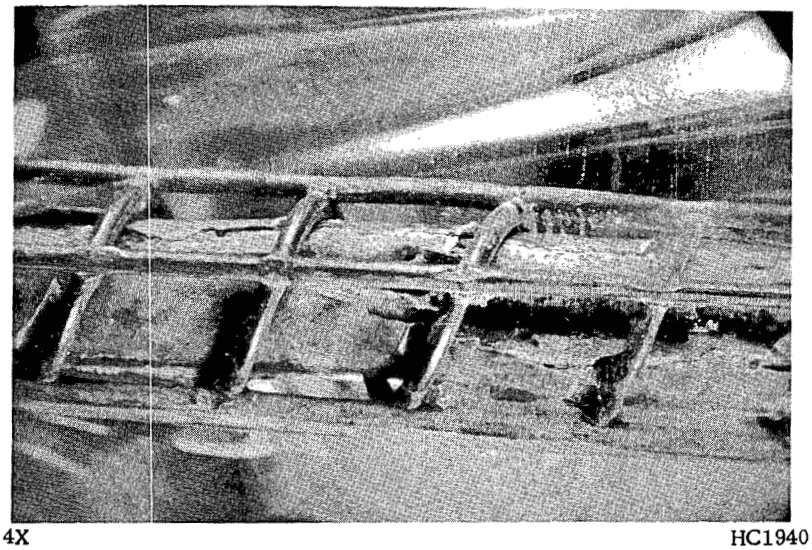

4X HC1940

FIGURE 45. SPECIMEN 10-2 IRRADIATED IN CAPSULE BMI-9-33

Photograph taken through wall of plastic vial.

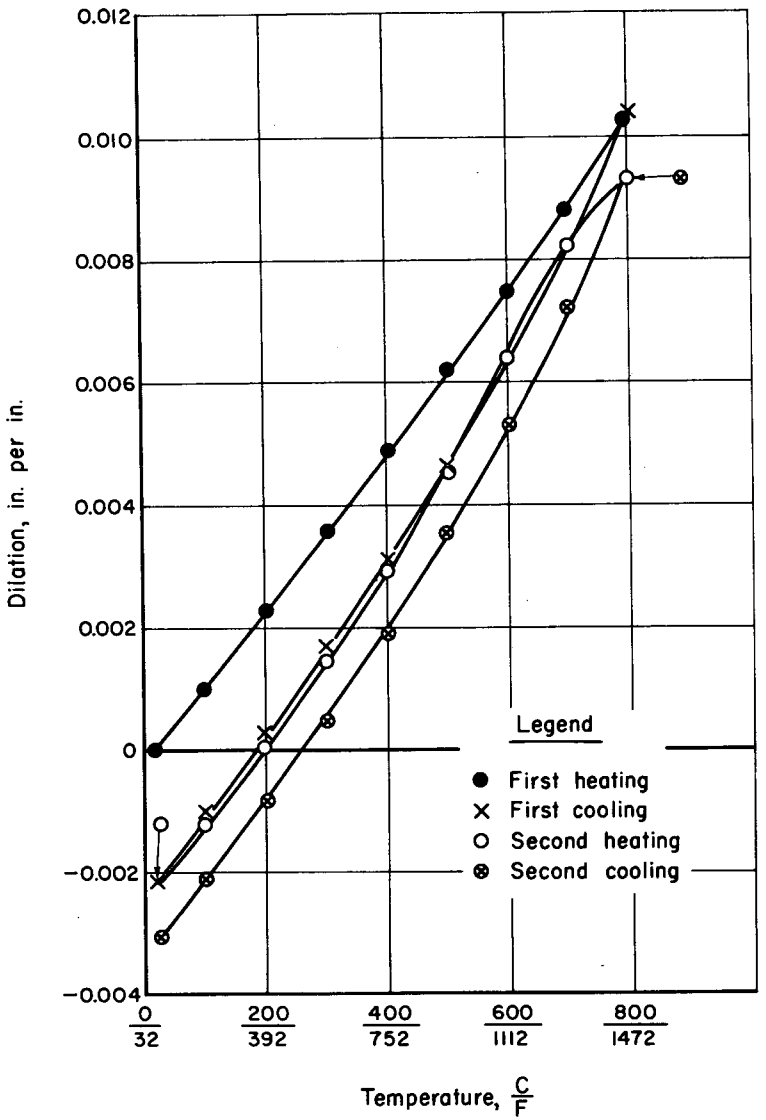

FIGURE 46. LINEAR EXPANSION VERSUS TEMPERATURE FOR HOT-ROLLED UNIRRADIATED CONTROL SPECIMEN HRC-2

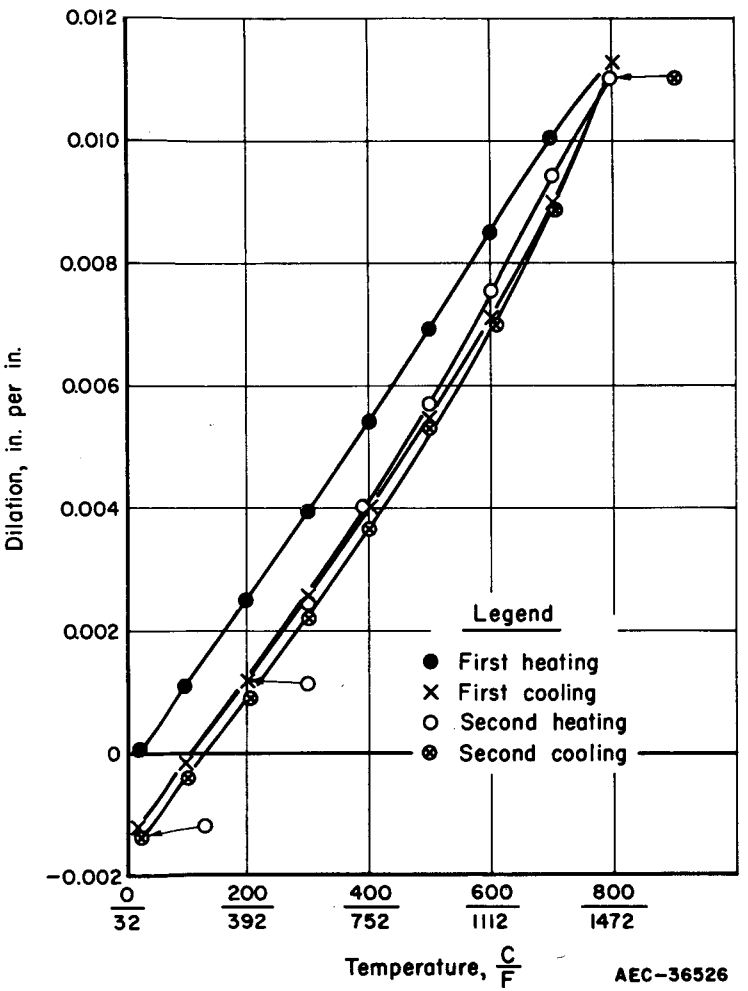

FIGURE 47. LINEAR EXPANSION VERSUS TEMPERATURE FOR COEXTRUDED UNIRRADIATED CONTROL SPECIMEN EC-2

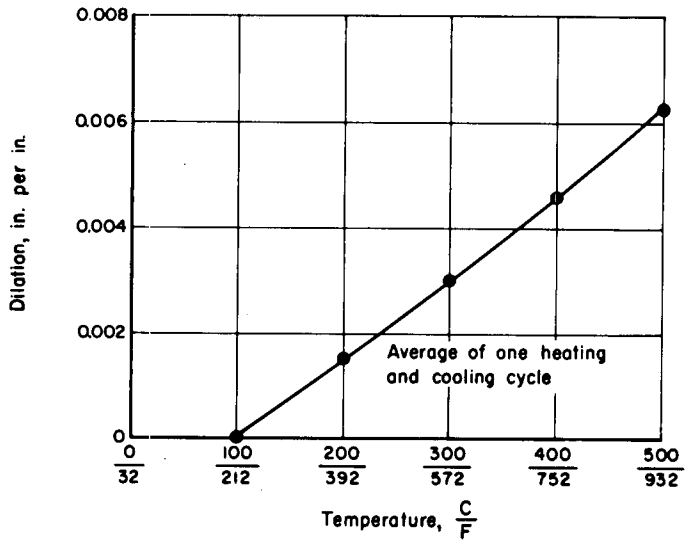

FIGURE 48. LINEAR EXPANSION VERSUS TEMPERATURE FOR IRRADIATED HOT-ROLLED SPECIMEN 10MoU-24

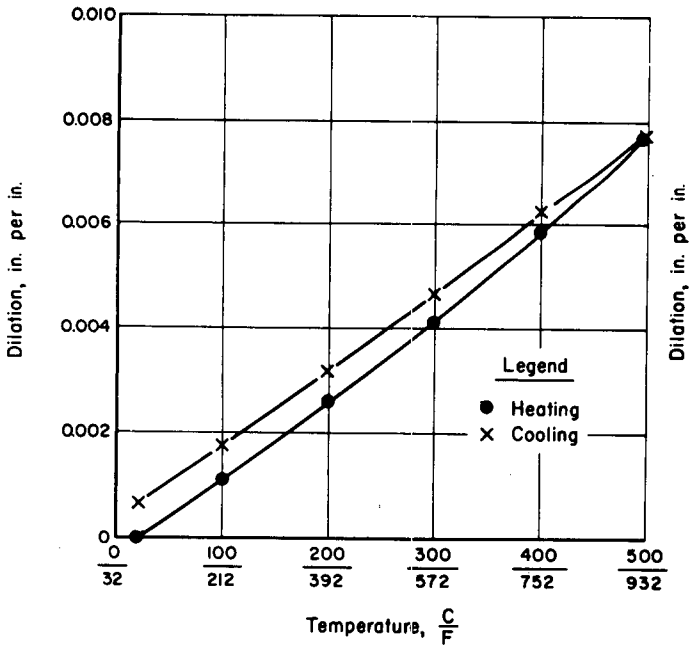

FIGURE 49. LINEAR EXPANSION VERSUS TEMPERATURE FOR IRRADIATED HOT-ROLLED SPECIMEN 10MoU-4

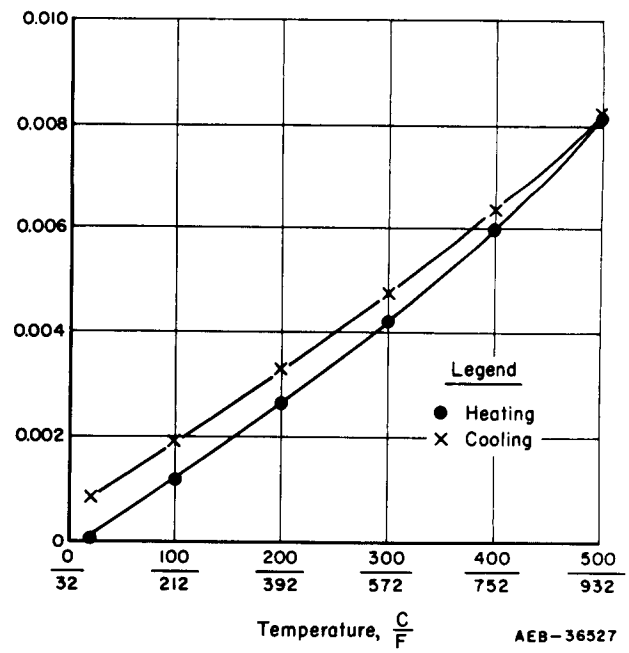

FIGURE 50. LINEAR EXPANSION VERSUS TEMPERATURE FOR IRRADIATED COEXTRUDED SPECIMEN HT-2

small change in the dilation rate and also a decrease in the electrical resistivity. The electrical resistivity of this specimen was observed to increase rather than decrease as in the case of the other irradiated specimens, probably as a result of increased porosity due to swelling.

The mean linear thermal-expansion coefficients for various temperature ranges are shown in Figure 52 as a function of burnup. The data obtained from the 1.3 total a/o burnup specimen at the three lower temperature ranges did not fit into the curves in a logical manner. Inspection of the data and experimental techniques has not revealed possible causes for the anomalous results. These data, denoted by x's in Figure 52, were not used to prepare the curves in the three temperature ranges of 212-392 F, 212-572 F, and 212-752 F.

POSTIRRADIATION HEAT TREATMENTS

Early in the irradiation program it seemed desirable to heat treat a few irradiated specimens at selected temperatures to obtain more data on the swelling of the fuel alloy. Consequently, one control and three irradiated specimens were selected for 100-hr heating studies at 1070 F.

The specimens were sealed in Vycor tubes under argon at pressures of about 0.02 mm of mercury. The capsules were placed in a furnace for 100 hr at 1070 F. After heating, the capsules were sampled for fission-gas content and the specimens recovered. The specimens were photographed, visually examined, and measurements of physical dimensions, density, and electrical resistivity completed. The results obtained from two of these heat treatments are presented in Table 14. A third heat treatment was performed, but the specimens disintegrated after the vials broke at temperature.

METALLOGRAPHIC EXAMINATION

During the course of this program, several specimens were metallographically examined to determine microstructural variations produced as a result of the irradiation exposure. Results of the examination of some of the specimens were reported previously to the Sponsor in quarterly, topical, or letter reports, and are not included in this report. The results of metallographic examination of specimens previously reported only in monthly letters are given.

The preirradiation variables contained in specimens receiving the metallographic examination are (1) alloy composition, (2) cladding thickness, and (3) heat treatment. Other variables introduced during the irradiation experiment, such as burnup and specimen operating temperature were given in Table 11.

Specimens were prepared for metallographic viewing by mounting in Bakelite, wet grinding through 600-grit silicon carbide paper, and polishing on water-lubricated wheels employing 6-, 1-, and 1/2-μ diamond paste as an abrasive. The specimens were electroetched with an 18:1 chromic-acetic acid solution at about 25 v dc on the open circuit.

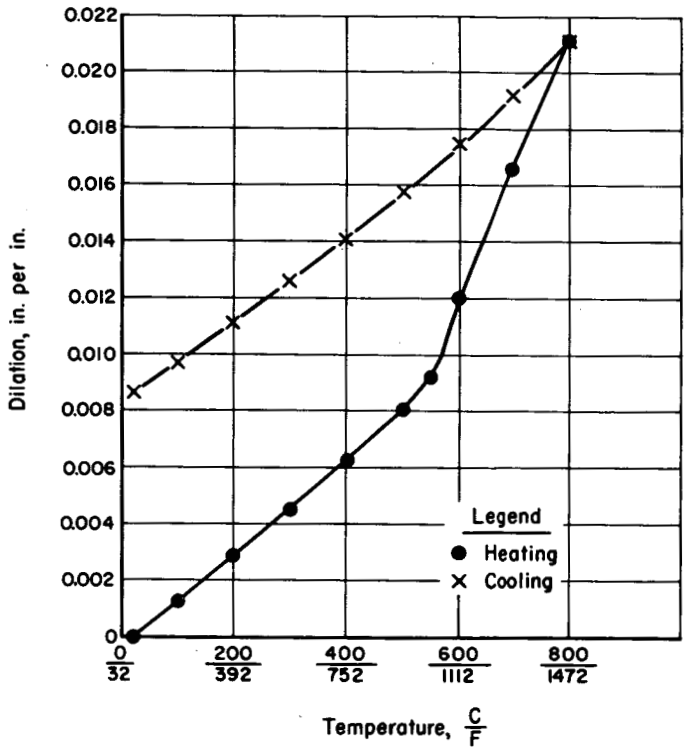

FIGURE 51. LINEAR EXPANSION VERSUS TEMPERATURE FOR IRRADIATED COEXTRUDED SPECIMEN HT-7

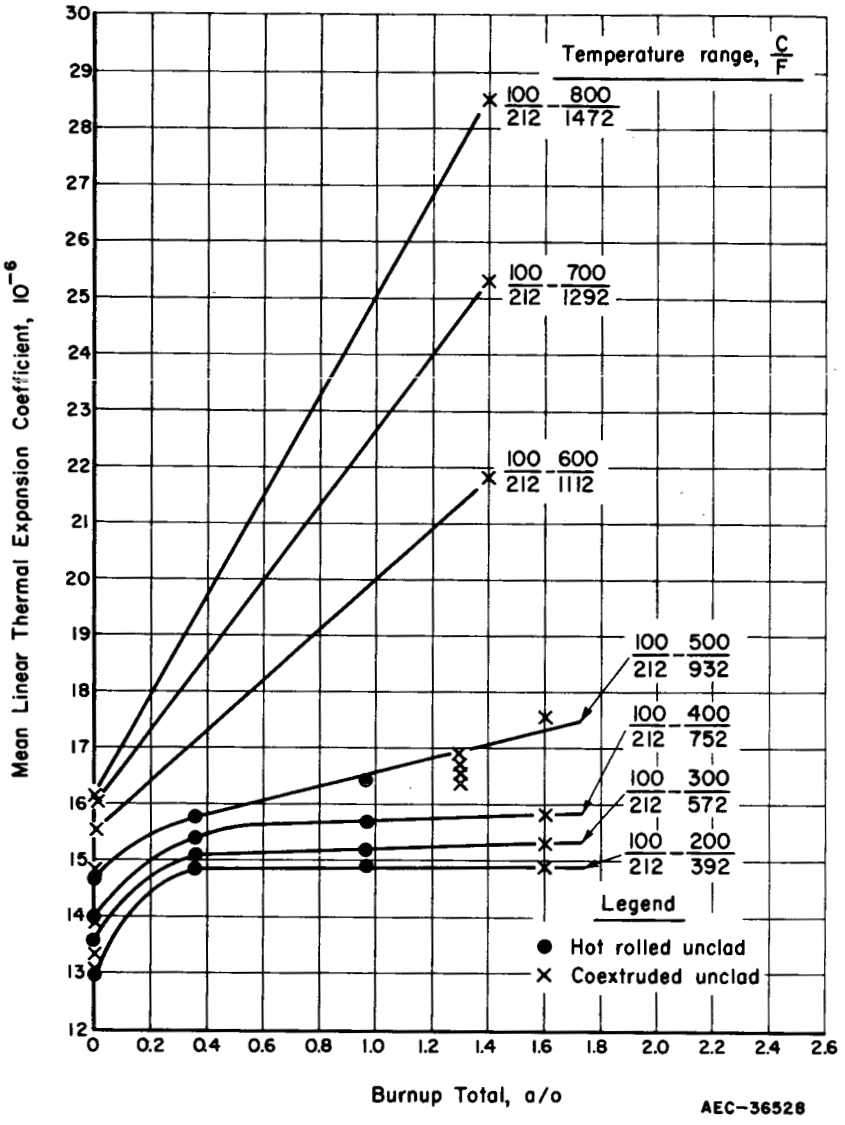

FIGURE 52. MEAN LINEAR THERMAL EXPANSION COEFFICIENTS OF URANIUM-10 w/o MOLYBDENUM AS A FUNCTION OF BURNUP

The microstructure of the unirradiated uranium-10 w/o molybdenum alloy given representative preirradiation heat treatments is shown in Figure 53. The typical microstructure of hot-rolled uranium-10 w/o molybdenum rod heated for 24 hr at 1652 F and water quenched to retain the gamma phase is shown in Figure 53a. Specimens receiving this preirradiation heat treatment were irradiated in Capsules BMI-302-19, and -20, and Capsules BMI-9-1, -2, -3, -4, -5, -12, and -13.

The reference APDA fabrication technique is to metallurgically bond approximately 4 mils of zirconium cladding to the surface of a uranium-10 w/o molybdenum fuel pin by a coextrusion process. The microstructure of the fuel alloy fabricated by this technique and subsequently heated for 15 min at 662 F and air cooled, is shown in Figure 53b. The postcoextrusion heat treatment has not completely eliminated the "swirl" structure produced by coextrusion of the somewhat inhomogeneous ingots, as shown in the photomicrograph by the presence of numerous dark wavy areas of high uranium. An area of oxide inclusions can be observed near the top of the photomicrograph.

The microstructure of the coextruded uranium-10 w/o molybdenum alloy heat treated for 1 hr at 1472 F and water quenched, then stress annealed for 15 min at 662 F is shown in Figure 53c. This was the reference heat treatment given to approximately 37 per cent of all specimens in the capsule program, and was designed to produce the gamma phase.

The microstructure of the reference fuel alloy after being given an alternate heat treatment designed to produce the alpha-plus-epsilon phases is depicted in the micrograph shown in Figure 53d. The light-colored phase is high-molybdenum-content uranium alloy and the dark phase is alpha uranium. The alloy responds to heat treatment below 1045 F to produce a lamellar-type transformation product which is dominant throughout the photomicrograph.

Specimens with nominally 4.7-, 8.1-, and 11-mil-thick zirconium cladding applied by coextrusion to the surface of nominally 0.100-in.-diameter uranium-10 w/o molybdenum alloy fuel pins were examined to determine the effects of cladding thickness on the irradiation stability of the reference fuel alloy. The microstructure of a fuel pin clad with 4.7 mils of zirconium is shown in Figure 54. Specimen 10CT4-27 was irradiated to a burnup of about 0.45 total a/o at a temperature of about 310 to 320 F. The specimen was in good physical condition after irradiation and exhibited no surface or end defects. Subsequent metallographic examination showed no obvious change from its preirradiation microstructure. A companion 4.7-mil-thick clad specimen, 10CT4-26 was irradiated to a burnup of about 3.4 total a/o at a specimen temperature of 1020 to 1440 F. The specimen decreased 17.0 per cent in density and a split on one end extending about 1/4 in. along its length. Metallographic examination revealed the core alloy contained a fine precipitate suggestive of gamma decomposition, although the precipitate was not the lamellar type normally associated with the alloy. It is believed that swelling and fission-gas formation may have affected the microstructure. A few large cracks generally terminating at the cladding-core interface, were observed, such as the one shown in Figure 55.

The microstructure of irradiated Specimen 10CT8-6 clad with 8.1 mils of zirconium is shown in Figure 56. This specimen received 1.0 total a/o burnup at a temperature of about 540 to 590 F. The specimen was in good physical condition after irradiation, with an apparent density decrease of 2.0 per cent. Preirradiation heat treatment produced the cubic gamma phase and postirradiation metallographic examination indicated that this phase was retained. A similar specimen, 10CT8-2, was irradiated to

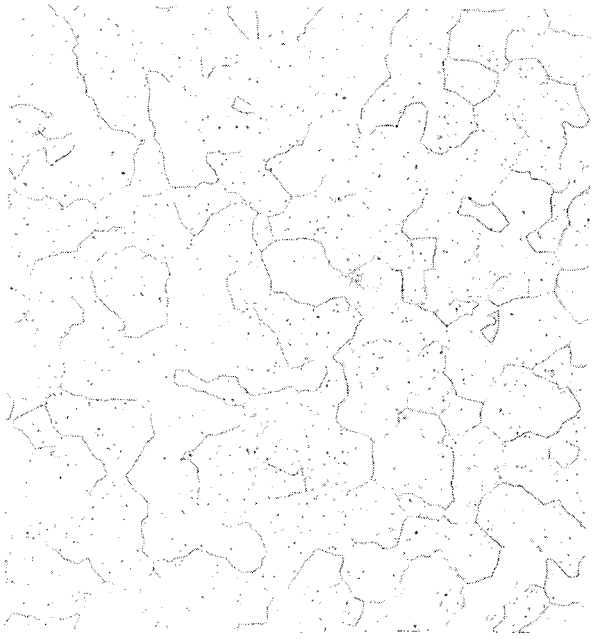

250X Etched RM3306

a. Hot Rolled, Heated 24 Hr at 1652 F, Water Quenched

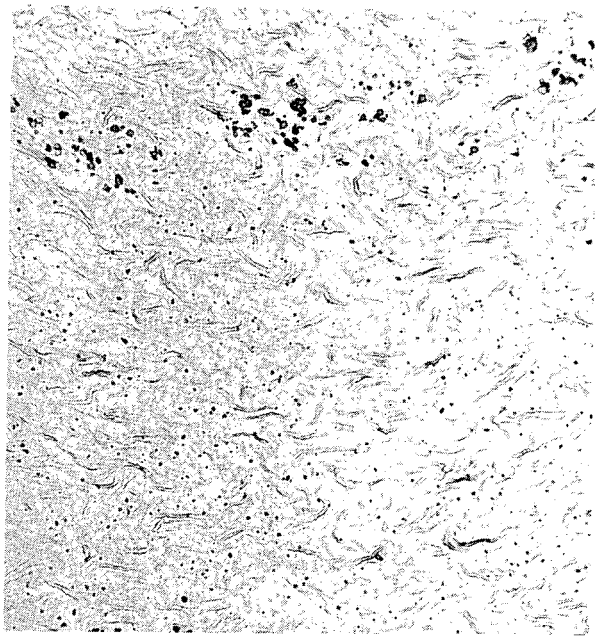

250X Etched RM7741

b. Extruded and Stress Annealed

Note swirl structure.

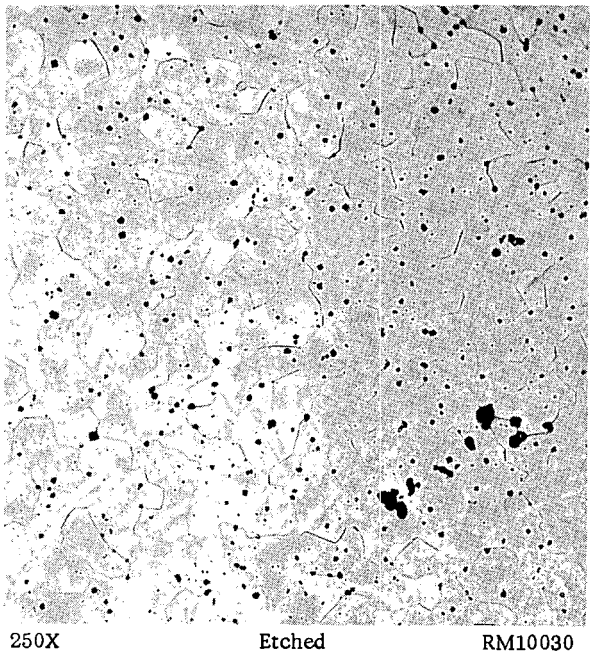

250X Etched RM10030

c. Extruded, Heated 1 Hr at 1472 F, Water Quenched, and Stress Annealed at 662 F for 15 Min

Gamma phase was produced.

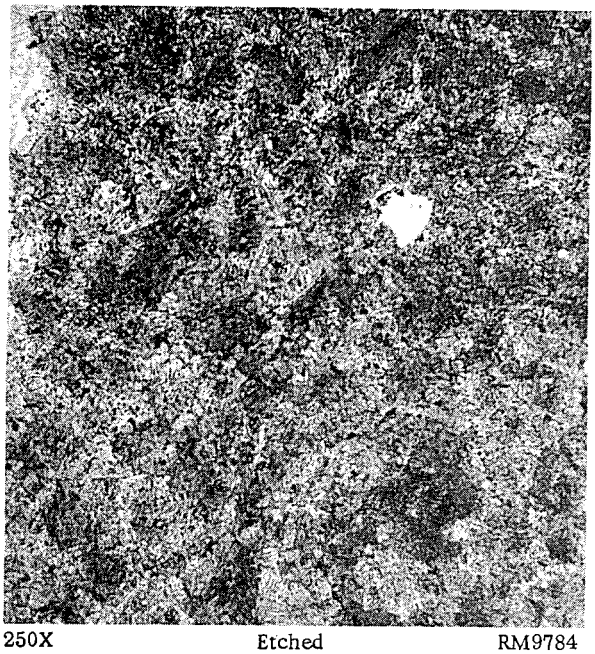

250X Etched RM9784

d. Extruded, Heated 1 Hr at 1472 F, Water Quenched, and Heated for 100 Hr at 932 F

Alpha-plus-epsilon phases were produced with slight remnant of gamma.

FIGURE 53. MICROSTRUCTURE OF UNIRRADIATED URANIUM-10 w/o MOLYBDENUM ALLOY

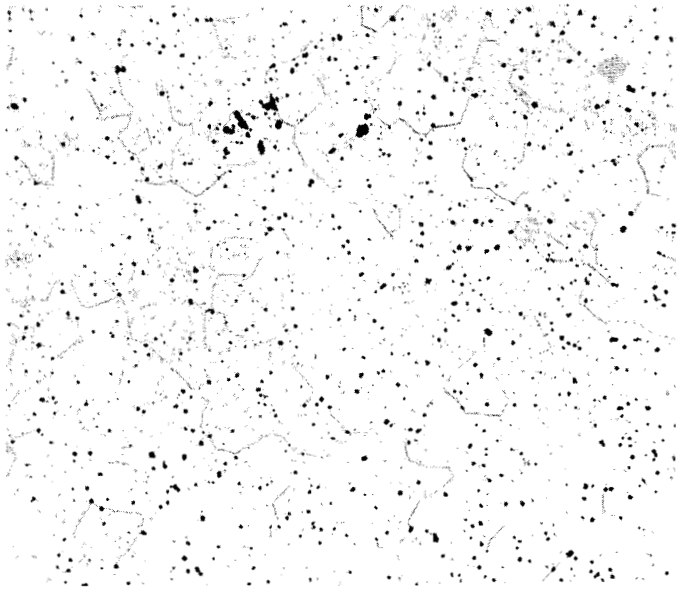

250X Etched HC1176

FIGURE 54. SPECIMEN OF URANIUM-10 w/o MOLYBDENUM ALLOY CLAD WITH 4.7 MILS OF ZIRCONIUM IRRADIATED TO ABOUT 0.45 TOTAL a/o BURNUP

This specimen, 10CT4-27, was irradiated at a center-line temperature of about 310 to 320 F. The specimen was in the gamma phase prior to and following irradiation exposure. Density decreased 1.2 per cent. The fission rate was 0.35×10^{14} fissions/(sec)(cm^3).

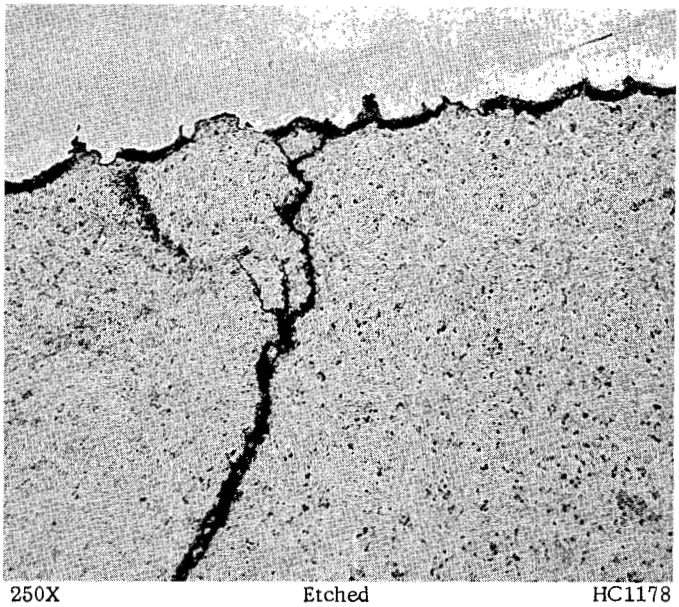

250X Etched HC1178

FIGURE 55. SPECIMEN OF URANIUM-10 w/o MOLYBDENUM ALLOY CLAD WITH 4.7 MILS OF ZIRCONIUM IRRADIATED TO 3.4 TOTAL a/o BURNUP

This specimen, 10CT4-26, was irradiated at a center-line temperature of 1020 to 1440 F. The specimen was in the gamma phase prior to irradiation but probably transformed during irradiation. Density decreased 17.0 per cent. The fission rate was 1.9×10^{14} fissions/(sec)(cm^3).

2.7 total a/o burnup at a temperature of 860 to 1120 F. The specimen contained a large crack on one end and underwent a density decrease 8.2 per cent. The presence of a fine precipitate in the core, seen in Figure 57, suggests the specimen has undergone transformation during irradiation. A large crack is present which terminates at the cladding-core interface. Patches of light, untransformed gamma-phase alloy are present to a limited degree in the area of the core adjacent to the cladding-core interface.

The microstructure of irradiated Specimen 10CT11-3, clad with 11 mils of zirconium, is shown in Figure 58. This specimen was irradiated to 3.0 total a/o burnup at a temperature of 930 to 1260 F. The specimen was split on one end and sustained a density decrease of 9.7 per cent. Metallographic examination of the core, Figure 58a, indicates nearly complete transformation has occurred of gamma to the alpha-plus-epsilon phases. The specimen contains numerous fine cracks in the core adjacent to the cladding interface. In the area of the core-cladding bond, Figure 58b, the gamma phase is largely present except at grain boundaries, where transformation to the alpha-plus-epsilon phases has been initiated. A large oxide-filled crack is present in the predominantly gamma-phase region, Figure 58c. Possibly, this untransformed region is a consequence of a uranium diffusion into the cladding with consequent uranium depletion of the core alloy. This untransformed area was noted, but to a lesser extent, in Specimen 10CT8-2 with an 8.1-mil-thick cladding.

A second 11-mil-thick zirconium-clad specimen, 10CT11-2, was examined after a burnup of 2.5 total a/o at a temperature of 820 to 1040 F. The specimen was mounted for longitudinal viewing of the cladding and core. The specimen, which showed a density decrease of 4.1 per cent was split on both ends. The as-polished section is shown in Figure 59a revealing numerous cracks and voids. It is possible that some of the cracks were produced during handling, particularly the cracks radiating from the right-hand edge of the specimen. The voids in the core were the result of pullout of chipped particles during metallographic operations.

A clue to the cause for the exaggerated splitting and cladding failures in the specimens with thicker cladding may be the extremely rough appearance of the zirconium cladding shown on the surface of Specimen 10CT11-2, Figure 59b. The rough granular appearance shown in this photomicrograph could conceivably lead to the formation of local stress risers as a result of swelling followed by possibly stress corrosion and subsequent cladding failure.

The etched appearance of the core is shown by Figure 59c. The specimen was apparently maintained essentially in the gamma phase during irradiation as indicated by the microstructure.

Specimens containing nominally 9 and 11 w/o molybdenum, balance uranium, were irradiated as part of a study of the effects of slight changes in composition of the fuel alloy. One of the specimens, 11MoCE-9, was subjected to a postirradiation metallographic examination. Hairline cracks were observed in the cladding, Figure 60, after a burnup of 1.1 total a/o at about 750 to 840 F. The density of the specimen had decreased by 2.1 per cent. Figure 60a shows the presence of two typical hairline cracks extending from the surface of the cladding to the cladding-core interface, where they terminate. The core alloy has been retained in the gamma phase, as shown by Figure 60b. Large patches of oxide inclusions are observed in the upper part of the photomicrograph.

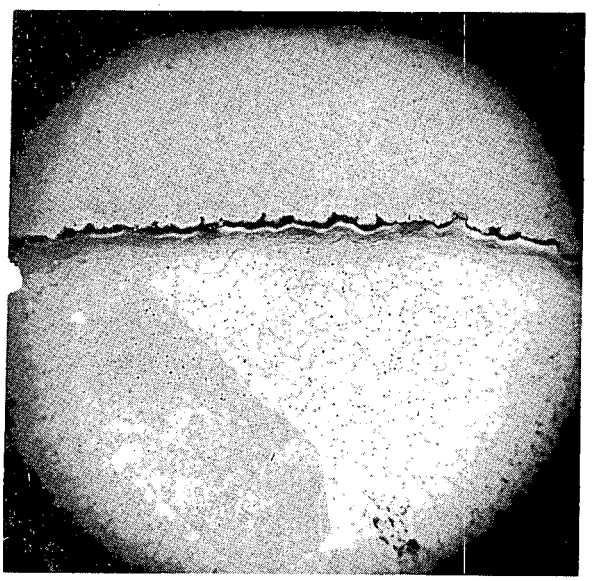

100X Etched HC1266

a. Over-All View of Cladding and Core

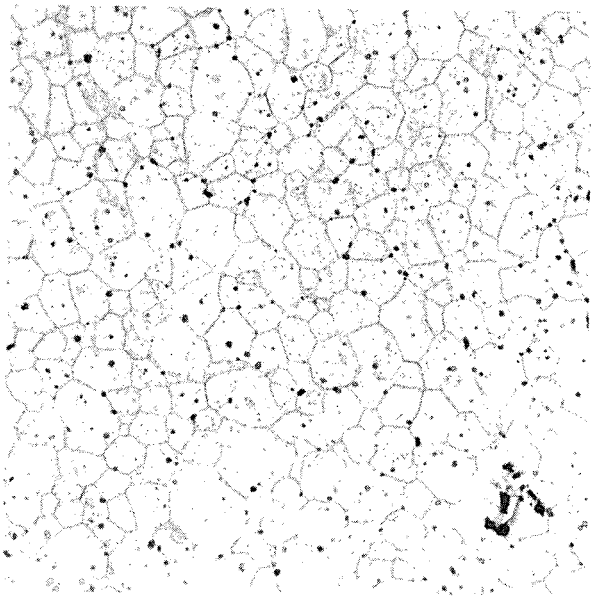

250X Etched HC1264

b. Typical Gamma-Phase Microstructure

FIGURE 56. SPECIMEN OF URANIUM-10 w/o MOLYBDENUM ALLOY CLAD WITH 8.1 MILS OF ZIRCONIUM IRRADIATED TO ABOUT 1.0 TOTAL a/o BURNUP

This specimen, 10CT8-6, was irradiated at a center-line temperature of 540 to 590 F. The specimen was in the gamma phase before and after irradiation. Apparent decrease in density was 2.0 per cent. The fission rate was 0.78×10^{14} fissions/(sec)(cm^3).

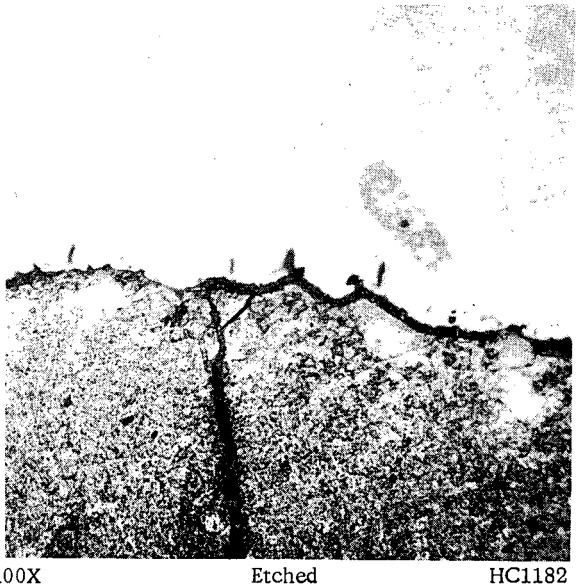

100X Etched HC1182

a. Untransformed Areas Near the Cladding

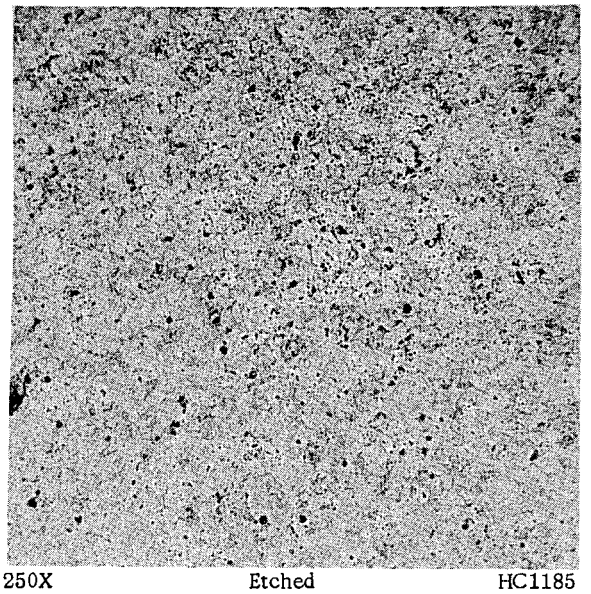

250X Etched HC1185

b. Area Near Center of Core

FIGURE 57. SPECIMEN OF URANIUM-10 w/o MOLYBDENUM ALLOY CLAD WITH 8.1 MILS OF ZIRCONIUM IRRADIATED TO 2.7 TOTAL a/o BURNUP

This specimen, 10CT8-2, was irradiated at a center-line temperature of 860 to 1120 F. The specimen contained a fine transformation product indicative of alpha-plus-epsilon phases. Density decreased 8.2 per cent. Note the large crack which terminates at the cladding-core interface. The fission rate was 1.5×10^{14} fissions/(sec)(cm^3).

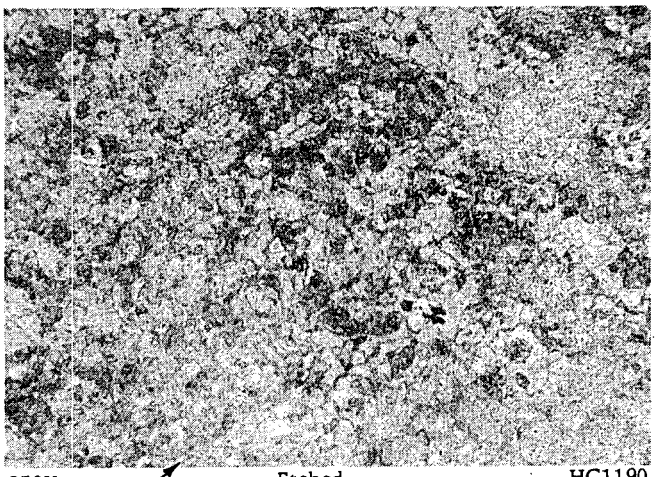

a. Fully Transformed Core Alloy

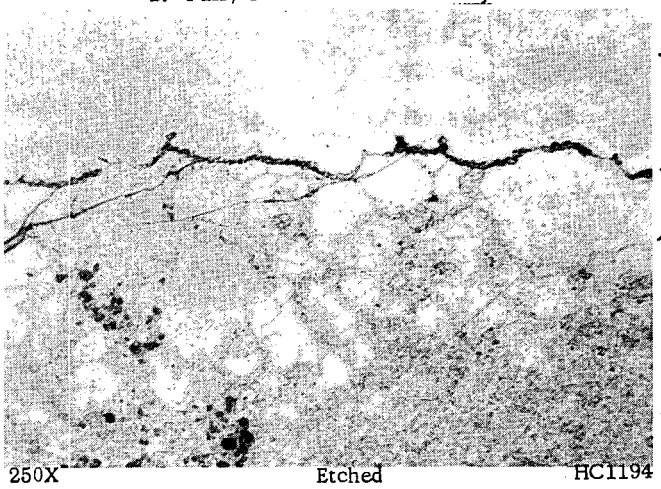

b. Area of Core-Cladding Bond

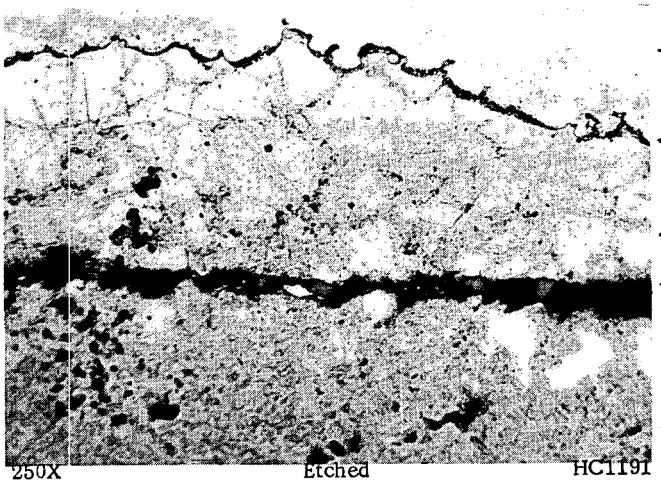

c. Crack in Core Near Interface

FIGURE 58. SPECIMEN OF URANIUM-10 w/o MOLYBDENUM ALLOY CLAD WITH 11 MILS OF ZIRCONIUM IRRADIATED TO 3.0 TOTAL a/o BURNUP

This specimen, 10CT11-3, was irradiated at a center-line temperature of 930 to 1260 F. The specimen was in the gamma phase before irradiation. It split on one end and decreased 9.7 per cent in density. Note that the alloy has transformed from its preirradiation gamma phase to the alpha-plus-epsilon phases except in the region adjacent to the cladding. The untransformed portion of the core contains numerous fine cracks, indicating a brittle microstructure. The fission rate was 1.7×10^{14} fissions/(sec)(cm^3).

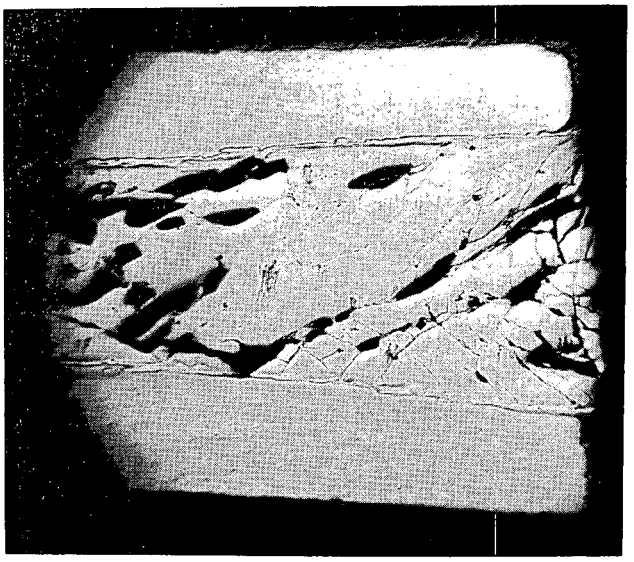

25X As Polished HC1171

a. Longitudinal Section of Cladding and Core

Note large amount of core cracking produced either during irradiation or by metallographic preparation. Voids are caused by pullout of core material.

250X As Polished HC1167

b. Extremely Rough Grainy Surface of Zirconium Cladding

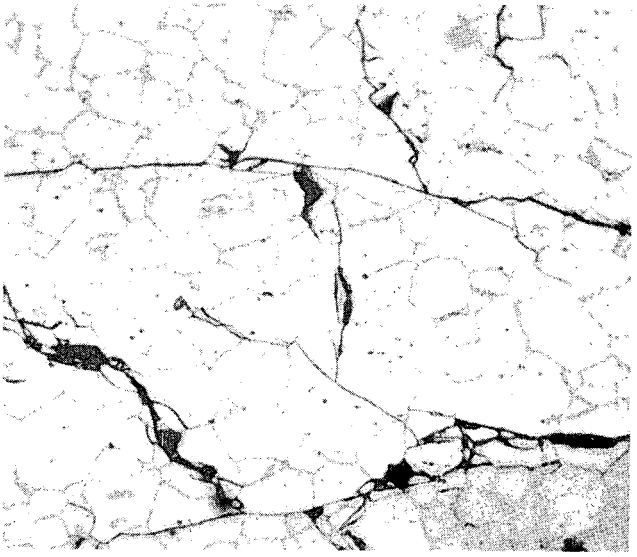

250X Etched HC1334

c. Microstructure Showing Cracks in Core Alloy

Some evidence of transformation to the alpha-plus-epsilon phases is suggested by the widened grain boundaries.

FIGURE 59. SPECIMEN OF URANIUM-10 w/o MOLYBDENUM ALLOY CLAD WITH 11 MILS OF ZIRCONIUM IRRADIATED TO 2.5 TOTAL a/o BURNUP

This specimen, 10CT11-2, was irradiated at a center-line temperature of 820 to 1040 F. The specimen was in the retained-gamma phase before irradiation and apparently remained in this phase throughout the irradiation. Both ends of the specimen were split when examined after irradiation. Density decreased 4.1 per cent. This fission rate was 1.4×10^{14} fissions/(sec)(cm^3).

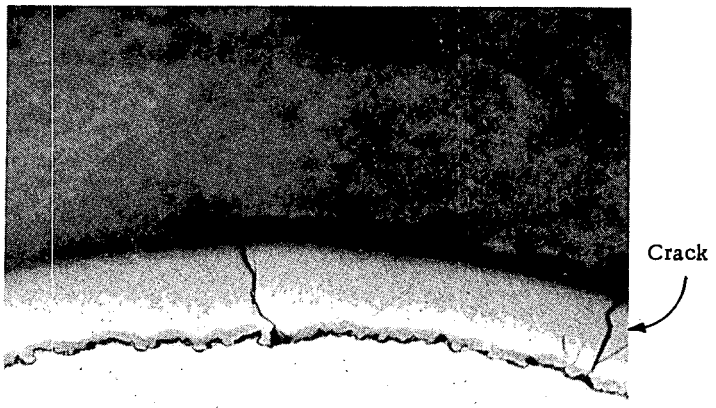

100X As polished HC1096

a. Hairline Cracks in Cladding

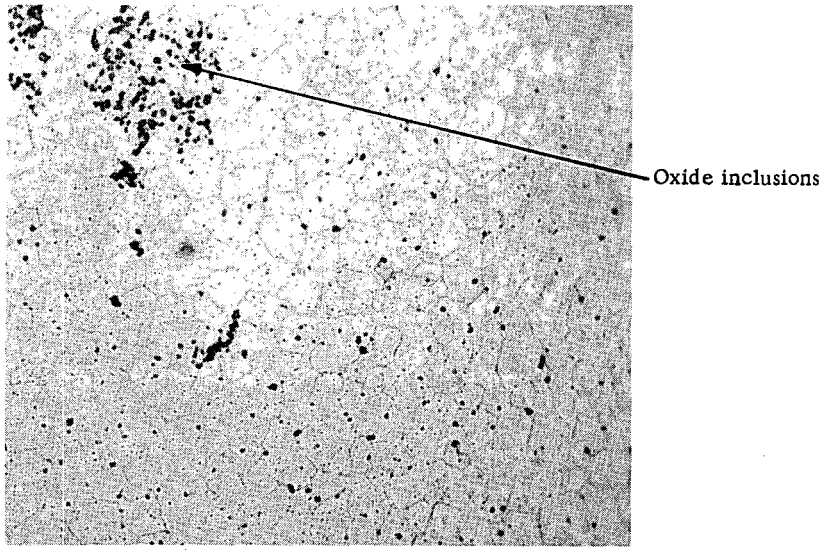

100X Etched HC1099

b. Gamma-Phase Microstructure With Oxide Inclusions

FIGURE 60. SPECIMEN OF URANIUM-11 w/o MOLYBDENUM ALLOY CLAD WITH 4.7 MILS OF ZIRCONIUM IRRADIATED TO 1.1 TOTAL a/o BURNUP

This specimen was irradiated at a center-line temperature of 750 to 840 F. This specimen was in the gamma phase prior to and following the irradiation exposure. Density decreased 2.1 per cent. The fission rate was 1.1×10^{14} fissions/(sec)(cm^3).

The microstructures of two bare specimens of coextruded uranium-10 w/o molybdenum alloy are shown in Figure 61. Specimen HT-4 was irradiated following a 15-min stress anneal at 662 F to 1.1 total a/o burnup at a specimen center-line temperature of 730 to 810 F. Examination reveals the presence of numerous swirls of inhomogeneous uranium-molybdenum alloy. The light areas contain high molybdenum concentrations while the darker areas are of high uranium content. During irradiation, transformation may have occurred in the high-uranium areas as evidenced by what appears to be a fine gray precipitate in the micrographs. The companion specimen, HT-5, was irradiated to 1.6 total atom per cent burnup at a specimen center-line temperature of 880 to 1000 F. The microstructure shown in Figure 61b, which was originally the same as for Specimen HT-4, indicates the specimen was maintained in the gamma phase during irradiation and that some homogenization may have occurred.

Sections from Specimen 10-1 from Capsule BMI-9-32 were also examined metallographically. The metallographic examination revealed that the fuel material around the circumference of the specimen was very porous. The number and size of the voids decreased toward the center of the specimen as shown in Figure 62. While some voids were small and round, many were much larger and very irregular in shape. It is believed that the larger and irregular voids followed grain boundaries. The extent of the porosity in the specimen is also shown in Figure 63. In addition, this photomicrograph shows a representative portion of the circumference of the specimen. Note the separation of the clad from the core. This separation was observed around the entire circumference of the specimen. There did not appear to be any transformation products in the matrix.

DISCUSSION AND EVALUATION OF RESULTS

The irradiation parameter most difficult to establish with any degree of accuracy in these irradiations was that of specimen temperature. The majority of the specimens were irradiated in capsules that were not equipped with any means for measuring temperatures, other than neutron-dosimeter wires. The neutron-flux data obtained from the dosimeters were used to calculate specimen burnup, and thus the production of fission heat. Using standard heat-flow theory for a radial geometry, as described in APDA-648, reasonably accurate temperature information could be obtained. This is evidenced by the agreement between the specimen temperatures and fuel burnup calculated for Specimen 10-1 from Capsule BMI-9-32 as determined by dosimetry and thermocouple readings, Table 6. Similar agreement was found in the case of Capsules BMI-9-19, -20, and -21, each of which was equipped with thermocouples and dosimeters. A problem arises in the calculation of specimen temperatures from dosimeter data only when the capsule is irradiated in several locations in the reactor at different neutron-flux intensities.

The neutron flux calculated from neutron-dosimeter data is an average for the entire irradiation period. Thus, the irradiation temperature calculated from such data is also the average temperature occurring during the entire irradiation period. An analysis of specimen swelling as a function of the irradiation temperature calculated from dosimeter data must therefore take into consideration the possibility of higher-than-average temperatures occurring if a capsule was moved from one location to another during irradiation. The only method of doing this is by a close study of the irradiation history of

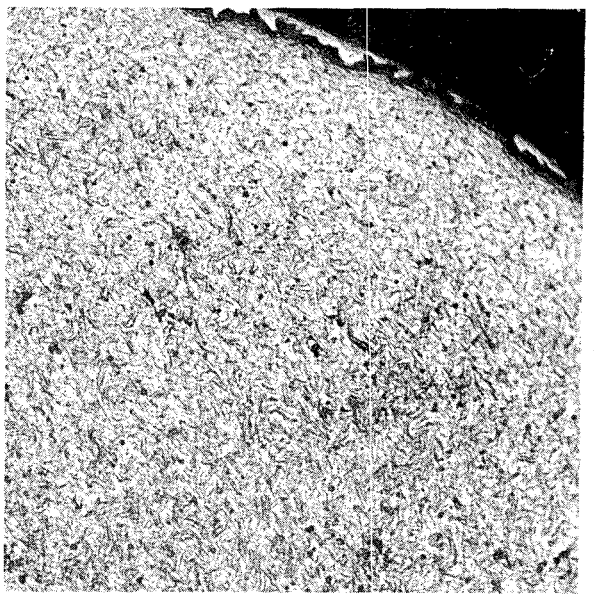

100X Etched HC1086

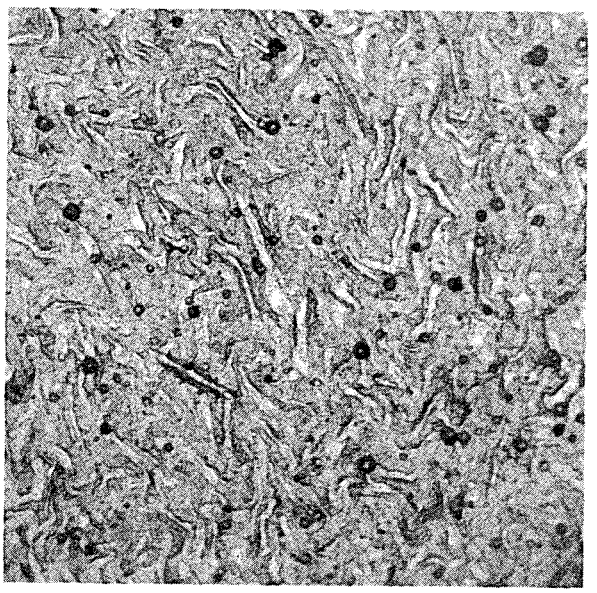

250X Etched HC1087

a. Specimen HT-4

This specimen was irradiated to 1.1 total a/o burnup of a center-line temperature of 730 to 810 F. The specimen was stress annealed for 15 min at 662 F prior to irradiation. Note "swirl" structure produced by coextrusion of inhomogeneous ingot. The alloy has apparently transformed to the alpha-plus-epsilon phases during irradiation. The fission rate was 1.2×10^{14} fissions/(sec)(cm^3).

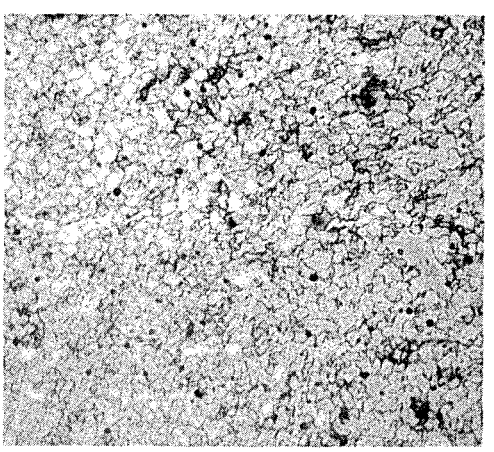

250X Etched HC1094

b. Specimen HT-5

This specimen was irradiated to 1.6 total a/o burnup at a center-line temperature of 880 to 1000 F. The specimen was stress annealed for 15 min at 662 F prior to irradiation. The gamma phase was maintained during irradiation. The fission rate was 1.7×10^{14} fissions/(sec)(cm^3).

FIGURE 61. SPECIMENS OF URANIUM-10 w/o MOLYBDENUM ALLOY IN WHICH THE COEXTRUDED ZIRCONIUM CLADDING WAS REMOVED PRIOR TO IRRADIATION

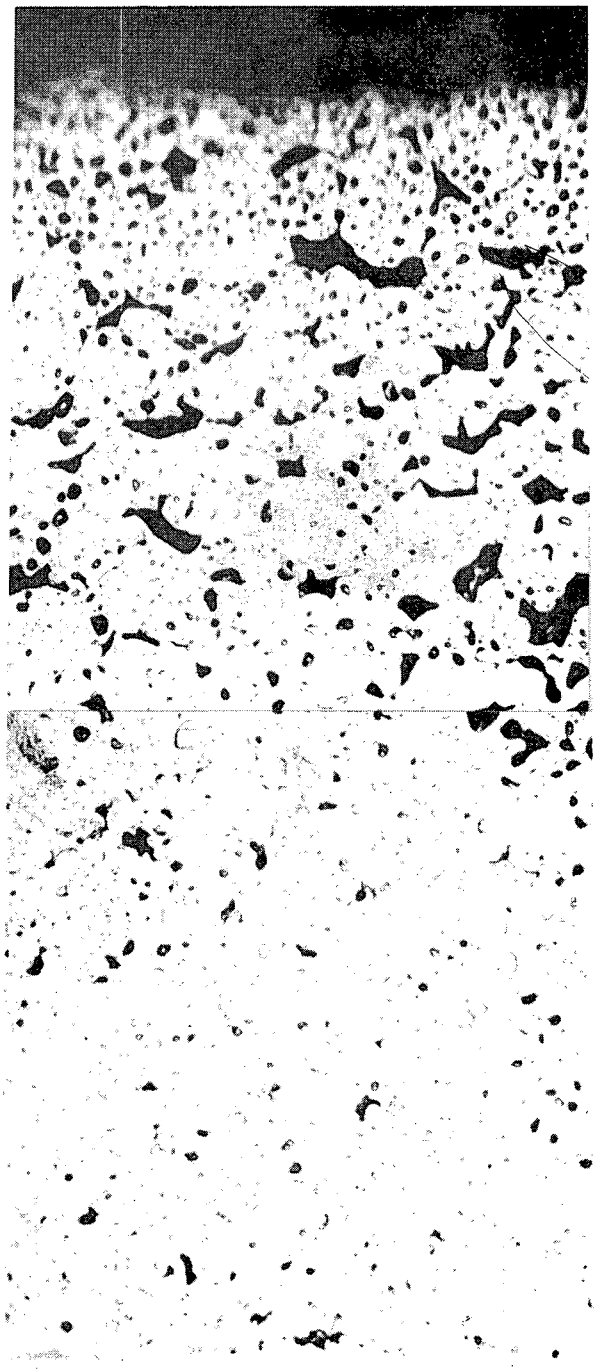

270X As Polished HC2530 and HC2531

FIGURE 62. COMPOSITE PICTURE OF SPECIMEN 10-1 SHOWING POROSITY FROM THE EDGE TOWARD THE CENTER OF THE SPECIMEN

Fission rate was 1.0×10^{14} fissions/(sec)(cm^3).

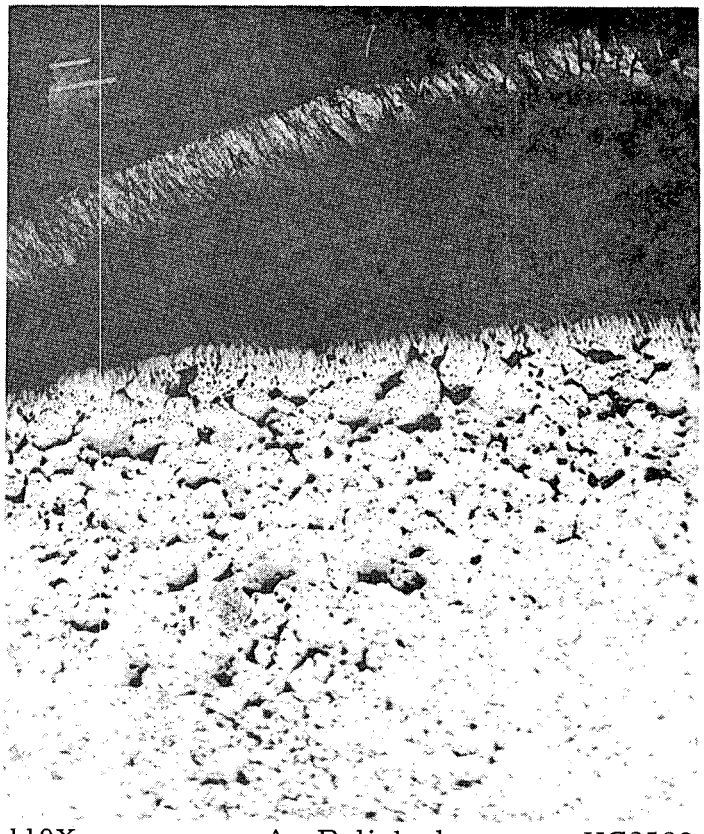

110X As Polished HC2529

FIGURE 63. AREA NEAR EDGE OF TRANSVERSE SECTION OF SPECIMEN 10-1

Note the separation of the cladding from the fuel material. The fission rate was 1.0×10^{14} fissions/(sec)(cm^3).

each particular capsule and by applying the experience gained from other thermocouple-equipped capsules which had been previously irradiated in the same position or were being irradiated at the same time in other sections of the reactor. The irradiation histories of all the capsules in this program have been reviewed as discussed above.

Heat-Treatment Phase

Capsules BMI-9-7 and -8 containing duplicate specimens were irradiated in only one position in the MTR. Irradiation temperatures calculated from cobalt dosimetry data should therefore be fairly representative of the entire irradiation, assuming that large neutron-absorber experiments were not placed near the capsule during the irradiation. The design burnups were achieved although the temperatures were lower than expected.

Three sections from one specimen from each of the two capsules were analyzed radiochemically for cesium-137 to determine the fuel burnup. The results are included in Table 15. The results obtained from the analysis of the specimen from Capsule BMI-9-7 agree well with the burnup determined by dosimetry. The burnup of the other two specimens in this capsule was then calculated by correlating the dosimeter flux data with the radiochemical burnup of the one specimen. The effective flux was then estimated by multiplying the effective dosimeter flux by the ratio of the radiochemically determined burnups of the analyzed specimen to the burnup of the same specimen determined by dosimetry, Table 11. The analyzed burnup of the specimen from Capsule BMI-9-8 was higher than that determined by dosimetry. Since there was considerable difference between duplicate analyses of the latter specimen, the burnup and temperature of this specimen from this capsule were calculated from dosimetry, Table 11.

The data obtained from these irradiations indicate that the three heat treatments used on the specimens prior to irradiation, had little effect on the radiation stability of the alloy. Swelling, as evidenced by increases in diameter and decreases in density, increased with increasing burnup but did not appear to be affected significantly by temperatures in the range of about 650 to 1000 F.

Metallographic studies indicated that the gamma-phase microstructure of a specimen (HT-4) irradiated to 1:1 total a/o burnup at a rate of 1.2×10^{14} fissions/(sec)(cm^3) of alloy and at center-line temperatures in the 730 to 810 F region had transformed to the alpha-plus-epsilon phases, Figure 61a. This is considered unusual since other data reported in BMI-APDA-625 indicate that the alloy should remain in the gamma phase under these irradiation conditions. Another gamma-phase specimen (HT-5) irradiated to 1.6 total a/o burnup at a rate of 1.7×10^{14} fissions/(sec)(cm^3) of alloy at center-line temperatures in the 880 to 1000 F region, had not transformed, Figure 61b. The fact that one specimen had apparently transformed while the other had not, did not appear to affect the swelling of the specimen. It should be noted that transformation in this case may have been influenced by inhomogeneities in the coextruded specimen as evidenced by the very pronounced "swirl" structure. The higher fission rate and temperature experienced by Specimen HT-5 may have homogenized the microstructure, thus eliminating the swirl structure. Both specimens were prepared from the same stock and were given identical preirradiation heat treatments (15 min at 662 F, air cooled).

Burnup Phase

All of the specimens used in this part of the program were heat treated (24 hr at 1652 F, water quenched) to produce the gamma phase prior to irradiation. Since the irradiations were generally quite long, most of the capsules were moved from one location to another. In cases where a capsule was moved, the MTR flux data were compared with dosimeter flux data, and the temperatures reported in Table 11 adjusted to show the probable maximum temperatures experienced by the specimens.

Capsules BMI-9-1, -2, and -3 were irradiated in only one location. Burnup and irradiation temperature were calculated from dosimetry data. Capsule BMI-9-4 was moved to three different vertical positions, but remained in one position at the highest flux for the last three out of six MTR cycles. The temperature given in Table 11 for this capsule was calculated by comparing the average flux obtained from MTR data with the dosimeter flux, and reducing the MTR flux for the last three cycles by the ratio of the two average flux values. The effective flux was then calculated by adjusting the reduced MTR flux to account for neutron perturbation.

Capsule BMI-9-5 was irradiated in several MTR locations including a lattice location during the last two cycles of a ten-MTR-cycle irradiation. The MTR estimated flux in the lattice location ranged from 8.3×10^{13} to 17×10^{13} nv. The temperatures for the specimens from this capsule, as presented in Table 11, were calculated by reducing the MTR estimated flux by the specimen perturbation factor. The specimens were badly swollen and disintegrated with some evidence of melting. Diameter and density measurements were obtained from a relatively good section of one specimen.

Capsule BMI-9-12 was irradiated in several locations in the MTR. However, the specimens were exposed to similar flux levels during the last eight of ten MTR cycles and the dosimeter flux was used to calculate burnup and irradiation temperatures. Nothing unusual was observed in the condition of the specimens.

Capsule BMI-9-13 was irradiated for 29 MTR cycles in five different vertical positions. The specimens had disintegrated and could not be examined. The burnup and irradiation temperature were estimated from MTR data by simply reducing the MTR estimated flux to account for neutron perturbation, since dosimeters were not recovered from the capsule.

Composition-Effects Phase

Capsule BMI-9-10 was irradiated for a total of seven MTR cycles. The capsule was in a lattice location during the last three cycles. Burnup and irradiation temperatures were calculated from MTR data by taking into account the perturbation factor. A brief examination of the failed specimens indicated evidence of melting.

Capsule BMI-9-11 was irradiated in two locations in the MTR. The capsule was in the highest flux during the last two out of four MTR cycles, according to MTR data. However, the dosimeter flux was about 5.9×10^{13} nv compared with a calculated average MTR estimated flux of 5.0×10^{13} nv. In almost every previous case the MTR estimates have been higher than the dosimeter flux by about 30 per cent. This indicates that reported MTR flux estimates were probably in error for this irradiation.

Two of the specimens from this capsule were sectioned for radiochemical analyses for cesium-137 to determine fuel burnup. Three small sections of one specimen were analyzed, while another was cut into six sections, each of which was analyzed. The results are given in Table 15. The burnup of the remaining two specimens was estimated by assuming that the dosimeter flux was correct for the burnup achieved in the top specimen, HT-4, as determined radiochemically, and by assuming that the burnup increase was linear from the top to the bottom specimen, which was also analyzed radiochemically. Temperatures were then estimated by using an effective flux calculated by multiplying the effective dosimeter flux for the top specimen by the ratio of the burnup of the appropriate specimen to that of the top specimen. The results are included in Table 11. The irradiation temperature of the specimens was estimated from these burnups. In general, the burnups determined by dosimetry alone was slightly lower than the analyzed values.

The data obtained from these irradiations did not indicate any major differences in radiation stability of the two alloys. One specimen of uranium-11 w/o molybdenum was examined metallographically with no indications of any change in the microstructure. However, fine hairline cracks were observed in the cladding.

Cladding-Thickness Phase

Capsule BMI-9-9 was irradiated in only one MTR location. The dosimeter data indicate a fairly uniform decrease in flux down the length of the capsule, except for the top specimen. A sharp decrease in flux between the top and second specimen was indicated, Table 10. A considerable amount of swelling was encountered in all of the specimens, with end cracks observed in four of the six specimens. The data indicate that swelling was reduced by the thicker cladding. However, specimens with the thicker claddings exhibited more of a tendency to crack than did the specimens with 4.7-mil cladding. In general, the specimens were considered to be in remarkably good condition considering the irradiation parameters.

Two specimens from this capsule were radiochemically analyzed for cesium-137 to determine fuel burnup, Table 15. The analyzed burnup values were much lower than the dosimeter values. Dosimeter values were used to calculate temperatures and burnups, Table 11, since dosimeter results obtained from other capsules (BMI-9-1, -2, -3, and -4) irradiated in or near the location of this capsule indicated similar flux intensities. The observed swelling of the specimens is also more indicative of either high irradiation temperature or high burnup.

Capsule BMI-9-14 was irradiated for four MTR cycles in one position and one MTR cycle in another position. According to MTR estimates, a steep flux gradient was imposed on the capsule during the last cycle, with the maximum flux occurring at the bottom of the capsule. This capsule was equipped with thermocouples which failed before any temperature readings could be obtained. Although the burnup and temperature data included in Table 11 were based on dosimeter data, it is estimated that the bottom specimen in this capsule could have experienced temperatures in the 750 to 850 F region during the last MTR cycle. The specimens from this capsule did not appear to be grossly affected by the irradiation. Again, it appeared that the swelling of the specimens had been restricted by the thicker cladding.

Metallographic examination of six specimens from these two capsules presented interesting information. Two specimens from Capsules BMI-9-14, 10CT4-27 and 10CT8-6, both retained the gamma phase during irradiation while three specimens, 10CT4-26, 10CT8-2, and 10CT11-3, from Capsule BMI-9-9 apparently transformed. One specimen, 10CT11-2, from Capsule BMI-9-9 remained essentially in the gamma phase with traces of transformation product at the grain boundaries.

The results of the metallographic examinations indicate that fission rates of 0.35×10^{14} and 0.78×10^{14} fissions/(sec)(cm^3) maintained the gamma phase under the irradiation conditions experienced by Specimens 10CT4-27 and 10CT8-6, respectively. However, very little, if any, transformation would have occurred in Specimen 10CT4-27 in the same amount of time at 300 F outside of a reactor.

The metallographic examinations also indicated that the specimens irradiated at high fission rates [1.4×10^{14} to 1.9×10^{14} fissions/(sec)(cm^3)] to burnups ranging from 2.5 to 3.4 total a/o transformed at irradiation temperatures ranging from 820 to 1440 F. The observed effect may have been the result of fission-gas bubbles but the microstructure closely resembled that of a transformed structure. These data suggest that at high burnups the transformation rate is increased drastically, possibly as a result of stresses due to swelling and/or contaminant fission products. The observation that transformation products were just beginning to appear at grain boundaries in Specimen 10CT11-2 while the specimen with the next highest burnup, Specimen 10CT8-2, was more or less fully transformed, may indicate the range of temperature and fission rate necessary to just maintain the gamma phase at a burnup of 2.4 total a/o.

Burnup-and-Heat-Treatment Phase

The specimens included in Capsules BMI-9-22 and -23 were identical. Capsule BMI-9-22 was irradiated for 11 MTR cycles in different vertical positions. During the last three cycles, the capsule was irradiated in a position in which the flux levels were estimated to be a factor of two higher than those encountered during the first eight MTR cycles. Temperatures calculated from dosimetry data indicate average levels of 400 to 500 F. However, it is estimated that the specimens achieved temperatures in the range of 620 to 840 F with a fission rate of about 1.2×10^{14} fissions/(sec)(cm^3), during the last three MTR cycles. Since in this case the condition of the specimen would be more affected by the temperatures encountered during the last three MTR cycles of the irradiation, the calculated irradiation temperature and fission rate existing during these cycles are reported in Table 11. However, it should be noted that fission rates of 0.4×10^{14} fissions/(sec)(cm^3) or lower were probably encountered by the top specimen in the capsule during the earlier part of the irradiation. Both specimens in this capsule exhibited considerable swelling, with small longitudinal cracks in the cladding. The top specimen, however, had swollen considerably more than the other specimen, possibly indicating the effects of transformation which could have occurred early in the irradiation due to low fission rates.

Capsule BMI-9-23 was irradiated for 16 MTR cycles with the capsule located in five different positions in one location in the MTR. The capsule was exposed to the highest flux levels during the last seven MTR cycles. The irradiation temperature and fission rate during the last seven MTR cycles was calculated using dosimeter data and MTR estimates of flux, Table 11. However, fission rates earlier in the irradiation

were probably in the range of 0.5×10^{14} fissions/(sec)(cm^3) or lower. Specimen 10MoBH-37 was split longitudinally and cracks were observed extending completely through the specimen.

The specimens included in Capsules BMI-9-24 and -25 were identical. Capsule BMI-9-24 was irradiated in several positions in one location in the MTR. The highest specimen temperatures were probably achieved during the last cycle, based upon MTR estimates of flux. Dosimeter data and MTR flux estimates were combined to permit the calculation of specimen temperatures during the last cycle, Table 11. Here again, there is a possibility that the specimens were irradiated at a low fission rate, particularly the top specimen, thus permitting transformation to occur. These results do not correlate too well with other data obtained under nearly similar conditions. Generally, it has been observed that this alloy swells at a linear rate of about 2.5 per cent per a/o burnup up to about 2.0 total a/o burnup at temperatures below about 1100 F. In the case of these specimens, the extra swelling may have resulted from transformation from the gamma phase since the fission rates were relatively low during part of the irradiation after significant burnup of the fuel had been achieved.

Capsule BMI-9-25 was irradiated for nine MTR cycles in several positions in the MTR. Although the location of the capsule was changed, there was little change in the estimated flux values in each position, according to MTR estimates. The dosimeter data were therefore used to calculate the irradiation parameters. However, there is a possibility that the neutron flux during MTR Cycles 95 and 96 which were run as part of the Atoms for Peace Program, was actually lower than MTR estimates, thus reducing the fission rates to levels where transformation could occur. This would be particularly true for the top specimen in the capsule due to the flux gradient. Both specimens had swollen considerably and split open, which does not correlate with other data at similar burnup and temperatures unless transformation did occur.

The specimens irradiated in Capsules BMI-9-30 and -31 were identical. Capsule BMI-9-30 was apparently irradiated in one position in one location in the MTR, although the MTR estimated flux was revised for the last cycle. Dosimeter data were used to calculate the irradiation temperatures and the burnup. The specimen with the lowest burnup, 10MoBH-6, exhibited a large brittle-type crack at one end. The other specimen, 10MoBH-8, exhibited small fine cracks at the higher burnup. The formation of cracks at burnups in the range experienced by these specimens is unusual. Even more unusual is the fact that the specimen with the lowest burnup was in the worst condition. This capsule was irradiated during the Atoms for Peace Program, MTR Cycles 95 and 96, which occurred near the end of the irradiation period. Reactor power was low during this time, and, although the MTR flux estimates do not indicate it, it is possible that the actual flux was lower than estimates. If this was the case, the fission rate may have been reduced to the point where transformation would occur. Since the specimens were at a significant burnup at this point, the fission rate would probably not have to decrease too much from the average of 0.8×10^{14} to 0.9×10^{14} fissions/(sec)(cm^3) to permit transformation.

Capsule BMI-9-31 was irradiated in several vertical positions in one location in the MTR. The capsule was exposed to the highest flux during the last four out of eleven MTR cycles. Dosimeter data and MTR flux estimates were therefore used to estimate the specimen temperatures and fission rate during the last four MTR cycles, Table 11. Both specimens were in relatively good condition after irradiation with the exception of fine longitudinal cracks in the cladding.

Three of the four specimens irradiated in Capsules BMI-9-30 and -31 survived the irradiation with only fine cracks in the cladding. These three specimens exhibited density decreases in the range of 2.3 to 2.8 per cent per a/o burnup, at burnups ranging from 1.6 to 3.0 total a/o. The fourth specimen, irradiated in Capsule BMI-9-30, to a burnup of 1.4 total a/o, exhibited a density decrease of 3.7 per cent per a/o burnup and also a large crack. Irradiation temperatures of all four were not markedly different. It is difficult to rationalize the behavior of the one specimen; although, such a behavior may have resulted from the presence of inhomogeneities or swirl structure in combination with a fission rate and temperature which promoted transformation. The presence of inhomogeneities does not seem likely since all of these specimens were prepared from the same fuel pin. It therefore appears possible that the excessive swelling of Specimen 10MoBH-6 may have been due to a combination of fission rate and temperature which promoted transformation, thus initiating excessive swelling. This appears more plausible when these data are compared with those obtained from specimens irradiated in Capsule BMI-9-24.

In general, it does not appear possible to evaluate the effect of the different heat treatments used in this phase of the program on the radiation stability of the specimens. This is due to the complications introduced by the possibilities of transformation due to low fission rates.

Capsule BMI-9-6 was included in the heat-treatment-and-burnup phase of the program for convenience. Irradiation temperatures were apparently very high and the specimens disintegrated.

Temperature-Effects Phase

The irradiation histories of the temperature-controlled capsules, BMI-9-19, -20, and -21, were described in detail earlier in this report. The three specimens in each capsule were given different heat treatments prior to irradiation, Table 1. One of the heat treatments was a gamma quench, one a gamma quench modified by a short-term slow cool, and the third produced the alpha-plus-epsilon structure. The specimens irradiated in Capsules BMI-9-19 and -21 to burnups of 1.1 and 1.5 total a/o at center-line temperatures of 800 and 590 F, respectively, did not exhibit any gross signs of damage. Swelling was uniform with density changes in the range of 2.5 per cent per a/o burnup, which corresponds to calculated theoretical swelling due to the formation of fission products. The fact that the specimens had received different preirradiation heat treatments did not appear to affect the swelling of the specimens.

The specimens irradiated in Capsule BMI-9-20 swelled severely and ruptured. Decreases in density ranged from 14 to 33 per cent per a/o burnup, indicating that abnormal swelling (i.e., swelling in excess of theoretical) had occurred. The only difference between the irradiation conditions of this capsule and the other two capsules of this phase was a slightly higher fission rate and a higher irradiation temperature. Since irradiation of other specimens under similar conditions of fission rate and burnup, but at lower temperatures than those occurring in Capsule BMI-9-20, did not result in abnormal swelling, it can be concluded that the abnormal swelling was the result of the higher irradiation temperature.

It should also be noted that the two specimens given a preirradiation gamma-quench and a modified-gamma-quench heat treatment swelled less than the specimen with the transformed alpha-plus-epsilon structure. Swelling of the latter specimen was almost twice that of the gamma specimens.

Reference-Diameter Phase

The irradiation histories of the four capsules, BMI-9-32, -33, -34, and -35, irradiated during this phase of the program, were described in detail earlier in this report. Only two specimens, one from Capsule BMI-9-32 and one from Capsule BMI-9-33 were recovered for examination. Both of these specimens had failed.

Capsule BMI-9-32 was equipped with several thermocouples positioned close to the specimen to provide a record of irradiation temperatures. This specimen had ruptured longitudinally and broken transversely. The cladding had almost peeled completely off the specimen. Metallographic examination indicated the presence of a considerable amount of gas bubbles in the matrix, with the quantity and size of the bubbles increasing toward the outer surface of the specimen. The condition of the specimen was probably the result of irradiation at temperatures in the 1100 F region (compare with results from Capsule BMI-9-20) and from the effects of the thermal cycling indicated by readings obtained from two of the four thermocouples located in the capsule. As noted earlier in this report, the thermal cycling indicated by the thermocouple readings may have been the result of movement of the thermocouples in respect to the specimen surface, probably as a result of vibrations caused by the flow of coolant water through the MTR core. If this was the case, thermal cycling did not occur in the specimen. If the thermal cycling was real, however, specimen center-line temperatures as high as 1400 F could have been obtained for short periods of time.

The specimen irradiated in Capsule BMI-9-33 to a burnup of 1.9 total a/o at center-line temperatures in the range of 1200 F swelled and ruptured longitudinally. This specimen had swelled until it contacted the specimen basket. The cladding generally did not appear to have peeled from the specimen as extensively as in the case of the specimen from Capsule BMI-9-32. The ruptures also did not appear to be of the brittle type, but indicated plastic deformation had occurred before rupture.

Generally, the results of these two irradiations indicate that the reference fuel alloy will swell abnormally at burnups as low as 0.78 total a/o when irradiated at temperatures in the 1100 to 1200 F range.

Release of Krypton-85 From Specimens During Irradiation

The release of krypton-85 from specimens irradiated in eight capsules was measured, Table 9. The data indicate that, in the case of unclad specimens, the release of krypton-85 is due to recoil and diffusion. In the case of clad specimens, the release of krypton-85 was too small to measure, indicating that there was little, if any, loss due to diffusion of the gas through the cladding during the irradiation period. Where specimens were ruptured, the release of krypton-85 increased drastically to levels as high as 38 per cent of the total krypton-85 formed.

Specimen Swelling

The swelling of a nuclear fuel alloy, such as uranium-10 w/o molybdenum, is a result of the formation of fission-product atoms whose total volume when substituted in the crystal lattice of the alloy exceeds that of the fissioned uranium atoms. Swelling from this effect is linear and is termed normal. Normal swelling, or volume increase, for the Fermi reference fuel has been estimated to be about 2.3 per cent at 1.0 total a/o burnup. Since rare gases make up part of the fission products, the swelling of a fuel is sometimes increased above normal due to the effect of gas in small pockets. This is termed abnormal swelling and is influenced by temperature since the pressure of a constant volume of gas is increased as the temperature is increased. Transformation apparently tends to agglomerate the gas in pockets and produce abnormal swelling. Data obtained from these irradiations have been used to prepare curves showing swelling as a function of burnup and temperature. Data originally presented in BMI-APDA-652 and in an APDA Memorandum, Mat-79, were used in preparing these curves.

The normal swelling of reference-alloy specimens as a result of irradiation is shown in Figure 64 as a function of burnup. The curve drawn through the points was placed so that most of the data points fell below the line. This should give a conservative estimate of swelling for specimens irradiated at average center-line temperatures of 1000 F or below, at fission rates sufficient to prevent the occurrence of transformation. The only data points located above the curve are those associated with specimens which were irradiated at center-line temperatures of about 1000 F or above, and those associated with specimens that were suspected to have transformed during irradiation as a result of low fission rates. The data indicate that conservatively the reference alloy will swell at a rate of about 3.0 per cent per a/o burnup, as long as irradiation temperatures are below a critical value of about 950 to 1100 F as discussed later, and transformation does not occur during the irradiation. This compares fairly well with the calculated value for normal swelling.

The effect of temperature on the swelling of reference-fuel-alloy specimens is shown in Figure 65. The data indicate that normal swelling occurs until specimen center-line irradiation temperatures of about 1000 F to 1100 F are reached. Above these temperatures, the swelling rate increases exponentially with temperature and rupturing of the specimens occurs. A range of temperature in the critical region is given because of a lack of data points with which to draw an accurate curve. The lower temperature was derived from a study of thermal-expansion data which indicated that irradiated specimens began to swell exponentially with increasing temperature in the region of 1000 F. The upper limit was chosen because almost all specimens irradiated above this temperature experienced abnormal swelling. The only data points which appeared above the curve were those obtained from specimens which were suspected of transforming during irradiation, thus increasing the swelling rate. There are some data points below the curve which were also obtained from specimens which were either known to, or were suspected of, transforming during irradiation. Apparently, some of these specimens did not transform during irradiation or the transformation did not cause the specimens to swell as in the case of other specimens. The reason for this is not clear.

Density data were used to prepare Figures 64 and 65 because measurements of this property will show small changes in volume more accurately than measurements of

physical dimensions, and because the physical-dimension measurements are affected by surface conditions. Curves have been prepared, however, showing the changes in diameter as a function of burnup and irradiation temperature since diameter increases are important from the standpoint of coolant flow in the reactor core, Figures 66 and 67.

The curve shown in Figure 66 indicates that the reference fuel alloy will increase in diameter at a rate of about 1.1 per cent per a/o burnup, at average specimen centerline temperatures up to about 1000 to 1100 F. The curve in this figure was drawn conservatively so that all data points would fall below the line except for those obtained from specimens suspected of transforming during irradiation.

The curve shown in Figure 67 was again drawn on the conservative side of the data and indicates a linear increase in diameter with increasing burnup up to about 1.5 to 1.6 total a/o. At this point, the data become scattered, probably because of the effect of surface conditions (roughness, cracks, etc.) on the measurements. The curve was then drawn on the conservative side of the data at the higher burnups. Acutally, this curve should probably be extended along the dashed line, where it would resemble the swelling curve shown in Figure 64, which was derived from density measurements.

An attempt was also made to show swelling as a function of fission rate. The data were rather scattered but indications were that fission rate did not affect swelling as long as the critical fission rate was exceeded.

Thermal Expansion and Postirradiation Heat Treatments

The thermal-expansion measurements and postirradiation heat treatments were combined for purposes of discussion since the expansion studies were essentially heat treatments. In general, the thermal-expansion data indicated that the length of irradiated specimens of the reference alloy increased linearly with increasing temperature up to about 1000 F, whereupon the length change increased exponentially up to the highest temperature measured, 1470 F, Figures 51 and 52. Only one specimen with a burnup of 1.3 total a/o was heated to these temperatures. However, the fact that the length of other specimens with burnups ranging from 0.36 to 1.6 total a/o increased linearly with temperature up to 1000 F, the maximum temperature used, indicates that the exponential swelling of the one specimen was an effect of temperature and not burnup. It is believed that the results of these experiments give an indication that abnormal swelling of the reference fuel alloy will occur at irradiation temperatures of 1000 F or above. This temperature may be slightly low compared to what may be observed during actual irradiation, probably as a result of transformation occurring during the heat treatments. Such transformation from the gamma phase would probably tend to induce swelling. Data presented earlier in Figures 65 and 66 indicate that specimens irradiated above about 1100 F swelled abnormally.

Data obtained from the postirradiation heat treatment of two specimens indicated that swelling of the specimen with a burnup of 0.5 total a/o leveled off after about 100 hr at 1050 F. The swelling of the other specimen increased exponentially until the specimen exhibited a 7.1 per cent decrease in density after 200 hr at 1050 F. An unirradiated control specimen did not show any signs of swelling. Electrical-resistivity measurements indicated that transformation from the gamma phase did not occur in either the control or the irradiated specimens. It is believed, based upon data presented

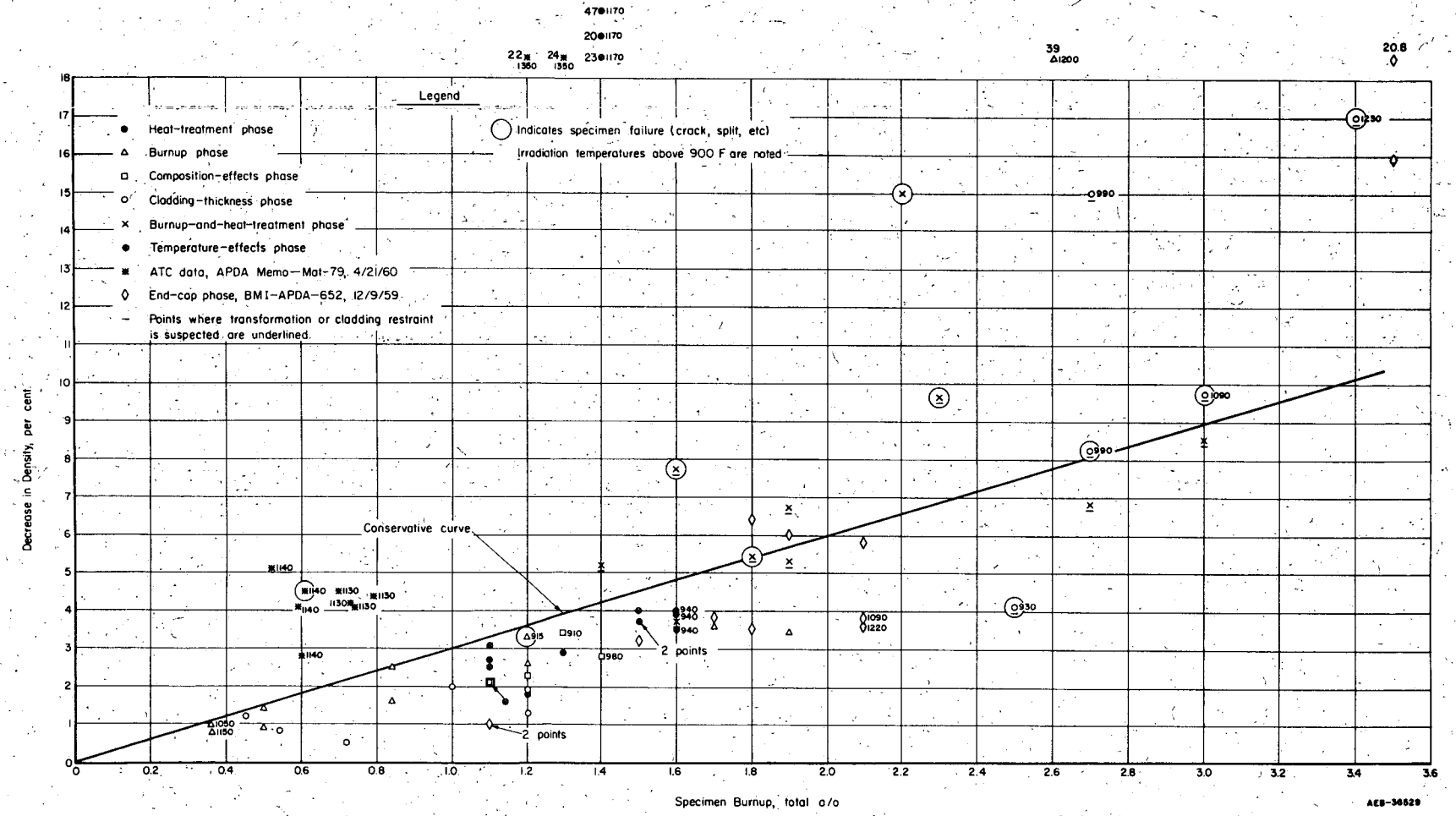

FIGURE 64. DECREASE IN DENSITY OF URANIUM-10 w/o MOLYBDENUM ALLOY SPECIMENS AS A FUNCTION OF BURNUP

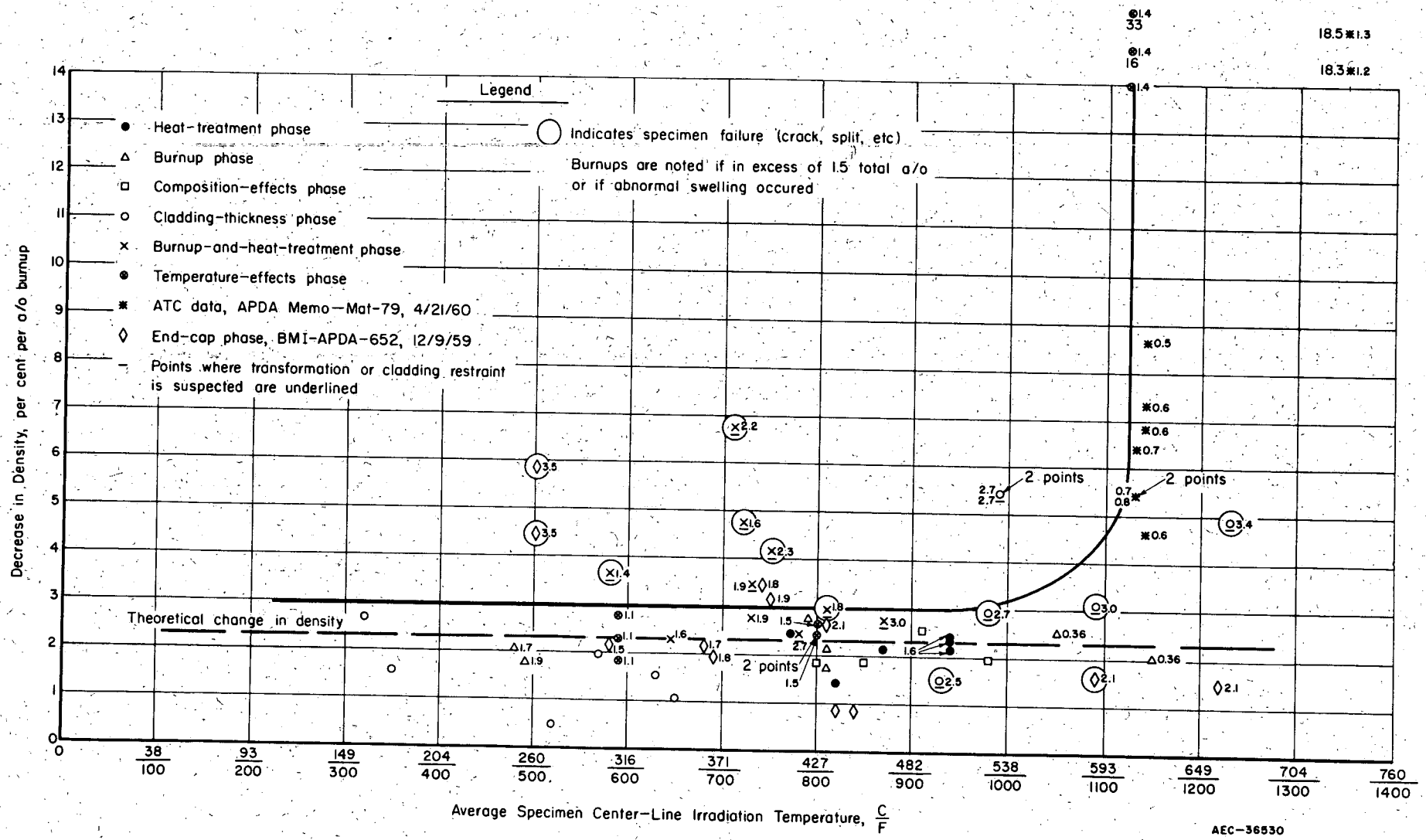

FIGURE 65. DECREASE IN DENSITY OF URANIUM-10 w/o MOLYBDENUM ALLOY SPECIMENS NORMALIZED TO 1.0 a/o BURNUP AS A FUNCTION OF AVERAGE CENTER-LINE IRRADIATION TEMPERATURE

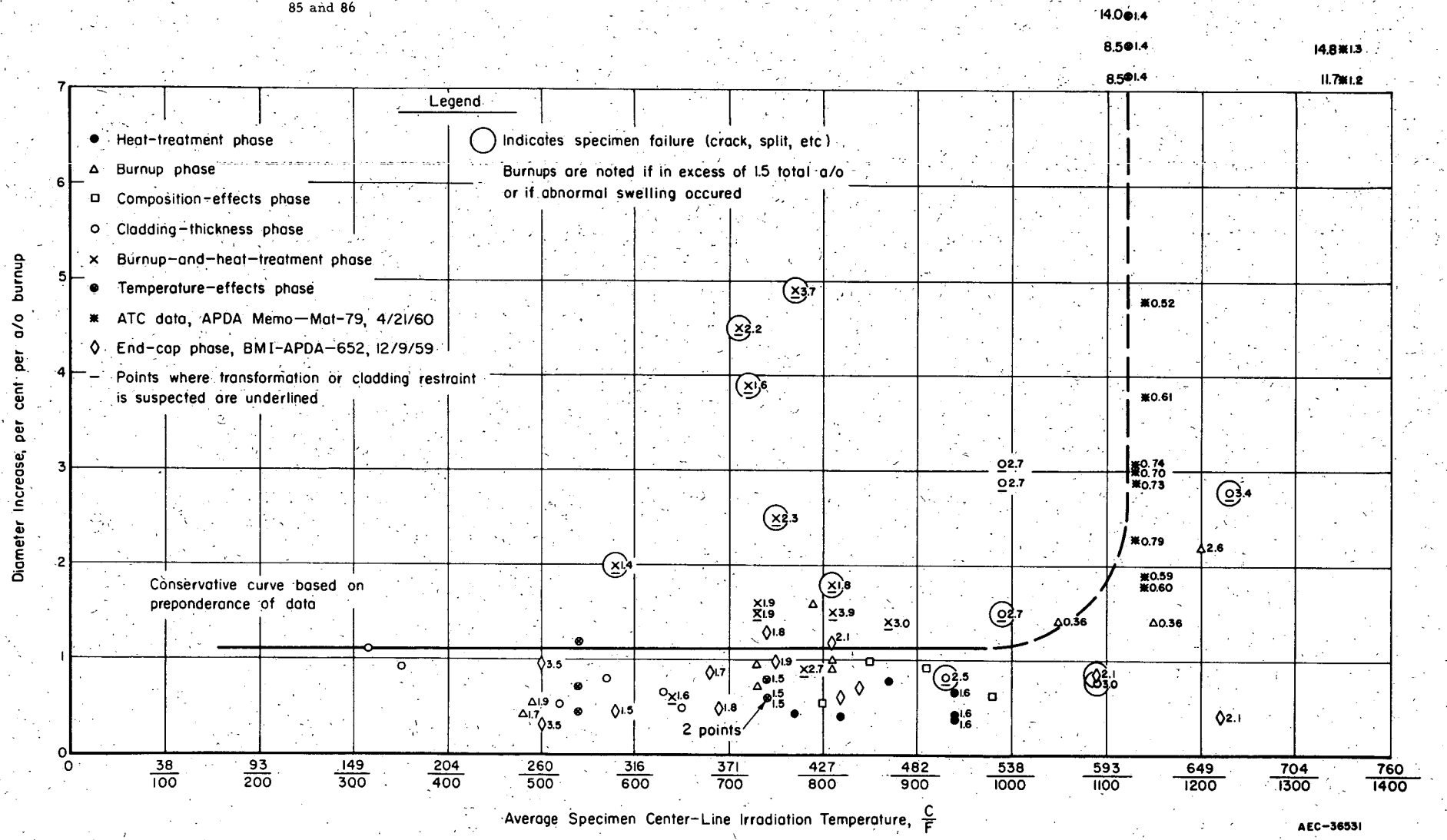

FIGURE 66. INCREASE IN DIAMETER OF URANIUM-10 w/o MOLYBDENUM ALLOY SPECIMENS NORMALIZED TO 1.0 TOTAL a/o BURNUP AS A FUNCTION OF AVERAGE CENTER-LINE IRRADIATION TEMPERATURE

87 and 88

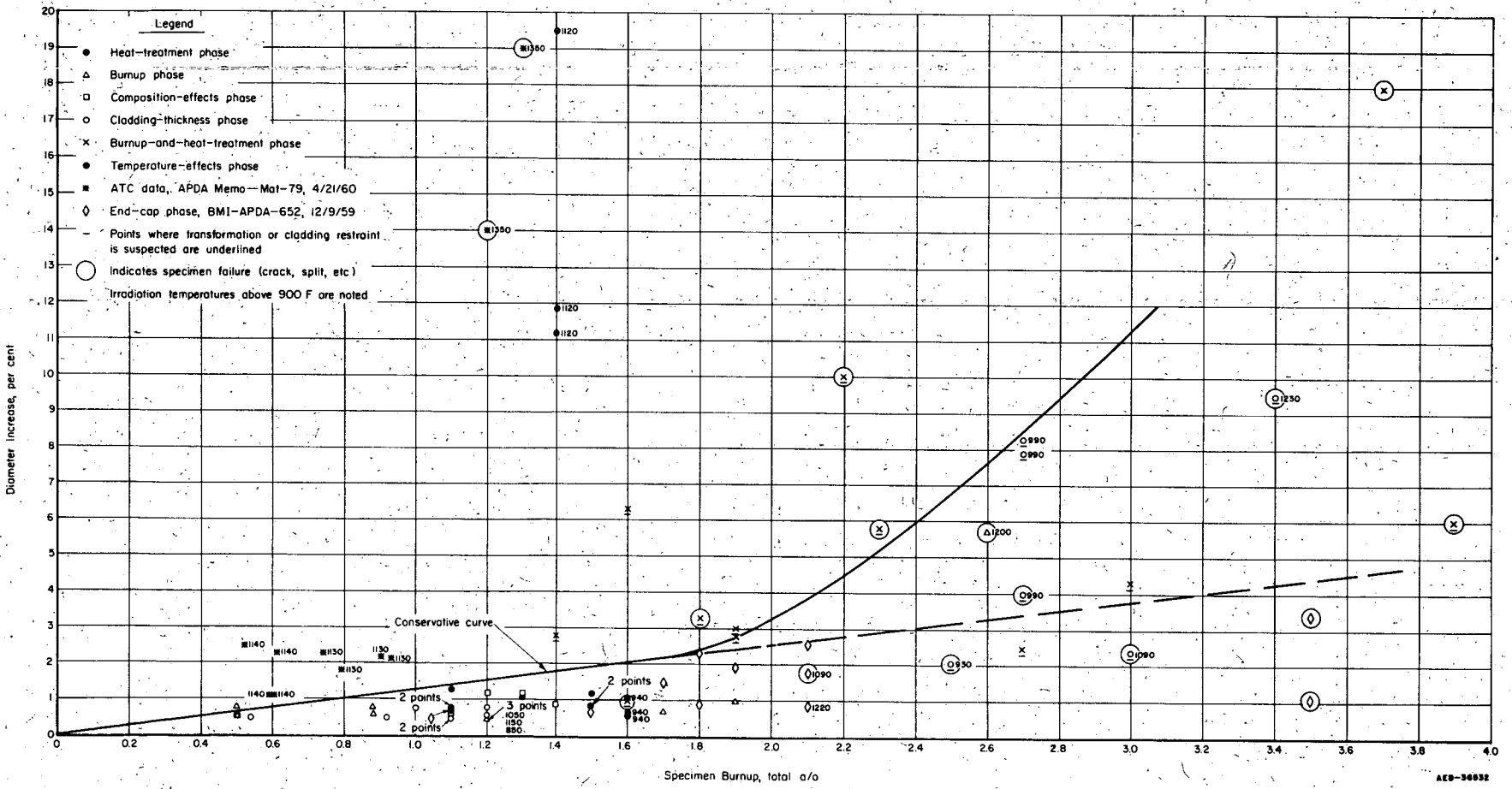

FIGURE 67. INCREASE IN DIAMETER OF URANIUM-10 w/o MOLYBDENUM ALLOY SPECIMENS AS A FUNCTION OF BURNUP

in BMI-APDA-646, that the swelling observed in the case of the specimen with a burnup of 0.84 total a/o was probably the result of oxidation. Such oxidation would also produce the high value observed for electrical resistivity.

General Discussion

The radiation stability of the uranium-10 w/o molybdenum alloy depends to a considerable extent upon the ability to retain the gamma phase during irradiation. However, when irradiations are conducted at low temperatures (below about 1060 F), the alloy tends to transform to the alpha and epsilon phases which are stable at the lower temperatures. The effect of fission-induced displacement and thermal spikes is to oppose this tendency, the spikes tending to disorder the epsilon phase and to produce a homogeneous gamma phase. The minimum number of displacement and thermal spikes required to maintain the gamma phase in opposition to the tendency of the alloy to transform defines a critical fission rate.

During the course of the irradiation experiments described in this report, there was no direct evidence that the critical fission rate was not exceeded, except for irradiations conducted under two conditions.

The first involved the irradiation of specimens in the coextruded and stress-relieved (15 min at 662 F) condition. The uranium-10 w/o molybdenum core alloy was highly segregated, reflecting coring during casting. Metallographic examination suggested that transformation had occurred in uranium-rich areas during irradiation, Figure 61a. Despite the transformation to the possibly less-radiation-resistant alpha and epsilon phases the fact that irradiation temperatures were extremely low (630 to 680 F) probably accounts for the absence of radiation-induced swelling. It is significant to note that a similar fuel specimen, irradiated at a somewhat higher temperature (880 to 1000 F) and fission rate, was apparently homogenized during the irradiation, Figure 61b.

While transformation probably occurred in the segregated uranium-10 w/o molybdenum alloy, indicating that the fission rate was less than critical, this critical rate applies only to areas which were considerably less rich in molybdenum than the 10 w/o which is average for the alloy. Consequently, the critical fission rate defined by this particular test applies to a single condition of prior history and to irradiation behavior at relatively low temperature.

The second condition under which the critical fission rate was not exceeded during irradiation was for irradiations conducted to burnups in excess of 2.0 total a/o. Again, metallographic examination indicates transformation occurring in specimens irradiated to burnups greater than this amount. Excessive swelling accompanied all such irradiations. However, again it is difficult to talk in terms of a critical fission rate for the 10 w/o molybdenum alloy for specimens at this burnup level. First, at this burnup level the alloy being irradiated is of about uranium-9 w/o molybdenum composition. While irradiation tests performed indicate little difference in irradiation behavior between 9, 10, and 11 w/o molybdenum alloys, the 2 a/o of uranium atoms fissioned has been replaced by 3 a/o of other solid fission-product atoms. Consequently, the transformation behavior of this type alloy can be expected to be extremely different from that of the original 10 w/o molybdenum alloy. Secondly, the alloy at this irradiation level is in a highly stressed condition, as evidenced by its extreme brittleness. It has been

shown that stress tends to accelerate transformation of the gamma phase. Thus, the apparent observation of gamma transformation products and excessive swelling in specimens irradiated to burnups in excess of 2 a/o is not regarded as providing a definition of the critical fission rate for the 10 w/o molybdenum alloy. Rather, it is regarded as defining the maximum burnup limit for the alloy. Whether this limitation results from a sharp increase in the critical fission rate required to maintain the alloy in the gamma phase, or just from a loss in properties required to maintain mechanical stability as a result of excessive lattice damage, cannot be determined.

The uranium-10 w/o molybdenum alloy exhibits a further critical point in its irradiation behavior, a critical temperature. This temperature is the temperature above which abnormal swelling is observed, abnormal swelling being defined as volume changes in excess of those which can be accounted for by accommodation of the solid fission-product atoms in the alloy lattice. Below the critical or swelling temperature, volume changes of about 3.0 per cent per a/o burnup are normally observed for specimens irradiated in the gamma-phase condition.

The critical swelling temperature for gamma-phase uranium-10 w/o molybdenum material, as defined by the results of the irradiations reported, is in the vicinity of 1000 to 1100 F. The swelling increases rapidly with increasing temperature for specimens irradiated above this temperature range. Swelling is attributed to increased mobility of fission-gas atoms and decreased mechanical strength with increasing temperature. Evidence of general atom mobility is indicated by the recrystallization temperature of the cold-worked gamma-phase uranium-10 w/o molybdenum alloy which is in the vicinity of 1100 to 1150 F. Hot-hardness data clearly show that the softening temperature of the alloy is about 1100 F. These observations are consistent with the observed swelling temperature.

Postirradiation dilation measurements tend to confirm the critical swelling temperature, although it is uncertain that postirradiation heating tests provide a reliable means of predicting in-pile behavior. However, in the case of the sample heated to 1472 F a rapid increase in length, indicative of the onset of swelling, occurred between about 1000 and 1100 F.

CONCLUSIONS

The following conclusions may be drawn from the results obtained during this program.

(1) The critical center-line irradiation temperature above which the reference fuel alloy of uranium-10 w/o molybdenum swelled abnormally was in the range of 1000 to 1100 F. There was some indication that specimens would not swell abnormally at temperatures over 1100 F, but only if the burnup was below about 0.5 total a/o.

(2) The reference alloy swelled normally with increasing burnup, at a maximum rate of about 3.0 per cent per a/o burnup, at irradiation temperatures below 1000 to 1100 F and if transformation of the gamma phase did not occur during irradiation. This corresponds to a rate of increase in diameter of about 1.1 per cent a/o burnup.

It should be noted that there was some indication that the rate of increase in diameter might become more rapid at burnups above 1.5 to 1.6 total a/o.

(3) The gamma phase of the reference alloy was normally maintained during irradiation at fission rates in the range of 0.7×10^{14} fissions/(sec)(cm^3) at temperatures below 1000 F and at burnups under 2.7 total a/o. The gamma phase apparently transformed during irradiation at burnups over 2.7 total a/o at temperatures in the range of 800 to 1000 F, and at fission rates ranging from 1.5×10^{14} to 1.9×10^{14} fissions/(sec)(cm^3). This apparently indicates that the transformation rate increased drastically at high burnups due to the effect of large quantities of fission products in the lattice and stresses from the attendant swelling, thus requiring large increases in the fission rate to maintain the gamma phase.

(4) The loss of krypton-85 fission gas from clad specimens was in the range of 0.04 per cent or less of the total gas formed, unless the cladding was cracked or the specimen was split. Loses as high as 38 per cent were measured in the case of severely swollen and ruptured specimens.

(5) Metallographic studies indicated that irradiation did not affect the microstructure of the reference alloy except in the case of burnups over 2.7 total a/o where transformation was observed, and swollen specimens irradiated at temperatures in excess of 1000 to 1100 F where gas bubbles or voids were observed in the metal matrix. The apparent homogenization of the structure of a coextruded specimen was also observed.

(6) The data did not indicate any effect of heat treatment prior to irradiation on the stability of the alloy during irradiation, as long as the alloy was in and remained in the gamma phase.

JEG:WEM:AAB:FAR/nb

TABLE 1. FABRICATION HISTORY OF APDA IRRADIATION SPECIMENS

BMI Capsule	Specimen	Lot	Fabrication Method[a]	Enrichment, per cent uranium-235	Molybdenum Content (Balance Uranium), w/o	Heat Treatment[b]	Nominal Gladding Thickness, mils	Type of End Caps
				Heat-Treatment Phase				
9-7	HT-1	--	E	19.35	10	2	0	None
	HT-4	--	E	19.35	10	3	0	None
	HT-7	--	E	19.35	10	4	0	None
9-8	HT-2	--	E	19.35	10	2	0	None
	HT-5	--	E	19.35	10	3	0	None
	HT-8	--	E	19.35	10	4	0	None
				Burnup Phase				
9-1	10MoU-17	1	HR	11.54	10	1	0	None
	10MoU-24	1	HR	11.54	10	1	0	None
9-2	10MoU-22	1	HR	11.54	10	1	0	None
	10MoU-15	1	HR	11.54	10	1	0	None
9-3	10MoU-16	1	HR	11.54	10	1	0	None
	10MoU-23	1	HR	11.54	10	1	0	None
9-4	10MoU-19	1	HR	11.54	10	1	0	None
	10MoU-26	1	HR	11.54	10	1	0	None
9-5	10MoU-20	1	HR	11.54	10	1	0	None
	10MoU-25	1	HR	11.54	10	1	0	None
9-12	10MoU-18	1	HR	11.54	10	1	0	None
	10MoU-27	1	HR	11.54	10	1	0	None
9-13	10MoU-21	1	HR	11.54	10	1	0	None
	10MoU-29	1	HR	11.54	10	1	0	None
				Composition-Effects Phase				
9-10	9MoCE-4	11074	E	19.35	9	2	4	None
	9MoCE-8	11074	E	19.35	9	2	4	None
	11MoCE-2	11075	E	19.35	11	2	4	None
	11MoCE-6	11075	E	19.35	11	2	4	None
9-11	9MoCE-6	11074	E	19.35	9	2	4	None
	9MoCE-9	11074	E	19.35	9	2	4	None
	11MoCE-4	11075	E	19.35	11	2	4	None
	11MoCE-9	11075	E	19.35	11	2	4	None
				Gladding-Thickness Phase				
9-9	10CT8-2	11076	E	19.35	10	2	8.1	None
	10CT4-25	11078	E	19.35	10	2	4.7	None
	10CT11-2	11079	E	19.35	10	2	11	None
	10CT8-3	11076	E	19.35	10	2	8.1	None
	10CT4-26	11078	E	19.35	10	2	4.7	None
	10CT11-3	11079	E	19.35	10	2	11	None

TABLE 1. (Continued)

BMI Capsule	Specimen	Lot	Fabrication Method[a]	Enrichment, per cent uranium-235	Molybdenum Content (Balance Uranium), w/o	Heat Treatment[b]	Nominal Cladding Thickness, mils	Type of End Caps
				Cladding-Thickness Phase (Continued)				
9-14	10CT8-6	11076	E	19.35	10	2	8.1	None
	10CT4-28	11078	E	19.35	10	2	4.7	None
	10CT11-5	11079	E	19.35	10	2	11	None
	10CT8-4	11076	E	19.35	10	2	8.1	None
	10CT4-27	11078	E	19.35	10	2	4.7	None
	10CT11-4	11079	E	19.35	10	2	11	None
	10CT4-34	11078	E	19.35	10	2	4.7	None
				Burnup-and-Heat-Treatment Phase				
9-22	10MoBH-35	11078	E	19.35	10	2	4	None
	10MoBH-43	11078	E	19.35	10	2	4	None
9-23	10MoBH-37	11078	E	19.35	10	2	4	None
	10MoBH-44	11078	E	19.35	10	2	4	None
9-24	10MoBH-1A	11078	E	19.35	10	3	4	None
	10MoBH-1B	11078	E	19.35	10	3	4	None
9-25	10MoBH-1C	11078	E	19.35	10	3	4	None
	10MoBH-5	11076	E	19.35	10	3	4	None
9-30	10MoBH-6	11078	E	19.35	10	5	4	None
	10MoBH-8	11078	E	19.35	10	5	4	None
9-31	10MoBH-7	11078	E	19.35	10	5	4	None
	10MoBH-9	11078	E	19.35	10	5	4	None
9-6	10PB-2	--	HR-PB	19.35	10	6	4	None
	10PB-3	--	HR-PB	19.35	10	6	4	None
				Temperature-Effects Phase				
9-19	10MoTE-31	11078	E	19.35	10	2	4	None
	10MoTE-30	11078	E	19.35	10	5	4	None
	10MoTE-40	11078	E	19.35	10	7	4	None
9-20	10MoTE-32	11078	E	19.35	10	2	4	None
	10MoTE-36	11078	E	19.35	10	5	4	None
	10Mo-TE-41	11078	E	19.35	10	7	4	None
9-21	10MoTE-33	11078	E	19.35	10	2	4	None
	10MoTE-39	11078	E	19.35	10	5	4	None
	10MoTE-42	11078	E	19.35	10	7	4	None

TABLE 1. (Continued)

BMI Capsule	Specimen	Lot	Fabrication Method[a]	Enrichment, per cent uranium-235	Molybdenum Content (Balance Uranium), w/o	Heat Treatment[b]	Nominal Cladding Thickness, mils	Type of End Caps
				Reference-Diameter Phase				
9-32	10-1	--	E	9.49	10	5	4	Swaged
9-33	10-2	--	E	9.45	10	5	4	Swaged
9-34	20-2	--	E	19.35	10	5	4	Swaged
9-35	20-3	--	E	19.35	10	5	4	Swaged

(a) HR = hot rolled; E = coextruded.

(b) The heat treatments were:

1 = 24 hr at 1652 F, water quenched
2 = 1 hr at 1472 F, water quenched; 17 min at 662 F, air cooled
3 = 1/4 hr at 662 F, air cooled
4 = 24 hr at 1652 F, water quenched; 1/4 hr at 662 F, air cooled
5 = 1 hr at 1472 F, slow cooled to 212 F (4-1/2 hr)
6 = As fabricated at 1544 F, furnace cooled
7 = 1 hr at 1472 F, water quenched; 2 weeks at 932 F, air cooled
8 = 24 hr at 1652 F, water quenched; 100 hr at 932 F, furnace cooled
9 = 24 hr at 1652 F, water quenched; 2 weeks at 932 F, furnace cooled.

TABLE 2. RESULTS OF PRE- AND POSTIRRADIATION DIMENSIONAL MEASUREMENTS OF APDA SPECIMENS

BMI Capsule	Specimen[a]	Preirradiation Measurements[b] Length, in.	Diameter, in.	Relative Density[c], g per cm^3	Postirradiation Measurements[b] Length, in.	Diameter, in.	Relative Density[c], g per cm^3
			Heat-Treatment Phase				
302-19	10MoU-1	0.7480	0.0999	17.28	0.7553	0.1004	16.68
	10MoU-5	0.7477	0.0999	17.26	0.7544	0.1008	16.73
	10MoU-13	0.7508	0.1000	17.11	0.7561	0.1004	16.73
302-20	10MoU-4	0.7423	0.1000	17.28	0.7523	0.1012	16.63
	10MoU-6	0.7475	0.1002	17.27	0.7543	0.1009	16.74
	10MoU-14	0.7486	0.1011	17.09	0.7534	0.1015	16.76
9-7	HT-4	0.7490	0.1000	16.79	0.7527	0.1003	16.34
	HT-1	0.7484	0.0988	17.06	0.7531	0.0993	16.75
	HT-7	0.7472	0.0995	16.96	0.7528	0.1006	16.47
9-8	HT-5	0.7498	0.0992	16.97	0.7668	0.0999	16.30
	HT-2	0.7477	0.0999	16.97	0.7553	0.1005	16.37
	HT-8	0.7474	0.0995	16.96	0.7550	0.1006	16.30
			Burnup Phase				
9-1	10MoU-17	0.7480	0.1018	17.13	0.7498	0.1023	16.97
	10MoU-24	0.7470	0.1014	17.10	0.7487	0.1017	16.97
9-2	10MoU-22	0.7514	0.1014	17.11	0.7544	0.1022	16.87
	10MoU-15	0.7463	0.1013	17.15	0.7503	0.1015	16.99
9-3	10MoU-16	0.7492	0.1017	17.14	--[d]	0.1070	16.58
	10MoU-23	0.7494	0.1001	17.20	0.7554	0.1012	16.76
9-4	10MoU-19	0.7499	0.1008	17.15	0.7555	0.1016	16.72
	10MoU-26	0.7483	0.1013	17.06	0.7538	0.1019	16.79
9-5	10MoU-20	0.7495	0.1005	17.22		Specimen disintegrated	
	10MoU-25	0.7512	0.1009	17.13	--[d]	0.1066	10.4
9-12	10MoU-18	0.7475	0.1003	17.22	0.7560	0.1013	16.64
	10MoU-27	0.7508	0.1010	17.23	0.7583	0.1017	16.61
9-13	10MoU-21	0.7484	0.1013	17.14		Specimen disintegrated	
	10MoU-29	0.7509	0.1007	17.18		Specimen disintegrated	
			Composition-Effects Phase				
9-10	11MoCE-6	0.7472	0.1113	15.37		Specimen disintegrated	
	11MoCE-2	0.7499	0.1114	15.36		Specimen disintegrated	
	9MoCE-4	0.7542	0.1114	15.55		Specimen disintegrated	
	9MoCE-8	0.7549	0.1113	15.58		Specimen disintegrated	
9-11	11MoCE-9	0.7516	0.1121	15.39	0.7550	0.1128	15.06
	11MoCE-4	0.7532	0.1117	15.40	0.7564	0.1130	15.04
	9MoCE-9	0.7490	0.1114	15.74	0.7434	0.1127	15.20
	9MoCE-6	0.7398[f]	0.1115	15.59	0.7522	0.1125	15.15

TABLE 2. (Continued)

BMI Capsule	Specimen[a]	Preirradiation Measurements[b] Length, in.	Diameter, in.	Relative Density[c], g per cm^3	Postirradiation Measurements[b] Length, in.	Diameter, in.	Relative Density[c], g per cm^3
			Cladding-Thickness Phase				
9-9	10CT4-26	0.7500	0.1121	15.59	0.7882	0.1227	12.90
	10CT8-3	0.7491	0.1165	14.26	0.7997	0.1257	12.10
	10CT11-3	0.7462	0.1209	13.30	0.7563	0.1238	12.01
	10CT4-25	0.7471	0.1121	15.56	0.7829	0.1214	13.15
	10CT8-2	0.7500	0.1166	14.20	0.7660	0.1211	13.03
	10CT11-2	0.7474	0.1211	13.23	0.7503	0.1237	12.69
9-14	10CT4-34[e]	0.7503	0.1123	15.37	0.7524	0.1125	15.24
	10CT4-27	0.7514	0.1121	15.54	0.7540	0.1123	15.35
	10CT8-4	0.7492	0.1172	14.25	0.7513	0.1178	14.13
	10CT11-4	0.7032	0.1210	13.42	0.7047	0.1212	13.35
	10CT4-28	0.7469	0.1120	15.54	0.7813	0.1129	15.25
	10CT8-6	0.7518	0.1166	14.16	0.7548	0.1175	13.88
	10CT11-5	0.7533	0.1210	13.47	0.7557	0.1217	13.30
			Burnup-and-Heat-Treatment Phase				
9-22	10MoBH-35	0.7502	0.1124	15.50	0.7620	0.1156	14.47
	10MoBH-43	0.7516	0.1120	15.85	0.7635	0.1153	15.01
9-23	10MoBH-37	0.7502	0.1121	15.53	0.7700	0.1241	--
	10MoBH-44	0.7526	0.1120	15.94	0.7664	0.1187	--
9-24	10MoBH-1B	0.7493	0.1120	15.32	0.7589	0.1190	14.14
	10MoBH-1A	0.7738	0.1120	15.30	0.7805	0.1157	14.47
9-25	10MoBH-1C	0.7756	0.1120	15.35	0.7887	0.1234	13.03
	10MoBH-5	0.7524	0.1085	15.47	0.7683	0.1148	13.99
9-30	10MoBH-6	0.7505	0.1091	15.38	0.7591	0.1122	14.58
	10MoBH-8	0.7503	0.1093	15.36	0.7573	0.1104	14.79
9-31	10MoBH-7	0.7506	0.1098	15.36	0.7595	0.1145	14.05
	10MoBH-9	0.7513	0.1091	15.94	0.7603	0.1118	14.86
9-6	10PB-2	0.7501	0.1089	15.44		Specimen disintegrated	
	10PB-3	0.7494	0.1097	15.46		Specimen disintegrated	
			Temperature-Effects Phase				
9-19	10MoTE-31	0.7516	0.1119	15.55	0.7546	0.1128	15.16
	10MoTE-30	0.7509	0.1122	15.55	0.7556	0.1128	15.23
	10MoTE-40	0.7503	0.1118	15.67	0.7571	0.1132	15.19
9-20	10MoTE-30	0.7494	0.1118	15.54	0.8120	0.1251	11.97
	10MoTE-36	0.7496	0.1122	15.55	0.7966	0.1248	12.49
	10MoTE-41	0.7496	0.1121	15.81	0.7931	0.1339	8.41

TABLE 2. (Continued)

BMI Capsule	Specimen[a]	Preirradiation Measurements[b] Length, in.	Diameter, in.	Relative Density[c], g per cm^3	Postirradiation Measurements[b] Length, in.	Diameter, in.	Relative Density[c], g per cm^3
			Temperature-Effects Phase (Continued)				
9-21	10MoTE-33	0.7455	0.1119	15.54	0.7559	0.1129	14.96
	10MoTE-39	0.7490[f]	0.1121	15.56	0.7508[f]	0.1134	14.99
	10MoTE-42	0.7491	0.1121	15.82	0.7578	0.1131	15.19
			Reference-Diameter Phase				
9-32	10-1	6.83	0.1592	14.31	Specimen disintegrated		
9-33	10-2	6.85	0.1591	14.27	Specimen disintegrated		
9-34	20-2	6.82	0.1591	14.44	Capsule not opened		
9-35	20-3	6.82	0.1591	14.42	Capsule not opened		

(a) The specimens are arranged in order from top to bottom of the capsule.
(b) The error in both the pre- and postirradiation dimensional measurements is estimated to be less than ±0.0005 in. and less than ±0.03 g per cm^3 in the case of density measurements.
(c) The relative density was measured by weight differences in air and carbon tetrachloride at ambient temperatures of 20 to 25 C.
(d) Length measurements were not made because one end of the specimen was damaged.
(e) A small hole was drilled longitudinally through this specimen for use in a dosimeter experiment.
(f) An error was apparently made during either the pre- or postirradiation measurements.

TABLE 3. SUMMARY OF DESIGN IRRADIATION CONDITIONS

BMI Capsule	Specimen Central-Core Temperature, F	Specimen Burnup, total a/o
	Heat-Treatment Phase	
302-19	1065	1.2
302-20	1065	1.2
9-7	1065	1.5
9-8	1065	1.5
	Burnup Phase	
9-1	1065	0.5
9-2	1065	1.0
9-3	1065	1.5
9-4	1065	2.0
9-5	1065	2.5
9-12	1065	2.5
9-13	1065	4.0
	Composition-Effects Phase	
9-10	1065	1.5
9-11	1065	1.5
	Cladding-Thickness Phase	
9-9	1065	1.5
9-14	1065	1.5
	Burnup-and-Heat-Treatment Phase	
9-22	1065	2.0
9-23	1065	3.0
9-24	1065	2.0
9-25	1065	3.0
9-30	1065	2.0
9-31	1065	3.0
9-6	1065	1.5
	Temperature-Effects Phase	
9-19	750	1.5
9-20	1290	1.5
9-21	1065	1.5
	Reference-Diameter Phase	
9-32	1200	1.5
9-33	1200	1.5
9-34	1200	1.5
9-35	1200	1.5

TABLE 4. MTR IRRADIATION HISTORY OF APDA CAPSULES

BMI Capsule	MTR Cycle	Irradiation Time: Megawatt - Days	Irradiation Time: Average Power Level, megawatts	Location in MTR	Distance From Top of Reflector to Top of Capsule, in.	Estimated Neutron Flux, 10^{13} nv: Capsule Bottom	Estimated Neutron Flux, 10^{13} nv: Capsule Top
				Heat-Treatment Phase			
9-7	77	473	38.0	A-28-SE	7-1/2	5.1	2.0
	78	539	38.7	A-28-SE	7-1/2	5.1	2.0
	79	527	38.2	A-28-SE	7-1/2	5.1	2.0
	80	556	38.5	A-28-SE	7-1/2	5.1	2.0
9-8	77	473	38.0	A-28-SE	14-3/4	5.7	5.1
	78	539	38.7	A-28-SE	14-3/4	5.7	5.1
	79	527	38.2	A-28-SE	14-3/4	5.7	5.1
	80	556	38.5	A-28-SE	14-3/4	5.7	5.1
				Burnup Phase			
9-1	68	677	39.6	A-27-NE	13-1/2	10.0	8.8
9-2	68	677	39.6	A-27-NE	16-1/2	11.0	10.0
	69	605	38.7	A-27-NE	16-1/2	11.0	10.0
9-3	68	677	39.6	A-27-NE	19-3/4	9.4	11.0
	69	605	38.7	A-27-NE	19-3/4	9.4	11.0
	70	611	39.4	A-27-NE	19-3/4	9.4	11.0
	71	764	39.3	A-27-NE	19-3/4	9.4	11.0
9-4	69	605	38.7	A-27-NW	15-1/2	8.8	7.9
	70	611	39.4	A-27-NW	15-1/2	8.8	7.9
	71	764	39.3	A-27-NE	13	11.0	8.6
	72	238	33.0	A-27-NE	16-1/4	13.0	11.0
	73	284	37.7	A-27-NE	16-1/4	13.0	11.0
	74	539	39.0	A-27-NE	16-1/4	13.0	11.0
9-5	69	605	38.7	A-27-NW	18-3/4	7.9	8.8
	70	611	39.4	A-27-NW	18-3/4	7.9	8.8
	71	764	39.3	A-27-NE	16-1/4	13.0	13.0
	72	238	33.0	A-27-NE	19-1/2	9.4	13.0
	73	284	33.7	A-27-NE	19-1/2	9.4	13.0
	74	539	39.0	A-27-NE	19-1/2	9.4	13.0
	75	510	37.0	A-27-NE	19-1/2	9.4	13.0
	76	537	39.6	A-13-SW	19-1/2	9.5	8.8
	78	539	38.7	L-51	6	15.0	8.3
	81	535	39.1	L-57	29	17.0	10.0
9-12	79	527	38.2	A-36-SW	24	1.5	1.5
	80	556	38.5	A-36-SW	24	1.5	1.5
	81	535	38.1	A-43-SW	24	6.1	7.3
	82	597	39.1	A-43-SW	24	6.1	7.3
	83	587	39.6	A-43-SW	24	6.1	7.3
	84	495	37.7	A-43-SW	24	6.1	7.3
	85	516	39.6	A-43-SW	24	6.1	7.3[a]
	87	650	38.8	A-2-NE	28	5.1	8.2
	88	526	39.1	A-2-NE	28	5.1	8.2
	89	631	39.2	A-2-NE	28	5.1	8.2

TABLE 4. (Continued)

BMI Capsule	MTR Cycle	Irradiation Time: Megawatt - Days	Irradiation Time: Average Power Level, megawatts	Location in MTR	Distance From Top of Reflector to Top of Capsule, in.	Estimated Neutron Flux, 10^{13} nv: Capsule Bottom	Estimated Neutron Flux, 10^{13} nv: Capsule Top
			Bumup Phase (Continued)				
9-13	79	527	39.1	A-36-SW	28	1.3	1.5
	80	556	38.5	A-43-SW	28	3.8	6.1
	81	535	38.1	A-43-SW	28	3.8	6.1
	82	597	39.1	A-43-SW	28	3.8	6.1
	83	587	39.6	A-43-SW	28	3.8	6.1
	84	495	37.7	A-43-SW	28	3.8	6.1
	85	516	39.6	A-43-SW	28	3.8	6.1
	86	614	39.2	A-43-SW	28	3.8	6.1
	87	650	38.8	A-2-NE	32	3.2	6.1
	88	526	39.1	A-2-NE	32	3.2	6.1
	89	631	39.2	A-2-NE	32	3.2	6.1
	90	590	38.9	A-2-NE	32	3.2	6.1
	91	615	39.2	A-2-NE	32	3.2	6.1
	92	602	39.7	A-2-NE	32	3.2	6.1
	93	558	39.0	A-2-NE	20	12.5	13.0
	94	590	39.1	A-2-NE	20	12.5	13.0
	95 and 96	686	26.4 (avg)	A-2-NE	20	8.3	8.6
	97	560	39.3	A-2-NE	20	12.5	13.0
	98	581	39.4	A-2-NE	20	12.5	13.0
	99	669	39.6	A-2-NE	24	9.7	12.4
	100	626	39.3	A-38-NW	30	9.5	16.0
	101	649	39.1	A-38-NW	30	9.5	16.0
	102	639	39.2	A-38-NW	30	9.5	16.0
	103	633	39.4	A-38-NW	30	9.5	16.0
	104	571	39.3	A-38-NW	30	9.5	16.0
	105	628	39.7	A-38-NW	30	9.5	16.0
	106	798	39.7	A-38-NW	30	9.5	16.0
	107	970	39.8	A-38-NW	30	9.5	16.0
			Composition-Effects Phase				
9-10	79	527	38.2	A-36-SW	7-1/2	1.6	0.83
	80	556	38.5	A-36-SW	7-1/2	1.6	0.83
	81	535	39.1	A-43-SW	7-1/2	6.3	0.23
	82	597	39.1	A-43-SW	7-1/2	6.3	0.23
	83	587	39.6	L-58	6-1/2	22.0	9.5
	84	495	37.7	L-58	6-1/2	22.0	9.5
	85	516	39.6	L-58	8	22.0	12.5
9-11	79	527	38.2	A-36-SW	16	3.5	2.8
	80	556	38.5	A-36-SW	16	3.5	2.8
	81	535	38.1	A-43-SW	16	7.3	6.3
	82	597	39.1	A-43-SW	16	7.3	6.3
			Cladding-Thickness Phase				
9-9	78	539	38.7	A-30-NE	14-1/2	12.0	14.5
	79	527	38.2	A-30-NE	14-1/2	12.0	14.5
	80	556	38.5	A-30-NE	14-1/2	12.0	14.5

TABLE 4. (Continued)

BMI Capsule	MTR Cycle	Irradiation Time: Megawatt - Days	Irradiation Time: Average Power Level, megawatts	Location in MTR	Distance From Top of Reflector to Top of Capsule, in.	Estimated Neutron Flux, 10^{13} nv: Capsule Bottom	Estimated Neutron Flux, 10^{13} nv: Capsule Top
			Cladding-Thickness Phase (Continued)				
9-9	81	535	39.1	A-30-NE	14-1/2	12.0	14.5
	82	597	39.1	A-30-NE	14-1/2	12.0	14.5
	83	587	39.6	A-30-NE	14-1/2	12.0	14.5
	84	495	37.7	A-30-NE	14-1/2	12.0	14.5
9-14	83	587	39.6	A-43-SW	10	7.3	3.2
	84	495	37.7	A-43-SW	10	7.3	3.2
	85	516	39.6	A-43-SW	10	7.3	3.2
	86	614	39.2	A-43-SW	10	7.3	3.2
	87	650	38.8	A-2-NE	5-1/2	11.0	2.0
			Burnup-and-Heat-Treatment Phase				
9-22	91	615	39.2	A-4-SW	1/2	4.0	1.0
	92	602	39.7	A-4-SW	1/2	4.0	1.0
	93	558	39.0	A-4-SW	1/2	4.0	1.0
	94	590	39.1	A-4-SW	1/2	4.0	1.0
	95 and 96	686	26.4	A-4-SW	1/2	2.6	0.7
	97	560	39.3	A-4-SW	6	6.3	3.4
	98	581	39.4	A-4-SW	8-1/2	8.5	5.3
	99	669	39.6	A-4-SW	17	15.0	13.0
	100	626	39.3	A-4-SW	18	15.0	14.0
	101	649	39.1	A-4-SW	18	15.0	14.0
9-23	91	615	39.2	A-4-SW	4	7.1	4.0
	92	602	39.7	A-4-SW	4	7.1	4.0
	93	558	39.0	A-4-SW	4	7.1	4.0
	94	590	39.1	A-4-SW	4	7.1	4.0
	95 and 96	686	26.4 (avg)	A-4-SW	4	4.7	2.6
	97	560	39.3	A-4-SW	9-1/2	9.5	6.3
	98	581	39.4	A-4-SW	12	12.0	8.5
	99	669	39.6	A-4-SW	24	12.5	15.0
	100	626	39.3	A-4-SW	25	11.5	14.5
	101	649	39.1	A-4-SW	25	11.5	14.5
	102	639	39.2	A-4-SW	25	11.5	14.5
	103	633	39.4	A-4-SW	25	11.5	14.5
	104	571	38.3	A-4-SW	25	11.5	14.5
	105	628	39.7	A-4-SW	25	11.5	14.5
	106	698	39.7	A-4-SW	25	11.5	14.5
9-24	91	615	39.2	A-4-SW	7-1/2	12.0	7.0
	92	602	39.7	A-4-SW	7-1/2	12.0	7.0
	93	558	39.0	A-4-SW	7-1/2	12.0	7.0
	94	590	39.1	A-4-SW	7-1/2	12.0	7.0
	95 and 96	686	26.4	A-4-SW	7-1/2	7.9	4.7
	97	560	39.3	A-4-SW	13	13.0	9.5
	98	581	39.4	A-4-SW	15-1/2	14.0	12.0
9-25	91	615	39.2	A-4-SW	11	17.0	12.0
	92	602	39.7	A-4-SW	11	17.0	12.0
	93	558	39.0	A-4-SW	11	17.0	12.0

TABLE 4. (Continued)

BMI Capsule	MTR Cycle	Irradiation Time: Megawatt – Days	Irradiation Time: Average Power Level, megawatts	Location in MTR	Distance From Top of Reflector to Top of Capsule, in.	Estimated Neutron Flux, 10^{13} nv: Capsule Bottom	Estimated Neutron Flux, 10^{13} nv: Capsule Top
			Burnup-and-Heat-Treatment Phase (Continued)				
9-25	94	590	39.1	A-4-SW	11	17.0	12.0
	95 and 96	686	26.4 (avg)	A-4-SW	11	11.2	7.9
	97	560	39.3	A-4-SW	16-1/2	14.5	13.0
	98	581	39.4	A-4-SW	19	15.0	14.0
	99	669	39.6	A-4-SW	27-1/2	9.1	12.5
9-30	91	615	39.2	A-4-SW	29	11.0	16.0
	92	602	39.7	A-4-SW	29	11.0	16.0
	93	558	39.0	A-4-SW	29	11.0	16.0
	94	590	39.1	A-4-SW	29	11.0	16.0
	95 and 96	686	26.4 (avg)	A-4-SW	29	7.3	8.9
	97	560	39.3	A-4-SW	29	9.0	11.0
9-31	91	615	39.2	A-4-SW	32-1/2	7.0	11.0
	92	602	39.7	A-4-SW	32-1/2	7.0	11.0
	93	558	39.0	A-4-SW	32-1/2	7.0	11.0
	94	590	39.1	A-4-SW	32-1/2	7.0	11.0
	95 and 96	686	26.4 (avg)	A-4-SW	32-1/2	4.6	7.3
	97	560	39.3	A-4-SW	32-1/2	3.0	7.4
	98	581	39.4	A-4-SW	32-1/2	3.0	7.4
	99	669	39.6	A-4-SW	20-1/2	15.0	15.0
	100	626	39.3	A-4-SW	21-1/2	14.5	15.0
	101	649	39.1	A-4-SW	21-1/2	14.5	15.0
	102	639	39.2	A-4-SW	19	15.0	14.5
9-6	76	530	39.6	L-56	1/2	7.2	5.0
	77	473	38.0	L-56	1/2	7.2	5.0
	78	539	38.7	L-56	7	25.0	16.0
	79	527	38.2	L-56	7	25.0	16.0
	80	556	38.5	L-56	13	43.0	35.0
	81			Canal			
	82	597	39.1	L-56	10-1/2	38.0	27.0
	83	587	39.6	L-56	17-1/2	49.0	45.0
	84	495	37.7	L-56	10	35.0	25.0
			Temperature-Effects Phase				
9-19	85	516	39.6	A-13-SE	14.5	11.0	7.0
	86	614	39.2	A-13-SE	14.5	11.0	7.0
	87	650	38.8	A-13-SE	14.5	11.0	7.0
	88	526	39.1	A-13-SE	14.5	11.0	7.0
	89	631	39.2	A-13-SE	14.5	11.0	7.0
	90	590	38.9	A-13-SE	14.5	11.0	7.0
	91	615	39.2	A-13-SE	14.5	11.0	7.0
9-20	88	526	39.1	A-7-SE	14.5	7.0	7.6
	89	631	39.2	A-7-SE	14.5	7.0	7.6
	90	590	38.9	A-7-SE	14.5	7.0	7.6
	91	615	39.2	A-7-SE	14.5	7.0	7.6
	92	602	39.7	A-7-SE	14.5	7.0	7.6
	93	558	39.0	A-7-SE	14.5	7.0	7.6
	94	590	39.1	A-7-SE	14.5	7.0	7.6

TABLE 4. (Continued)

BMI Capsule	MTR Cycle	Irradiation Time: Megawatt - Days	Irradiation Time: Average Power Level, megawatts	Location in MTR	Distance From Top of Reflector to Top of Capsule, in.	Estimated Neutron Flux, 10^{13} nv: Capsule Bottom	Estimated Neutron Flux, 10^{13} nv: Capsule Top
			Temperature-Effects Phase (Continued)				
9-21	88	526	39.1	A-9-SE	14.5	3.5	4.2
	89	631	39.2	A-9-SW	13.0	7.2	6.2
	90	590	38.9	A-9-SW	13.0	7.2	6.2
	91	615	39.2	A-9-SW	13.0	7.2	6.2
	92	602	39.7	A-9-SW	13.0	7.2	6.2
	93	558	39.0	A-9-SW	13.0	7.2	6.2
	94	590	39.1	A-9-SW	13.0	7.2	6.2
	95 and 96	686	26.4	A-9-SW	13.0	4.7	4.1
	97	560	39.0	A-9-SW	13.0	7.2	6.2
			Reference-Diameter Phase				
9-32	112	554	38.6	A-38-NW	11.5	18.0	20.0
	113	572	37.6	A-38-NW	11.5	18.0	20.0
	114	568	38.5	A-38-NW	11.5	18.0	20.0
9-33	105	628	39.7	A-38-NW	9.5	17.5	5.9
	106	698	39.7	A-38-NW	9.5	17.5	5.9
	107	970	39.8	A-38-NW	9.5	17.5	5.9
	108	262	19.0	A-38-NW	9.5	7.9	2.7
	109	163	39.6	A-38-NW	9.5	17.5	5.9
	110	585	38.9	A-38-NW	9.5	17.5	5.9
	111	608	39.7	A-38-NW	9.5	17.5	5.9
9-34	99	669	39.6	A-38-NW	1.0	21	3.4
	100	626	39.3	A-38-NW	1.0	13	1.0
	101	649	39.1	A-38-NW	1.0	13	1.0
	102	639	39.2	A-38-NW	1.0	13	1.0
	103	633	39.4	A-38-NW	1.0	13	1.0
	104	571	38.3	A-38-NW	1.0	13	1.0
9-35	100	626	39.3	A-4-SE	9.0	12	4.6
	101	649	39.1	A-4-SE	9.0	12	4.6
	102	639	39.2	A-4-SE	9.0	12	4.6
	103	633	39.4	A-4-SE	9.0	12	4.6
	104	571	38.3	A-4-SE	9.0	12	4.6

TABLE 5. CALCULATED SURFACE AND CENTER-LINE TEMPERATURES FOR SPECIMENS OF URANIUM 10 w/o MOLYBDENUM ALLOY FROM CAPSULES BMI-9-19, -20, AND -21

	Capsule BMI-9-19		Capsule BMI-9-20		Capsule BMI-9-21	
Cycle	Maximum Calculated Surface Temperature, F	Maximum Calculated Center-Line Temperature, F	Maximum Calculated Surface Temperature, F	Maximum Calculated Center-Line Temperature, F	Maximum Calculated Surface Temperature, F	Maximum Calculated Center-Line Temperature, F
85	850	910				
86	860	920				
87	750	810				
88	840	900	1120	1180	530	580
89	880	940	1090	1150	--	--
90	630	690	1090	1150	--	--
91	610	670	1090	1150	--	--
92			1070	1120	580	640
93			1070	1120	580	640
94			1000(a)	1070(a)	560	610
95 and 96					490	540
97					--	--

(a) The heaters failed near the end of Cycle 94 and temperatures decreased about 450 F.

TABLE 6. CALCULATED BURNUP AND TEMPERATURES FOR SPECIMEN 10-1 IRRADIATED IN CAPSULE BMI-9-32

Basis of Calculation	Thermocouple Data			Average Calculated Specimen Temperature[a], F		Heat-Generation Rate, Btu/(hr)(in.)			Average Burnup, total a/o
	No.	Reading	Measured Temperature, F	Surface	Center Core	Initial	Final	Average	
Dosimetry	--	--	--	990	1130	2980	2800	2890	0.78
Heat meter	1	Average	680	950	1110	--	--	2700	0.75
		Maximum	970	1380	1600		--		--
	2	Average	630	860	1000	--	--	2410	0.67
		Maximum	990	1400	1630		--		--
	3	Average	680	970	730	--	--	2750	0.76
		Maximum	840	1200	1380		--		--
	4	Average	640	900	1040	--	--	2500	0.69
		Maximum	790	1110	1270		--		--
Heat meter modified by dosimetry	3	Average	680	970	1130	2980	2800	2890	0.78

(a) Average of initial and final irradiation temperature.

TABLE 7. CALCULATED BURNUP AND TEMPERATURE BASED ON DOSIMETRY FOR SPECIMEN 10-2 IRRADIATED IN CAPSULE BMI-9-33

Average Calculated Specimen Temperature, F		Heat-Generation Rate, Btu/(hr)(in.)			Average Burnup, total a/o
Surface	Center Core	Initial	Final	Average	
1080	1240	3340	2820	3080	1.9

TABLE 8. TEMPERATURE VARIATIONS RECORDED BY THERMOCOUPLES IN CAPSULE BMI-9-32

Thermocouple	Distance From Top of Specimen, in.	Reading[(a)]	Temperature Variation, F per 5 min		
			Cycle 112	Cycle 113	Cycle 114
1	1.2	Daily maximum average	149	221	176
		Cycle maximum	256	392	356
2	2.6	Daily maximum average	194	194	131
		Cycle maximum	329	248	230
3	4.0	Daily maximum average	95	77	86
		Cycle maximum	149	95	131
4	5.4	Daily maximum average	59	50	68
		Cycle maximum	95	59	68

(a) Daily maximum average: The average of the daily maximum temperature variations recorded for the irradiation cycle. Cycle maximum: The maximum temperature variation observed during the irradiation cycle.

TABLE 9. FISSION-GAS RELEASE FROM URANIUM-10 w/o MOLYBDENUM SPECIMENS DURING IRRADIATION

BMI Capsule	Length of Irradiation, days	Specimen Burnup, total a/o	Specimen Surface Irradiation Temperature, F	Type of Cladding	Measured Release of Krypton-85 Atoms(a)	Krypton-85 Atoms Formed	Krypton-85 Released, per cent	Remarks
9-1	17.1	0.36	920-1020	None	5.7×10^{14}	1.0×10^{17}	0.6	--
9-2	32.6	0.50	700-730	None	5.7×10^{14}	1.5×10^{17}	0.4	--
9-3	67.6	1.2	780-890	None	510×10^{14}	3.5×10^{17}	15.0	One specimen partially melted
9-4	79.3	0.84	540-560	None	6.5×10^{14}	2.4×10^{17}	0.3	--
9-12	144.8	1.9 1.7	460-480	None	19×10^{14}	5.2×10^{17}	0.4	--
9-19	106.1	1.1	740	4-mil zirconium	$<0.5 \times 10^{14}$	1.4×10^{17}	<0.04	Specimen 10MoTE-31
		1.1	740	4-mil zirconium	$<0.8 \times 10^{14}$	1.4×10^{17}	<0.04	Specimen 10MoTE-30
		1.1	740	4-mil zirconium	$<0.5 \times 10^{14}$	1.4×10^{17}	<0.04	Specimen 10MoTE-40
9-20	101.2	1.4	1070	4-mil zirconium	300×10^{14}	2.1×10^{17}	14.0	Specimen 10MoTE-36 cracked
		1.4	1070	4-mil zirconium	800×10^{14}	2.1×10^{17}	38.0	Specimen 10MoTE-41 cracked
		1.4	1070	4-mil zirconium	350×10^{14}	2.1×10^{17}	17.0	Specimen 10MoTE-32 cracked
9-21	145.3	1.5	540	4-mil zirconium	$<0.5 \times 10^{14}$	2.3×10^{17}	<0.02	Specimen 10MoTE-42
		1.5	540	4-mil zirconium	$<0.5 \times 10^{14}$	2.3×10^{17}	<0.02	Specimen 10MoTE-39
		1.5	540	4-mil zirconium	$<0.5 \times 10^{14}$	2.3×10^{17}	<0.02	Specimen 10MoTE-33

(a) Calculated from $V = A \times \frac{V_S}{V_A} \left(\frac{t_{1/2}}{0.693 \times f} \right)$ cm^3 at STP,

where

V = volume of krypton-85 at STP, cm^3

A = measured quantity of 0.52-Mev photons emitted from gas aliquot

V_S = volume of sampling system, cm^3

V_A = volume of aliquot of gas, cm^3

$t_{1/2}$ = half-life of krypton-85, 5.41×10^6 min

f = fraction of krypton-85 decaying by emission of 0.52-Mev photon, 0.0036.

TABLE 10. SUMMARY OF DOSIMETER DATA

BMI Capsule	Specimen	Irradiation Time(c), days	Average Neutron Flux, 10^{13} nv	Calculated Effective Neutron Flux, 10^{13} nv
		Heat-Treatment Phase		
9-7	HT-4	54.5	4.6	2.5
	HT-1		5.0	2.7
	HT-7		5.5	3.0
9-8	HT-5	54.5	7.3	3.9
	HT-2		7.3	3.9
	HT-8		7.2	3.9
		Burnup Phase		
9-1	10MoU-17	17.1	9.8	6.6
	10MoU-24		11	7.4
9-2	10MoU-22	32.6	7.1	4.8
	10MoU-15		7.5	5.0
9-3	10MoU-16	67.6	8.0	5.4
	10MoU-23			5.4
9-4	10MoU-19	79.3	5.3	3.6
	10MoU-26		5.2	3.5
9-5	10MoU-20	134.3	--(a)	--
	10MoU-25		--(a)	--
9-12	10MoU-18	144.8	4.4	3.0
	10MoU-27		4.1	2.8
9-13	10MoU-21	157.5	--(a)	--
	10MoU-29		--(a)	--
		Composition-Effects Phase		
9-10	11MoCE-6	115.2	--(a)	--
	11MoCE-2		--(a)	--
	9MoCE-4		--(a)	--
	9MoCE-8		--(a)	--
9-11	11MoCE-9	57.5	6.0	3.2
	11MoCE-4		5.6	3.0
	9MoCE-9		6.3	3.4
	9MoCE-6		5.8	3.1

TABLE 10. (Continued)

BMI Capsule	Specimen	Irradiation Time(c), days	Average Neutron Flux, 10^{13} nv	Calculated Effective Neutron Flux, 10^{13} nv
		Cladding-Thickness Phase		
9-9	10CT4-26	99.4	11.0	5.9
	10CT8-3		8.4	4.5
	10CT11-3		9.5	5.1
	10CT4-25		8.4	4.5
	10CT8-2		8.2	4.4
	10CT11-2		7.6	4.1
9-14	10CT4-34	73.4	--	--
	10CT4-27		1.7	0.90
	10CT8-4		2.0	1.1
	10CT11-4		3.5	1.9
	10CT4-28		4.4	2.4
	10CT8-6		4.0	2.1
	10CT11-5		4.7	2.5
		Burnup-and-Heat-Treatment Phase		
9-22	10MoBH-35	164.6	3.3	1.8
	10MoBH-43		3.3	1.8
9-23	10MoBH-37	248.3	4.9	2.6
	10MoBH-44		5.2	2.8
9-24	10MoBH-1B	115.2	4.2	2.2
	10MoBH-1A		4.5	2.4
9-25	10MoBH-1C	132.1	5.6	3.0
	10MoBH-5		5.9	3.2
9-30	10MoBH-6	100.5	4.1	2.2
	10MoBH-8		4.6	2.5
9-31	10MoBH-7	181.6	5.1	2.8
	10MoBH-9		4.5	2.4
9-6	10PB-2	111.5	--(a)	--
	10PB-3		--(a)	--
		Temperature-Effects Phase		
9-19	10MoTE-31	106	2.7	1.5
	10MoTE-30	106	2.9	1.5
	10MoTE-40	106	2.7	1.5

TABLE 10. (Continued)

BMI Capsule	Specimen	Irradiation Time[c], days	Average Neutron Flux, 10^{13} nv	Calculated Effective Neutron Flux, 10^{13} nv
		Temperature-Effects Phase (Continued)		
9-20	10MoTE-32	101	3.0; 3.1[b]	1.6
	10MoTE-36	101	3.1; 3.1[b]	1.6
	10MoTE-41	101	3.1; 3.2[b]	1.6
9-21	10MoTE-33	145	2.4	1.3
	10MoTE-39	145	2.3	1.2
	10MoTE-42	145	2.2	1.2
		Reference-Diameter Phase		
9-32	10-1	44.3	5.6	2.4
9-33	10-2	106	6.2	2.7
9-34	10-3	Irradiation not completed		--
9-35	10-4	Irradiation not completed		--

(a) Dosimeters not recovered.
(b) Neutron flux calculated from dosimeters positioned outside the subcapsules.
(c) Irradiation time calculated from MTR data concerning total MTR operating time (MWD) and average power level (megawatts). See Table 4.

TABLE 11. IRRADIATION PARAMETERS AND RESULTING DIMENSIONAL AND DENSITY CHANGES OF URANIUM-10 w/o MOLYBDENUM SPECIMENS[a]

BMI Capsule	Specimen	Burnup, total a/o	Average Fission Rate, 10^{14} fissions/(sec)(cm^3)	Calculated Specimen Irradiation Temperature, F				Dimensional and Density Changes After Irradiation				
				Surface		Center Line		Total Change, per cent			Change per a/o Burnup, per cent	
				Start	Finish	Start	Finish	Length	Diameter	Density	Diameter	Density
				Heat-Treatment Phase								
9-7[b]	HT-4	1.1	1.2	700	630	810	730	0.49	<0.5	-2.7	<0.45	-2.5
	HT-1	1.2	1.3	740	670	860	770	0.63	0.5	-1.8	0.42	-1.5
	HT-7	1.3	1.4	790	700	920	820	0.75	1.1	-2.9	0.79	-2.2
9-8	HT-5	1.6	1.7	850	750	1000	880	2.4	0.7	-4.0	0.44	-2.5
	HT-2	1.6	1.7	850	750	1000	880	1.0	0.6	-3.5	0.38	-2.2
	HT-8	1.6	1.7	850	750	1000	880	1.0	1.1	-3.9	0.69	-2.4
				Burnup Phase								
9-1	10MoU-17	0.36	1.2	920	860	1080	1010	0.24	0.5	-0.93	1.4	-2.6
	10MoU-24	0.36	1.2	1020	950	1190	1100	0.23	<0.5	-0.76	<1.4	-2.1
9-2	10MoU-22	0.50	0.88	700	640	820	750	0.40	0.8	-1.4	1.6	-2.8
	10MoU-15	0.50	0.88	730	660	850	770	0.54	<0.5	-0.93	<1.0	-1.9
9-3	10MoU-16	1.2	1.0	(890)[b]	(690)[b]	(1030)[b]	(800)[b]	--	5.2	-3.3	4.3	-2.8
	10MoU-23	1.2	1.0	780	630	900	720	0.80	1.1	-2.6	0.92	-2.2
9-4	10MoU-19	0.84	0.61	--	(630)[c]	--	(730)[c]	0.75	0.8	-2.5	0.95	-3.0
	10MoU-26	0.84	0.61	--	(630)[c]	--	(730)[c]	0.73	0.6	-1.6	0.71	-1.9
9-5[d]	10MoU-20	(2.6)	(0.66)	Estimated 2200 F				Specimen melted				
	10MoU-25	(2.6)	(0.66)	Estimated 1200-1600 F					5.7	-39	2.2	15
9-12	10MoU-18	1.9	0.76	480	370	550	430	1.1	1.0	-3.4	0.53	-1.8
	10MoU-27	1.7	0.68	460	360	530	420	1.0	0.7	-3.6	0.41	-2.1
9-13[e]	10MoU-21	(5.0)	(1.8)	Estimated 1000-1500 F				Specimen disintegrated				
	10MoU-29	(5.0)	(1.8)	Estimated 1000-1500 F				Specimen disintegrated				

TABLE 11. (Continued)

BMI Capsule	Specimen	Burnup, total a/o	Average Fission Rate, 10^{14} fissions/(sec)(cm^3)	Calculated Specimen Irradiation Temperature, F				Dimensional and Density Changes After Irradiation				
				Surface		Center Line		Total Change, per cent			Change per a/o Burnup, per cent	
				Start	Finish	Start	Finish	Length	Diameter	Density	Diameter	Density
Composition-Effects Phase												
9-10[e]	11MoCE-6	(2.2)	(1.1)	Estimated 1100-2100 F				Specimen melted and disintegrated				
	11MoCE-2	(2.2)	(1.1)	Estimated 1100-2100 F				Specimen melted and disintegrated				
	9MoCE-4	(2.2)	(1.1)	Estimated 1100-2100 F				Specimen melted and disintegrated				
	9MoCE-8	(2.2)	(1.1)	Estimated 1100-2100 F				Specimen melted and disintegrated				
9-11[f]	11MoCE-9	1.1	1.1	720	650	840	750	0.45	0.6	-2.1	0.55	-1.9
	11MoCE-4	1.2	1.2	780	690	900	800	0.42	1.2	-2.3	1.0	-1.9
	9MoCE-9	1.3	1.3	830	730	970	850	0.75	1.2	-3.4	0.92	-2.6
	9MoCE-6	1.4	1.4	890	780	1040	910	--	0.9	-2.8	0.64	-2.0
Cladding-Thickness Phase												
9-9	10CT4-26	3.4	1.9	1220	860	1440	1020	5.1	9.5	-17.0	2.8	-5.0
	10CT8-3	2.7	1.5	960	740	1120	860	6.6	7.9	-15.0	2.9	-5.5
	10CT11-3	3.0	1.7	1070	790	1260	930	1.4	2.4	-9.7	0.80	-3.2
	10CT4-25	2.7	1.5	960	740	1120	860	4.8	8.3	-15	3.1	-5.5
	10CT8-2	2.7	1.5	960	740	1120	860	2.1	4.0	-8.2	1.5	-3.0
	10CT11-2	2.5	1.4	890	700	1040	820	0.39	2.1	-4.1	0.84	-1.6
9-14	10CT4-34	0.70	0.56	Dosimeter test specimen				0.28	<0.5	-0.9		-1.3
	10CT4-27	0.45	0.35	290	280	320	310	0.35	<0.5	-1.2	<1.1	-2.7
	10CT8-4	0.54	0.42	320	310	360	340	0.28	0.5	-0.84	0.93	-1.6
	10CT11-4	0.92	0.72	470	430	540	500	0.21	<0.5	-0.5	<0.54	-0.5
	10CT4-28	1.2	0.94	570	510	660	590	--	0.8	-1.9	0.67	-1.6
	10CT8-6	1.0	0.78	510	470	590	540	0.40	0.8	-2.0	0.80	-2.0
	10CT11-5	1.2	0.94	590	530	680	610	0.32	0.6	-1.3	0.50	-1.1
Burnup-and-Heat-Treatment Phase												
9-22[g]	10MoBH-35	1.9	1.2	720	530	840	620	1.6	2.8	-6.7	1.5	-3.5
	10MoBH-43	1.9	1.2	720	530	840	620	1.6	3.0	-5.3	1.6	-2.8
9-23[g]	10MoBH-37	3.7	1.2	790	530	920	620	2.6	18.	--	4.9	--
	10MoBH-44	3.9	1.3	830	560	970	650	1.8	6.0	--	1.5	--

TABLE 11. (Continued)

BMI Capsule	Specimen	Burnup, total a/o	Average Fission Rate, 10^{14} fissions/(sec)(cm^3)	Calculated Specimen Irradiation Temperature, F				Dimensional and Density Changes After Irradiation				
				Surface		Center Line		Total Change, per cent			Change per a/o Burnup, per cent	
				Start	Finish	Start	Finish	Length	Diameter	Density	Diameter	Density
Burnup-and-Heat-Treatment Phase (Continued)												
9-24[g]	10MoBH-1B	1.6	0.80	620	610	730	710	1.2	6.3	-7.7	3.9	-4.8
	10MoBH-1A	1.8	0.90	700	690	820	800	0.87	3.3	-5.4	1.8	-3.0
9-25	10MoBH-1C	2.2	1.1	680	540	790	620	1.7	10.	-15.	4.5	-6.8
	10MoBH-5	2.3	1.2	720	560	840	650	2.1	5.8	-9.6	2.5	-4.2
9-30	10MoBH-6	1.4	0.80	530	470	610	540	1.1	2.8	-5.2	2.0	-3.7
	10MoBH-8	1.6	0.92	590	510	680	590	0.87	1.0	-3.7	0.63	-2.3
9-31[g]	10MoBH-7	3.0	1.4	810	700	940	800	1.2	4.3	-8.5	1.4	-2.8
	10MoBH-9	2.7	1.3	730	630	840	720	1.2	2.5	-6.8	0.93	-2.5
9-6[h]	10PB-2	(3.5)	(1.8)	Estimated 1500-2000 F				Disintegrated				
	10PB-3	(3.5)	(1.8)	Estimated 1500-2000 F				Disintegrated				
Temperature-Effects Phase												
9-19[i]	10MoTE-31	1.1	0.60	740 (avg)		800 (avg)		0.60	0.8	-2.1	0.73	-1.9
	10MoTE-30	1.1	0.60	740 (avg)		800 (avg)		0.63	0.5	-2.5	0.45	-2.3
	10MoTE-40	1.1	0.60	740 (avg)		800 (avg)		0.80	1.3	-3.1	1.2	-2.5
9-20[i]	10MoTE-32	1.4	0.80	1070 (avg)		1120 (avg)		8.3	11.9	-23.0	8.5	-16.0
	10MoTE-36	1.4	0.80	1070 (avg)		1120 (avg)		6.3	11.2	-20.0	8.0	-14.0
	10MoTE-41	1.4	0.80	1070 (avg)		1120 (avg)		5.8	19.5	-47.0	14	-33.0
9-21[i]	10MoTE-33	1.5	0.60	540 (avg)		590 (avg)		1.4	0.9	-3.7	0.6	-2.5
	10MoTE-39	1.5	0.60	540 (avg)		590 (avg)		--[j]	1.2	-3.7	0.8	-2.5
	10MoTE-42	1.5	0.60	540 (avg)		590 (avg)		1.2	0.9	-4.0	0.6	-2.7
Reference-Diameter Phase												
9-32	10-1	0.78	1.0	See Table 6		See Table 6		Split and cracked				
9-33	10-2	1.9	1.1	1080 (avg)		1240 (avg)		Split and cracked				
9-34	10-3	--	--	Not estimated, natural uranium				Capsule not opened				
9-35	10-4	--	--	Not estimated, natural uranium				Capsule not opened				

Footnotes appear on following page.

Footnotes for Table 11

(a) All temperature and burnup data were calculated from neutron-dosimeter data except as noted.
(b) The bottom end of this specimen melted, apparently as a result of the capsule being inverted during irradiation, allowing the end of the specimen to extend above the NaK. The average temperature determined by dosimetry is given.
(c) Temperatures were calculated for last three MTR cycles in the highest flux encountered during the irradiation.
(d) This capsule was irradiated for the last two reactor cycles in an MTR lattice position. Although the reported flux was 15×10^{13} nv, it is known that flux estimates in the lattice were low during the period of time the capsule was irradiated. Burnup and temperatures were estimated from MTR data and appearance of specimens.
(e) This capsule was irradiated in a neutron flux in excess of the design flux. Dosimeter wires were not recovered. Temperatures and burnups were estimated from MTR data.
(f) Burnup was determined by radiochemical analyses and correlation with dosimeter flux. Temperatures were calculated from effective flux derived from radiochemical burnup.
(g) These are estimated temperatures and fission rates achieved near the end of the irradiations when the capsules were placed in positions where the flux was higher than experienced during the first part of the irradiation.
(h) This capsule was irradiated in an MTR lattice position in the highest flux available in the reactor. Burnup and temperature were estimated from MTR data and appearance of specimens.
(i) Burnups were determined by radiochemical analysis. Temperatures were measured by thermocouple.
(j) An error was apparently made during measurement of the pre- or postirradiation length.

TABLE 12. PHYSICAL PROPERTIES OF URANIUM-10 w/o MOLYBDENUM DILATION SPECIMENS

Specimen	Burnup, total a/o	Maximum Test Temperature, C/F	Measurement[a]	Diameter, in.	Length, in.	Density, g per cm^3	Electrical Resistivity[b], 10^{-6} ohm-cm
HRC-2	0	800/1472	1	0.1009	0.7511	17.1[b]	73.1[b]
			3[c]	0.1009	0.7501	17.09	72.4
			Per cent change	0	-0.1	0	-1.0
EC-2	0	800/1472	1	0.1009	0.7512	17.1[b]	73.1[b]
			3[c]	0.1009	0.7503	17.06	70.9
			Per cent change	0	-0.1	0	-3.0
10MoU-24[d]	*0.36*	*500/932*	1	0.1014	0.7470	17.10	73.5
			2	0.1017	0.7487	16.97	74.1
			3	0.1017	0.7623[d]	16.74[d]	79.4[d]
			Per cent change[e]	0	--	--	--[d]
10MoU-4	0.97	500/932	1	0.1000	0.7423	17.28	34.2
			2	0.1012	0.7523	16.63	75.6
			3	0.1019	0.7535	16.50	74.6
			Per cent change[e]	0.7	0.2	-0.8	-1.4
HT-2	1.6	500/932	1	0.0999	0.7477	16.97	73.2
			2	0.1005	0.7553	16.37	76.0
			3	0.1014	0.7570	16.03	73.6
			Per cent change[e]	0.9	0.2	-2.1	-3.2
HT-7	1.3	800/1472	1	0.0995	0.7472	16.96	75.2
			2	0.1006	0.7528	16.47	76.3
			3	0.1016	0.7601	15.94	81.0
			Per cent change[e]	1.0	1.0	-3.2	6.2

(a) Measurements were made (1) before irradiation, (2) after irradiation, (3) after dilation measurements.

(b) The predilation data were estimated from average values from gamma-quenched material.

(c) Dual cycles to 800 C were performed on the control specimen. The measurements completed after the second cycle to 800 C are shown.

(d) This specimen was plated with nickel and tin on one end for thermal-diffusivity measurements. This material was not completely removed from the specimen prior to the dilation measurements and may have affected the length, density, and electrical-resistivity measurements.

(e) The per cent change between the postirradiation and postdilation values is shown.

TABLE 13. MEAN LINEAR THERMAL-EXPANSION COEFFICIENTS FOR URANIUM-10 w/o MOLYBDENUM SPECIMENS

Temperature Range, F	Mean Linear Thermal-Expansion Coefficients, 10^{-6}															
	Unirradiated Control Specimens								Irradiated Specimens							
	HRC-2				EC-2				10MoU-24[a]		10MoU-4		HT-7		HT-2	
	H[b]	C[c]	H	C	H	C	H	C	H	C	H	C	H	C	H	C
68-212	12.5	13.9	12.3	12.3	13.3	13.3	12.6	12.4	--	--	14.3	13.6	16.4	13.8	14.4	13.3
68-392	12.7	13.9	12.8	12.4	13.6	13.3	12.9	12.6	--	--	14.6	13.9	16.4	13.9	14.7	13.5
68-572	12.9	14.0	13.2	12.8	13.9	13.4	13.2	13.0	--	--	14.9	14.3	16.5	14.3	15.1	14.0
68-752	12.9	14.1	13.7	13.2	14.1	13.6	13.7	13.4	--	--	15.4	14.7	16.6	14.5	15.6	14.5
68-932	13.0	14.3	14.3	13.8	14.4	13.9	14.4	14.0	--	--	16.1	14.7	16.8	14.9	17.1	15.3
68-1022	--	--	--	--	--	--	--	--	--	--	--	--	17.5	--	--	--
68-1112	12.9	14.7	14.8	14.5	14.6	14.4	15.1	14.6	--	--	--	--	21.0	15.3	--	--
68-1292	12.9	15.2	15.4	15.1	14.8	15.0	15.7	15.3	--	--	--	--	24.2	15.7	--	--
68-1472	13.3	16.2	14.8	15.9	14.5	16.1	15.7	16.0	--	--	--	--	27.3	16.2	--	--
212-392	12.9	13.9	13.2	12.6	13.9	13.3	13.1	12.8	14.9	14.9	14.9	14.1	16.4	14.1	14.9	13.7
212-572	13.0	14.1	13.6	13.0	14.2	13.5	13.4	13.2	15.1	15.1	15.2	14.5	16.5	14.5	15.4	14.3
212-752	13.1	14.2	14.0	13.4	14.4	13.7	13.9	13.7	15.4	15.4	15.7	15.0	16.7	14.7	15.9	14.9
212-932	13.1	14.4	14.7	14.1	14.6	14.1	14.8	14.3	15.8	15.8	16.4	14.9	16.9	15.1	17.6	15.7
212-1022	--	--	--	--	--	--	--	--	--	--	--	--	17.7	--	--	--
212-1112	13.0	14.8	15.3	14.8	14.8	14.6	15.5	14.9	--	--	--	--	21.8	15.5	--	--
212-1292	13.0	15.4	15.8	15.5	15.0	15.3	16.1	15.7	--	--	--	--	25.3	16.0	--	--
212-1472	13.4	16.4	15.1	16.4	14.6	16.4	16.1	16.4	--	--	--	--	28.5	16.5	--	--
1112-1292	--	--	--	--	--	--	--	--	--	--	--	--	42.9	--	--	--
1112-1472	--	--	--	--	--	--	--	--	--	--	--	--	45.5	--	--	--

(a) This material had nickel and tin plated on one end. This material was not completely removed prior to the expansion measurements and may have affected the results to some extent.

(b) Heating cycle.

(c) Cooling cycle.

TABLE 14. EFFECT OF POSTIRRADIATION HEAT TREATMENTS AT 1070 F ON PHYSICAL DIMENSIONS, DENSITY, AND ELECTRICAL RESISTIVITY OF SPECIMENS

Specimen	Burnup, total a/o	Property	Before Heat Treatment	After 100 Hr at 1070 F	Change, per cent	After 200 Hr at 1070 F	Change, per cent	Measured Loss of Krypton-85, per cent
Control B	0.00	Length, in.	0.7176	0.7170	0	--(b)	--	Less than detectable
		Diameter, in.	0.0883	0.0989	0	--(b)	--	
		Density, g per cm^3	17.17	17.21	0	--(b)	--	
		Electrical resistivity, 10^{-6} ohm-cm	73.1(a)	66.4	-9.1	--(b)	--	
10MoU-15	0.50	Length, in.	0.7503	0.7513	0.1	0.7512	0.1	Less than detectable (about 0.1 per cent of total formed) after both heat treatments
		Diameter, in.	0.1015	0.1019	0	0.1015	0	
		Density, g per cm^3	16.99	16.89	-0.59	16.87	-0.71	
		Electrical resistivity, 10^{-6} ohm-cm	75.3	--(c)	--	73.6	0	
10MoU-19(d)	0.84	Length, in.	0.7555	0.7601	0.61	0.7808	3.4	Less than detectable (about 0.06 per cent of total formed) after first heat treatment and about 4 per cent after the second heat treatment
		Diameter, in.	0.1016	0.1024	0.79	0.1051	3.4	
		Density, g per cm^3	16.72	16.47	-1.5	15.54	-7.1	
		Electrical Resistivity, 10^{-6} ohm-cm	79.4	--(c)	--	104.0	31.0	

(a) Estimated from average electrical resistivity of 10 similar specimens.
(b) The control was given only one heat treatment before the study was discontinued.
(c) Electrical resistivities were not measured due to equipment difficulties.
(d) The ends of this specimen began to chip after 200 hr at 1070 F. This is possible reason for detection of krypton-85 only after the second treatment.

TABLE 15. RESULTS OF RADIOCHEMICAL BURNUP ANALYSES[a]

BMI Capsule	Specimen	Burnup, total a/o	Burnup From Dosimetry, total a/o	Location of Analyzed Section and Remarks
9-11	11MoCE-9	2.0	1.2	Top end of specimen
		1.1		Center section
		1.1		End of specimen adjacent to another specimen
9-11	9MoCE-6[b]	1.2	1.1	End adjacent to upper specimen, 0.5841 in. remaining length
		1.3		0.4436 in. remaining length
		1.3		0.3592 in. remaining length
		1.5		0.2196 in. remaining length
		1.5		0.1012 in. remaining length
		1.8		End adjacent to capsule bottom
9-7	HT-4	1.2	0.9	End section
		1.1		Center section
		1.2		End section
9-8	HT-5	2.1	1.6	End section
		1.9		Center section (25 per cent difference between duplicate analyses)
		2.7		End section
9-9	10CT-4-26	1.7	3.4	Center section; results believed to be low
	10CT-11-2	0.6	2.5	Center section; results believed to be low
9-19	10MoTE-40	1.1	1.2	Center section
9-20	10MoTE-32	1.4	1.2	Center section
9-21	10MoTE-42	1.5	1.3	Center section

(a) Details of the radiochemical techniques were given in BMI-APDA-625.
(b) Original length of specimen 0.7526 in.